Nadine Hammer

Hydrogels for the Controlled Release of Protein Pharmaceuticals

Hydrogels for the Controlled Release of Protein Pharmaceuticals

DISSERTATION ZUR ERLANGUNG DES DOKTORGRADES DER NATURWISSENSCHAFTEN (DR. RER. NAT.) DER FAKULTÄT FÜR CHEMIE UND PHARMAZIE DER UNIVERSITÄT REGENSBURG

vorgelegt von

Nadine Hammer
aus Frankfurt am Main

März 2017

Diese Arbeit entstand in der Zeit von September 2010 bis März 2017 am Lehrstuhl für Pharmazeutische Technologie an der Universität Regensburg.

Die Arbeit wurde von Herrn Prof. Dr. Achim Göpferich angeleitet.

Promotionsgesuch eingereicht am:	13.03.2017
Datum der mündlichen Prüfung:	15.05.2017
Prüfungsausschuss:	Prof. Dr. Sigurd Elz (Vorsitzender)
	Prof. Dr. Achim Göpferich (Erstgutachter)
	Prof. Dr. Torsten Blunk (Zweitgutachter)
	Prof. Dr. Jens Schlossmann (Drittprüfer)

Hydrogels for the Controlled Release of Protein Pharmaceuticals

In der Wissenschaft gleichen wir alle nur den Kindern, die am Rande des Wissens hie und da einen Kiesel aufheben, während sich der weite Ozean des Unbekannten vor unseren Augen erstreckt.

Sir Isaac Newton

Contents

Chapter 1

Introduction and Goals of the Thesis

1.1. Challenges in Protein Formulations

1.1.1. Protein Therapeutics

Over the last decades the importance of proteins in their application as therapeutics increased significantly. Especially, their benefit for the treatment of serious diseases such as cancer, auto immune diseases (e.g. multiple sclerosis), cardiovascular and metabolic diseases was discovered [1].

The developed protein therapeutics are potent and highly specific biomacromolecules with a molecular weight of more than 5 kDa or consisting of more than 50 amino acids [2]. In contrast to other drugs, proteins consist of complex and sensitive three-dimensional structures of polypeptides (primary structure). These polypeptides are arranged in secondary, tertiary and sometimes quaternary structure.

The secondary structure of a protein describes the arrangement and folding of the polypeptide. Due to this folding, the energetic level of the structure is reduced [3]. Drawn by forces, such as hydrogen bonding, electrostatic forces or van der Waals forces, the peptide strands form α-helices, ß-sheets, hinges, turns, and loops [3]. α-Helices are right hand side coils stabilized by hydrogen bonding. For schematic drawing, see exemplarily the green coils in the tertiary structure of lysozyme (**Figure 1.1**). ß-Sheets consist of extended, zigzag ß-strands associated by hydrogen bonding [4]. In Figure 1.1 the ß-strand domains are shown as blue arrows with the tip representing the C-terminal end. The different structural domains of α-helices and ß-sheets are connected via so called loops or shorter turns, respectively [4]. Turns, as shown schematically in magenta, purple and red in Figure 1.1, are 180° turns of different length [4]. 3-turns consist of three amino acid residues, 4-turns of four and so on. Within a turn, the carbonyl residue of the first amino acid is connected via hydrogen bonding with the amino group of the last one [4].

The tertiary structure is the three-dimensional arrangement of secondary structure segments as shown exemplarily for lysozyme in Figure 1.1. These arrangements are stabilized by disulfide bridges (Figure 1.1), isopeptide bonds, hydrophobic interactions, hydrogen bonding, electrostatic interactions or van der Waals forces [3].

In some proteins the tertiary structures aggregate to more complex structures or multimers called quaternary structure [3]. These structures are primarily stabilized by hydrophobic interactions [3].

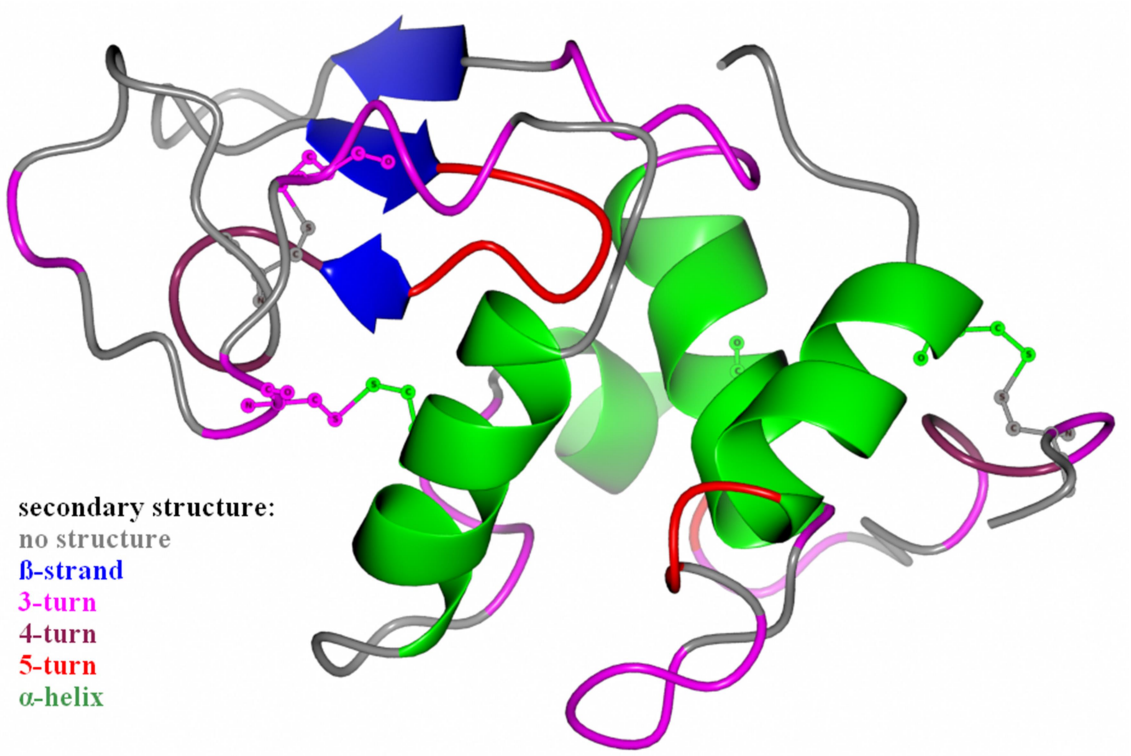

Figure 1.1: Tertiary structure of lysozyme. The shown structure model was created using the CCP4 Molecular Graphics software [5]. Structural information used to create this model is based on results from Diamond (PDB ID: 2 LYZ) [6].

Protein Stability and Activity

This complex three-dimensional structure described above makes proteins more susceptible for instabilities than other common, small-molecule drugs.

The tertiary structure forms the active site of a protein, which is essential for its activity and efficacy [3]. For this reason, the complex structure of proteins is closely related to their therapeutic effect, which makes formulation development very tricky [1, 7]. The activity of the protein drug at the site of action is the most important factor for an effective treatment. Furthermore, well-defined activity of the final formulation is desirable [8]. Damage to the fragile protein structures such as degradation, structural breakdown or aggregation is associated with loss of activity and immune reactions [1]. So, the challenge of protein formulations is to prevent degradation during the whole process of preparation, sterilization and subsequent release in order to maintain protein activity [2, 9].

Aggregation is one of the most frequent complications, when working with proteins [10]. It has to be differentiated between physical and chemical (covalent) aggregation

[10]. While physical aggregation is mostly reversible, chemical aggregation is irreversible in most of the cases.

Aggregates can lead to B-cell activation and recruitment of T-cells [11]. This results in formation of antibodies and consequently product inactivation [11, 12]. Additionally, aggregates containing degraded epitopes can cause anaphylactic reactions [11]. In any case, the appearance of aggregates inhibits the release of the developed formulation to the market [10].

Bioavailability

Another important issue for every agent, but especially for biomacromolecular agents is to make it available at the desired target. The application of biomacromolecules can be performed via invasive (e.g. parenteral or subcutaneous injections, implants etc.) or non-invasive (e.g. oral, nasal, pulmonary, etc.) routes [2]. However, each route involves its own specific difficulties: the large size of the biomacromolecules leads to low transdermal availability and hampers crossing other anatomical barriers such as the blood brain barrier [1, 3]; oral availability is poor due to low absorption in the gastrointestinal tract [1, 13]; in addition, protein degradation by proteolytic enzymes in the gastrointestinal tract, the eye and the nasal mucosa hampers these ways of application [1]. So the right choice of the application route is very important for the success of the formulation.

A further challenge is the stability of proteins inside the body after application. Many proteins show a very short half-life of few minutes to maximal hours [14]. Glucagon for the treatment of hypoglycemia, for example, has a half-life of less than 10 min [14]. For antibodies longer residence times in the body were observed [14]; cetuximab has a half-life of 2.9 d, bevacizumab of 9.7 d (in cynomolgus monkeys) [14]. However, despite the longer half-life of antibodies periodic application is required to ensure the therapeutic benefit. Ranibizumab (anti-VEGF Fab) for the treatment of age-related macular degeneration, for example, needs to be injected intravitreous monthly [9]. However, intravitreous injections are associated with the risk of hemorrhages, retinal detachment, cataract or endophthalmy [9]. Furthermore, they can be painful and traumatic at the injection site [9].

1.1.2. Controlled Delivery – Chance and Challenge

As described above, the challenge is to make a protein available at the desired target site and to retain its structure during formulation and subsequent delivery in order to obtain the best therapeutic benefit.

One possibility to improve availability is the application of depot formulations directly to the site of action. Implants or in-situ gelling systems are very promising tools to increase the efficiency of protein drugs. The controlled release directly at the target tissue ensures the availability over a longer period of time, while the depot matrix protects the sensitive protein against degradation and denaturation.

Furthermore, the controlled delivery prevents dose-dependent side reactions. Protein therapeutics are generally considered as highly specific and well tolerable [15]. However, like for other drugs the side effects of proteins are dose-dependent [9]. For a safe application of proteins, formulations for controlled delivery are a good strategy to prevent dose-dependent side effects [9]. In addition, the sustained release improves patient compliance and reduces the risk of traumas and infections during application due to reduced application frequency. The delivery system should ideally be injectable and biodegradable [9].

However, especially for depot formulations, the compatibility of drug and the used matrices and solvents is important due to the long contact time of the components. Of course internal factors such as primary and secondary structure of the protein influence the tendency towards instabilities such as aggregation [10]. These factors depend on the protein drug itself and could not be tailored by the formulation. However, some of the described issues of protein therapeutics such as aggregation, instability and inactivity are associated with the formulation and formulation conditions. Incompatibility between protein and polymer, for example may result in stability problems during storage and release [1]. Especially in depot formulations, protein stability may be affected by the long time exposure to physiological temperature, the used polymer matrix and its degradation products [16]. Additionally, mechanical forces even via simple shaking can induce aggregation [7]. Due to increased air/water interfaces caused by shaking, the exposure of hydrophobic residues to the air is increased leading to higher risk towards aggregation [10]. Further important factors influencing the tendency towards aggregation are the temperature, the pH of the formulation, protein concentration, solvents and additives [7, 10]. The temperature during formulation preparation is an

important factor to maintain protein integrity. Higher temperatures increase the risk of aggregation [7, 10]. Above 40 °C the tendency towards the formation of so called fibrils is increased. Therefore, low temperatures are more appropriate also during storage [7]. In contrast to high-temperature, denaturation at low temperature is reversible in most of the cases [7].

Also the pH of a formulation is of great importance to retain protein stability and activity. Deamidation (hydrolysis of aspargine or glutamine), for example, is catalyzed by acidic as well as basic pH values [17]. Outside the optimal pH range proteins tend to aggregation and denaturation [18]. High charge density within the protein, caused by pH values different from the isoelectric point (pI) of the protein, lead to unfolding due to charge repulsion [18]. Furthermore, electrostatic interactions within the tertiary protein structure can be affected by changing charges [18]. On the other hand, the availability of both charges at pH values near to the pI may lead to protein assembling in form of aggregates [18]. Low pH values may lead to hydrolytic protein degradation and formation of aggregates [1]. Especially pH values below 3 or above 10 induce the formation of so called fibrils [7]. Degradation of PLGA for example lowers the pH of the microenvironment which may result in protein denaturation [1]. Zhu et al. described peptide hydrolysis and non-covalent aggregation of BSA encapsulated in PLGA implants [19]. Here, a pH < 3 during degradation of PLGA triggered the unfolding of BSA resulting in site effects [19]. In contrast, the addition of a strong base ($Ca(OH)_2$) resulted in covalent aggregation of BSA via disulfide bonds [19]. Due to the basic pH, the cysteine residues formed free thiolates which is a precondition for the formation of disulfides [19]. However, not only the pH itself, also the type and concentration of the used buffer influence the tendency towards aggregation [10]. On the other hand, the protein itself and its buffer capacity may influence the pH of the formulation. Van de Weert et al., for example, observed some buffering effect of BSA and lactalbumin in contrast to lysozyme [20]. The slightly lower pH of lysozyme and the catalyzing effect of the amine residues triggered faster degradation of the used polymer, resulting in accelerated protein release [20]. Furthermore, hydrophobic, organic solvents (e.g. methylene chloride, dimethyl sulfoxide etc.) induce the exposure of hydrophobic amino groups, normally buried inside the protein, leading to destroyed protein structure and increased tendency towards aggregation. For this reason, solvent-free formulation preparation in water should be preferred. The approved product Eligard™ is a depot formulation of the LHRH agonist leuprolide acetate in PLGA and N-methyl-2-

pyrrolidone [21]. After injection a gel-like precipitation of the polymer is formed by phase separation due to penetration of water in the organic N-methyl-2-pyrrolidone phase [21]. Eligard™ needs to be injected within 30 min after mixing to prevent protein denaturation caused by the organic solvent [21].

Similar stability problems may also be triggered by hydrophobic polymers such as PLGA itself [12]. Electrostatic and hydrophobic interactions of PLGA and incorporated proteins result in incomplete protein release [22]. Furthermore, reactions between the protein and the used polymer can result in loss of activity and undesired immune response. For example incorporation of proteins in PLGA microparticles can lead to amide bonds between primary protein amines and carboxyl groups of the degrading polymer [22]. Lucke et al. described the acylation of atrial natriuretic peptide and salmon calcitonin by lactic and glycolic acid units during the degradation of PLA and PLGA microspheres. The described protein acylation may result in loss of activity or changed receptor specificity [23]. With regard to the matrix, side reactions of the protein with functional groups of the used polymer should be kept in mind. The formation of disulfide bonds between thiol groups of the protein and thiol groups of the used polymer are one example for unwanted side reactions during cross-linking of hydrogels. The formation of disulfides can result in aggregates and should be prevented for thiol-functionalized polymers [24]. The tendency towards these reactions depends on the polymer and the protein. Qiu et al. for example did not observe any side reactions with BSA and EPO during cross-linking of the poly(ethylene glycol)(PEG)-based thiol-containing copolymer and a divinylsulfone-derivative [24]. In contrast, Hiemstra et al. reported side reactions of the amino or thiol groups of IgG, BSA, and lysozyme with the functional groups of tetrafunctional mercapto-PEG or dextran vinyl sulfone during cross-linking [25]. These side reactions resulted in denaturation, aggregation and subsequent precipitation of the proteins incorporated in the analyzed hydrogels [25].

In addition, protein modifications can impact the biological efficacy [7]. Protein modification with PEG (PEGylation) is a popular method to enhance the stability and half live of proteins [26]. However, PEGylation may also result in loss of activity depending on the number of attached polymer chains and the binding sites [26]. In the study of Maiser et al., lysozyme PEGylated at lysine 33 showed 35 % activity, while PEGylation at lysine residue 1 resulted in 24 % activity [26]. The number of attached PEG chains and the binding sites highly depends on the PEGylation conditions (e.g. pH, PEG excess, etc.) [26]. For that reason, batch-to-batch variations regarding the degree

and site of PEGyaltion and subsequently the activity of PEG-asparaginase (Oncospar® from Enzon) led to recalls in the past [26].

1.1.3. Conclusion

Compared to other drugs proteins have a complex and sensitive structure as described above. This requires a special careful handling to prevent degradation, to retain protein activity and to ensure drug availability at the target site. Consequently, the development of protein formulations is very challenging. Many factors such as instabilities, side effects, availability and loss of activity may hamper the successful realization. The most serious issue is the formation of aggregates, which finally stops market release of the formulation.

Depot formulations applied at the site of action are a promising strategy to overcome these issues. In-situ gelling hydrogels, for example, may improve bioavailability by application at the target site und protect the sensitive structure against degradation and denaturation. However, also the formulation itself and the formulation conditions may affect protein stability. Solvent free manufacturing, the use of compatible polymers, moderate temperatures and optimized pH values are important to maintain protein integrity and activity.

In the following chapters, suitable hydrogels as depot formulations for controlled protein delivery were developed and investigated. A special focus was set on the conservation of protein integrity and activity during hydrogel formulation and subsequent protein delivery. Additionally, the formation of side products between cross-linking agents and proteins was examined in order to prevent side effects and loss of efficacy.

1.2. Goals of the Thesis

The goal of the thesis was to develop hydrogels as depot formulations for the controlled delivery of protein drugs at the target site.

To investigate release profiles, protein compatibility and side reactions a commercial available model protein was used. Due to its well characterized structure and properties, lysozyme is ideally suited as model drug. A further advantage of lysozyme is the established and well known activity assay to verify integrity and lytic activity after protein release.

Due to its advantages in handling and application, poly(ethylene) glycol (PEG) was chosen as polymeric backbone of the developed formulations. PEG is an approved polymer for parenteral applications. Hydrogel preparation occurs without organic solvents in water preventing incompatibilities at the application site and with incorporated proteins. End-group functionalization can be performed with simple procedures under moderate conditions. PEGs of different chain length and branching are commercially available enabling the variation of mesh size and further hydrogel properties.

To match the goal of controlled delivery, two different strategies to tailor release kinetics were investigated. Firstly, release kinetics was regulated by reversible covalent attachment of the protein to the hydrogel backbone via hydrolytically cleavable linkers. Secondly, release was controlled by the interplay of protein size and hydrogel mesh size. For both cases, a special focus was set on protein integrity and activity after release.

To realize controlled release via cleavable linkers, the protein was tethered to the hydrogel backbone via carbamate linkers with different cleaving kinetics. For this purpose, lysozyme was first PEGylated with the linker. Statistically one arm of the four-armed PEG was modified with the linker group, while the remaining arms were functionalized with an alkyne group. Via copper-catalyzed click reactions of the alkyne group with azide functionalized four-armed PEG the protein was reversibly incorporated into the hydrogel during cross-linking.

In **Chapter 2**, the synthesis of the gel precursors and the used linkers is described in detail. Furthermore, **Chapter 2** reports on the influence of the protein and linker incorporation on the gel characteristics (gel stiffness, swelling and gelation time). In addition, the suitability of these click hydrogels as model systems to investigate protein release is discussed.

Carbamate linkers are hydrolytically cleavable making cleavage and subsequent protein release independent of special conditions of the surrounding tissues such as the presence of enzymes for example. Furthermore, cleavage occurs without the formation of toxic leaving groups or remaining ‘tags’ at the released protein indicating good tolerability of these formulations. The kinetics of linker hydrolysis and subsequent protein release can be controlled by the substitution pattern of the aromatic linker group. The influence of three different substitution patterns on cleaving kinetics was investigated in **Chapter 3**. For this purpose, firstly, PEGylation and De-PEGylation of protein amino groups was

analyzed by Sodium dodecyl sulfate (SDS) polyacrylamide gel electrophoresis (PAGE) using linear methoxy-PEG. A special focus was set on protein integrity and activity after PEGylation and PEG chain elimination. To this end, effects on protein secondary structure were determined by CD spectroscopy (circular dichroism spectroscopy) and an activity assay was performed. The influence of the different linkers on subsequent protein release was investigated using the non-degradable click-hydrogels described above.

SDS-PAGE is an excellent method to investigate PEGylation and follow PEG chain elimination. However, the experimental procedure is time consuming and requires toxic acrylamide for gel preparation. Furthermore, sample preparation including freezing in order to stop elimination and thawing before starting the experiments might negatively affect the protein samples. To overcome these drawbacks a non-toxic, automated real-time measurement was realized using a SEC (size exclusion chromatography) method to investigate PEGylation and PEG chain elimination (**Chapter 4**).

Another possibility to control protein release is by adjusting the hydrogel mesh size and its degradation. After cross-linking the protein is trapped in the hydrogel network due to its large hydrodynamic diameter. During hydrogel swelling and degradation the mesh size increases resulting in increasing protein mobility and subsequent controlled protein release. Using this strategy the incorporated drug should remain unaffected during cross-linking increasing the chance of protein integrity during formulation and subsequent release. Different delivery systems based on this mechanism have already been developed. Michael addition, Diels-Alder reactions or radical polymerization are common cross-linking reactions to prepare those hydrogels. A critical factor for successful application of such delivery systems is once more the compatibility with the incorporated protein. For that purpose, side reactions between frequently used cross-linking agents and lysozyme were analyzed using SDS-PAGE (**Chapter 5**).

A specially promising strategy is cross-linking via Dials-Alder reactions. Hydrogel preparation occurs without catalyst or initiator making the reaction excellently suitable for in-situ gelation at the target site. Furthermore, due to the retro-Diels-Alder reaction the hydrogels are biodegradable enabling degradation controlled release. The suitability of Diels-Alder hydrogels for controlled release was investigated in **Chapter 6**. Two further model proteins, α-CT (α-Chymotrypsin) and γ-globulin were used besides lysozyme to determine protein mobility inside the prepared hydrogels by FRAP

(fluorescence recovery after photobleaching) and to study release profiles. A special focus was again set on possible side reactions and protein activity.

Chapter 2

Synthesis and Characterization of Click Hydrogels

Abstract

Hydrolytically cleavable carbamte linkers were integrated in the hydrogel network using DCC/NHS chemistry of branched poly(ethylene glycol) (PEG) amine. Statistically one arm was modified with the linker group (**5a**, **5b**, **5c**) by choosing the adequate molar ratio. The other arms were functionalized with an alkyne group in a similar way for cross-linking with 4armPEG-azide. The incorporation of linker groups resulted in defects in the hydrogel network. The influence of the linker group and the resulting network defects on gel stiffness, hydrogel swelling, and gelation time was investigated in this chapter to evaluate the suitability of the used hydrogels as model systems to analyze protein release. The complex shear modulus was significantly lower compared to the reference gels (without linker groups, without lysozyme (Ctrl): 7908 ± 634 Pa / without linker, with lysozyme (w/o): 7923 ± 506 Pa) due to defects in the network structure caused by the linker groups (**5a**: 3564 ± 57 Pa / **5b**: 2897 ± 174 Pa / **5c**: 4325 ± 114 Pa). The extent of swelling increased to 152 ± 3.0 % (M_t/M_0) (**5b**) with decreasing cross-linking density due to the network defects. Gelation of all tested gels occurred after a few minutes (Ctrl.: 19.4 ± 0.5 min / w/o: 19.1 ± 0.1 min / 5a: 15.9 ± 0.4 min / 5b: 15.5 ± 0.4 min / 5c: 15.1 ± 0.1 min).

2.1. Introduction

Different ways to control the release of incorporated proteins have been reported since hydrogels were investigated as suitable carriers for protein delivery. The reversible covalent attachment of proteins to the hydrogel backbone is a promising strategy to control protein release. For this purpose, the protein is PEGylated by the linker in the first step (**Figure 2.1** Illus. 1). Afterwards, the linker with the attached protein is incorporated in the hydrogel network during cross-linking (Figure 2.1 Illus. 2). This allows controlling protein release by the cleavage kinetics of the used linker (Figure 2.1 Illus. 3). In order to achieve this goal, three poly(ethylene glycol) (PEG) based carbamte linkers with different rates of hydrolysis were developed.

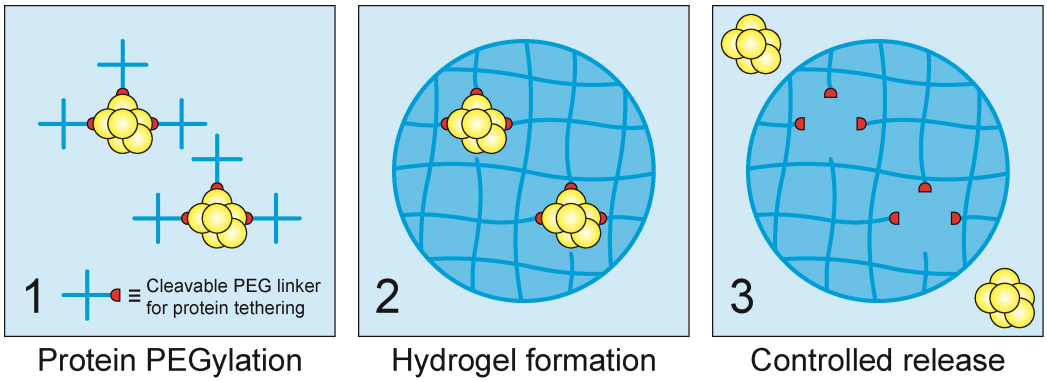

Figure 2.1: Reversible covalent protein attachment to the hydrogel network. Published as graphical abstract in Hammer, Nadine; Brandl, Ferdinand P.; Kirchhof, Susanne; Goepferich, Achim M, Cleavable carbamate linkers for controlled protein delivery from hydrogels, Journal of Controlled Release (2014) 183, S. 67–76.

To investigate the incorporation of linker groups and proteins in the hydrogel matrix, a model hydrogel was developed. For this model hydrogel, cross-linking via a copper-catalyzed click reaction was chosen. Copper-catalyzed click chemistry is highly specific, which is essential to prevent side reactions with incorporated proteins [27, 28]. Cross-linking occurs fast without the formation of side products, which is important for sample preparation of model hydrogels. The gelation time should be fast enough to allow timesaving sample preparation and slow enough for accurate handling. Furthermore, using PEG as backbone, these hydrogels are non-biodegradable, which allows studying protein release without the influence of hydrogel degradation.

Further hydrogel properties, such as swelling and hydrogel stiffness, play an important role for the suitability of a hydrogel as model system to study protein release. The hydrogel stiffness is closely associated with the cross-linking density [29], which has a

great impact on protein mobility within the hydrogel and consequently protein release [12]. Furthermore, the cross-linking density affects the swelling capacity, which influences the release kinetics due to the increased water content and enlarged pore size [30]. An ideal model system should show a similar degree of swelling for all samples, because increasing the degree of swelling, increases the diffusion coefficient resulting in enhanced protein mobility [31]. In addition, swelling lowers the mechanical strength of a hydrogel [32]. The mechanical stiffness is important for handling the gels during the experiments.

In this chapter, the synthesis of linkers and hydrogel precursors is described. Furthermore, this chapter focuses on the characterization of click hydrogel preparations containing cleavable carbamate linkers and its suitability as model systems. For this purpose, the influence of linkers on gelation time and gel stiffness of the hydrogels was determined by rheological measurements and the swelling behavior in the presence of linkers and attached protein was investigated. Protein PEGylation, cleaving kinetics of the linkers and the resulting protein release from hydrogels is discussed in detail in the next chapter (Chap. 3).

2.2. Materials and Methods

2.2.1. Materials

3-Hydroxybenzoic acid, 3-(4-hydroxyphenyl)propionic acid, phthalimide and toluene were purchased from Acros Organics (Geel, Belgium). Deuterated Chloroform ($CDCl_3$) was obtained from Deutero GmbH (Kastellaun, Germany). Dulbecco's phosphate-buffered saline (DPBS) was purchased from Invitrogen GmbH (Karlsruhe, Germany). Four-armed poly(ethylene glycol) (molecular weight 10 kDa, 4armPEG10k-OH) was purchased from JenKem Technology (Allen, TX, USA). Acetonitril, *N*,*N'*-dicyclohexylcarbodiimide (DCC), *N*-hydroxysuccinimide (NHS), diisopropyl azodicarboxylate (DIAD), *N*,*N'*-discuccinimidyl carbonate (DSC), fluorescamine, 4-hydroxybenzoic acid, lysozyme (from chicken egg white), magnesium sulfate, sodium tetraborate decahydrate, 4-pentynoic acid, and tetrahydrofuran were obtained from Sigma-Aldrich (Taufkirchen, Germany). Acetone, methylene chloride (DCM), diethyl ether and ethanol were purchased from CSC Jäcklechemie (Nürnberg, Germany). All other chemicals were from Merck KGaA (Darmstadt, Germany). Deionized water was

prepared freshly every day using a Milli-Q water purification system from Millipore (Schwalbach, Germany).

2.2.2. ^{1}H-NMR Measurement

^{1}H-NMR measurements were performed on a Bruker Avance 300 spectrometer (Bruker BioSpin GmbH, Rheinstetten, Germany). All spectra were recorded in $CDCl_3$ at room temperature. The polymer concentration was about 30 mg/mL.

2.2.3. Fluram Assay

For the determination of free amino groups, a fluorescamine stock solution (0.3 mg/mL) was prepared in acetone [33]. The sample (0.2 µmol/mL) was dissolved in 50 mM borate buffer pH 8.5 and mixed with 1300 µL of borate buffer and 100 µL of the fluorescamine stock solution. The fluorescence intensity (λ_{ex} = 390 nm, λ_{em} = 480 nm) was measured on a PerkinElmer LS 55 Fluorescence spectrometer (Perkin-Elmer, Wiesbaden, Germany). The number of free amino groups was calculated using a calibration curve prepared with 4armPEG10k-amine (compound **3**).

2.2.4. Synthesis of Compound 3 (4armPEG10k-NH_2)

4armPEG10k-NH_2 was synthesized according to a protocol published by Brandl et al. [34]. In brief, 12.5 g of 4armPEG10k-OH, 0.88 g of phthalimide (0.006 mmol) and 1.57 g of triphenylphosphine (PPh_3) (0.006 mmol) were dissolved in tetrahydrofuran. Then, 0.006 mmol of DIAD in 15 mL of Tetrahydrofuran were added dropwise. The mixture was stirred for 72 h at room temperature. Afterwards, the solvent was evaporated under reduced pressure. The residue was dissolved in 100 mL of water, filtered, and washed twice with 100 mL of diethylether. After evaporation of water, the raw product was dissolved in 25 mL of DCM and crystallized at 0 °C under addition of 250 mL of diethylether. 4armPEG10k-phthalimide was collected by filtration and dried under vaccum to yield 10.7 g (81.8 %).

^{1}H-NMR ($CDCl_3$, 300 MHz): δ 3.66 ppm (s, -OC*H*$_2$C*H*$_2$-), 7.74 ppm (d, 8H, Ar-*H*), 7.84 ppm (d, 8H, Ar-*H*).

Then, 10.7 g of 4armPEG10k-phthalimide were dissolved in 100 mL of ethanol. After addition of 1061 µL of hydrazine hydrate, the mixture was refluxed for 5 h at 85 °C. The reaction mixture was cooled to room temperature and the formed precipitate was filtered off. After adjusting the pH to 2 - 3, the solvent was evaporated. The residue was

dissolved in 50 mL of water and the pH was adjusted to 9 - 10. The raw product was extracted four times with DCM and the combined organic phases were dried over anhydrous $MgSO_4$. The solvent was evaporated and the residue was taken up in 20 mL of DCM. The product was crystallized at 0 °C by addition of diethylether. The precipitate was dried under vacuum to yield 9.7 g (95.6 %).

^{1}H-NMR ($CDCl_3$, 300 MHz): δ 2.93 ppm (t, 8H, –C*H*$_2$NH$_2$), 3.66 ppm (s, –OC*H*$_2$-C*H*$_2$–).

2.2.5. Synthesis of Compound 4 (4armPEG10k-pentyne)

4armPEG10k-pent-4-yne-amide was synthesized as already published [35]. In brief, 0.24 g of 4-pentynoic acid (2.4 mmol), 0.28 g of NHS (2.4 mmol) and 0.50 g of DCC (2.4 mmol) were dissolved in 10 mL of 1,4-dioxane und stirred at room temperature for 6 h. Afterwards, the precipitated dicyclohexylurea was filtered off and the filtrate was combined with a mixture of 4armPEG10k-NH_2 (0.3 mmol) and $NaHCO_3$ (2.4 mmol) in water. After stirring overnight at 50 °C, the solvent was evaporated under reduced pressure. The residue was taken up in water and the raw product was extracted four times with DCM. The organic phases were combined and dried over anhydrous $MgSO_4$. The solution was concentrated and the product was crystallized by dropwise addition of diethylether at 0 °C. 4armPEG10k-pentyne was dried under vacuum to yield 2.8 g (90 %).

^{1}H-NMR ($CDCl_3$, 300 MHz): δ 2.05 ppm (t, 4 H, *H*C≡C–), 2.44 ppm (t, 8 H, –C(O)-*CH*$_2$CH$_2$–), 2.55 ppm (t, 8 H, –C(O)CH$_2$*CH*$_2$–), 3.66 ppm (s, –O*CH*$_2$*CH*$_2$–).

2.2.6. Synthesis of Compound 5a

5a was synthesized as previously published [35]. In brief, 0.03 g of 4-hydroxybenzoic acid (0.2 mmol), 0.02 g of NHS (0.2 mmol), and 0.04 g of DCC (0.2 mmol) were dissolved in 7 mL of 1,4-dioxane. After stirring at room temperature for 6 h, the precipitated dicyclohexylurea was filtered off. The filtrate was combined with 2.0 g of 4armPEG10k-NH_2 (0.2 mmol) and 0.02 g of $NaHCO_3$ (0.22 mmol) in 7 mL of water. The mixture was stirred overnight at 50 °C. The solvent was evaporated and the residue was taken up in 20 mL of water the next day. The raw product was extracted four times with DCM. The organic phases were combined and dried over anhydrous $MgSO_4$. The solvent was evaporated to a volume of 5 mL and the product was crystallized at 0 °C by

dropwise addition of diethylether. The reaction intermediate of **5a** was dried under vacuum to yield 1.81 g (90 %).

^{1}H-NMR ($CDCl_3$, 300 MHz): δ 2.97 ppm (t, 6 H, –*CH$_2$*-NH_2), 3.66 ppm (s, –O*CH$_2$*-*CH$_2$*–), 6.91 ppm (d, 2 H, –C_6H_4OH), 7.73 ppm (d, 2 H, –C_6H_4OH).

The degree of end-group conversion was 30 % as calculated from the number of free amino groups. In a second step, the remaining amino groups were functionalized with 4 pentynoic acid as described above to yield 1.62 g (77 %).

^{1}H-NMR ($CDCl_3$, 300 MHz): δ 2.04 ppm (t, 3 H, *HC*≡C–), 2.44 ppm (t, 6 H, –C(O)-*CH$_2$*CH_2–), 2.55 ppm (t, 6 H, –C(O)CH_2*CH$_2$*–), 3.66 ppm (s, –O*CH$_2$CH$_2$*–), 6.93 ppm (d, 2 H, –C_6H_4OH), 7.75 ppm (d, 2 H, –C_6H_4OH).

The degree of end-group conversion was almost 100 %. In the last step, the phenolic hydroxyl group was activated. To this end, 1.6 g of the intermediate (0.15 mmol) and 0.2 g of DSC (0.75 mmol) were dissolved in anhydrous acetonitrile. Then, 96 µL of pyridine (1.2 mmol) were added and the mixture was stirred at room temperature overnight. The next day, the solvent was evaporated and the residue was taken up in DCM. The raw product was filtrated and concentrated to 5 mL. Compound **5a** was crystallized at 0 °C by addition of diethylether and dried under vacuum to yield 1.38 g (92 %).

^{1}H-NMR ($CDCl_3$, 300 MHz): δ 2.05 ppm (t, 3 H, HC≡C–), 2.44 ppm (t, 6 H, –C(O)-*CH$_2$*CH_2–), 2.55 ppm (t, 6 H, –C(O)CH_2*CH$_2$*–), 2.91 ppm (s, 4 H, –C(O)*CH$_2$CH$_2$*C(O)-), 3.66 ppm (s, –O*CH$_2$CH$_2$*–), 6.92 ppm (d, 2 H, –C_6H_4OSu), 7.75 ppm (d, 2 H, –C_6H_4-OSu).

2.2.7. Synthesis of Compound 5b

5b was synthesized in the same way as described for **5a** using 3-hydroxybenzoic acid as phenolic compound. The first intermediate was synthesized in 90 % yield (1.81 g).

^{1}H-NMR ($CDCl_3$, 300 MHz): δ 2.97 ppm (t, 6 H, –*CH$_2$*-NH_2), 3.66 ppm (s, –O*CH$_2$*-*CH$_2$*–), 7.00 ppm (d, 1 H, –C_6H_4OH), 7.27 ppm (d, 1 H, –C_6H_4OH), 7.37 ppm (d, 1 H, –C_6H_4OH).

The degree of end-group conversion was 32 %, as calculated from the number of free amino groups. In a second step, the remaining amino groups were modified as described for **5a.** The yield was 1.52 g (72 %).

^{1}H-NMR ($CDCl_3$, 300MHz): δ 2.05 ppm (t, 3 H, *HC*≡C–), 2.44 ppm (t, 6 H, –C(O)*CH_2*-CH_2–), 2.55 ppm (t, 6 H, –C(O)CH_2*CH_2*–), 3.66 ppm (s, –O*CH_2CH_2*–), 7.00 ppm (d, 1 H, –C_6H_4OH), 7.31 ppm (d, 1 H, –C_6H_4OH), 7.39 ppm (d, 1 H, –C_6H_4OH).

The end-group conversion was almost quantitative as determined by a fluram assay. The intermediate was activated by DSC in 86 % yield (1,29 g) as described above.

^{1}H-NMR ($CDCl_3$, 300 MHz): δ 2.05 ppm (t, 3 H, HC≡C–), 2.44 ppm (t, 6 H, –C(O)-*CH_2*CH_2–), 2.55 ppm (t, 6 H, –C(O)CH_2*CH_2*–), 2.91 ppm (s, 4 H, –C(O)*CH_2CH_2*-C(O)–), 3.66 ppm (m, –O*CH_2CH_2*–), 7.38 ppm (d, 1 H, –C_6H_4OSu), 7.52 ppm (d, 1 H, –C_6H_4OSu), 7.79 ppm (d, 1 H, –C_6H_4OSu).

2.2.8. Synthesis of Compound 5c

5c was synthesized according to previously published protocols [35]. In brief, 0.12 g of 4-pentynoic acid (1.2 mmol), 0.06 g of 3-(4-hydroxyphenyl)propionic acid (0.4 mmol), 0.15 g of NHS (1.6 mmol) and 0.33 g of DCC (1.6 mmol) were dissolved in 7 mL of 1,4-dioxane. After stirring for 6 h at room temperature, the precipitated dicyclohexylurea was filtered off. The filtrate was combined with 2 g of 4armPEG10-NH_2 (0.2 mmol) and 0.13 g of $NaHCO_3$ dissolved in 7 mL water. The mixture was stirred overnight at 50 °C. Then, the solvent was evaporated and the residue was dissolved in water. After extraction with DCM (4x), the combined organic phases were dried over anhydrous $MgSO_4$. The raw product was concentrated to 5 mL and crystallized at 0 °C by dropwise addition of diethylether. The intermediate was dried under vaccum to yield 1.52 g (73 %).

^{1}H-NMR ($CDCl_3$, 300 MHz): δ 2.05 ppm (t, 3 H, *HC*≡C–), 2.43 ppm (t, 2 H, C(O)*CH_2*CH_2–), 2.46 ppm (t, 6 H, –C(O)*CH_2*CH_2–), 2.55 ppm (t, 6 H, –C(O)CH_2-*CH_2*–), 2.89 ppm (t, 2 H, –C(O)CH_2*CH_2*–), 3.66 ppm (s, –O*CH_2CH_2*–), 6.79 ppm (d, 2 H, –C_6H_4OH), 7.06 ppm (d, 2 H, –C_6H_4OH).

The degree of end-group conversion was 98 %, as determined by a fluram assay. The intermediate was activated using DSC to yield 1.13 g (77 %) as described above.

^{1}H-NMR ($CDCl_3$, 300 MHz): δ 2.05 ppm (t, 3 H, HC≡C–), 2.44 ppm (t, 6 H, –C(O)-*CH_2*CH_2–), 2.55 ppm (t, 6 H, –C(O)CH_2*CH_2*–), 2.86 ppm (s, 4 H, –C(O)*CH_2CH_2*-C(O)–), 2.89 ppm (t, 2 H, –C(O)CH_2*CH_2*–), 3.66 ppm (s, –O*CH_2CH_2*–), 6.79 ppm (d, 2 H, –C_6H_4-OH), 7.06 ppm (d, 2 H, –C_6H_4OH).

2.2.9. Synthesis of Compound 6 (4armPEG10k-azide)

Imidazole-1-sulfonyl azide hydrochloride was synthesized according to a method described by Goddard-Borger et al. [36]. As already published, 3.0 g of 4armPEG10k-NH_2 (0.3 mmol), 292 µL of triethylamine and 3.0 mg of copper(II) sulfate were dissolved in 10 mL of methanol [35]. 0.3 g of imidazole-1-sulfonyl azide (1.44 mmol) was added and the mixture was stirred overnight at room temperature. Then, the mixture was concentrated under reduced pressure and diluted with water. Afterwards the mixture was acidified with HCl. The raw product was extracted four times with DCM and the combined organic phases were dried over anhydrous $MgSO_4$. The raw product was concentrated to 10 mL and crystallized at 0 °C by addition of diethylether. The product was dried under vacuum to yield 2.85 g (95 %).

^{1}H-NMR ($CDCl_3$, 300 MHz): δ 3.66 ppm (s, –O*CH$_2$CH$_2$*–).

2.2.10. Preparation of Hydrogels

Hydrogels with a total polymer content of 5 % were prepared as previously described [35]. For the control group (Ctrl) equal amounts of four-armed PEG functionalized with alkyne (compound 4 / 4armPEG10k-pentyne) and azido (compound 6 / 4armPEG10k-azide) groups were dissolved in 25 mM phosphate buffer pH 7.4. In all other cases, a lysozyme stock solution (1.33 mg/mL) was prepared in 25 mM phosphate buffer pH 7.4. For the group without linker (w/o) equal amounts of 4armPEG10k-pentyne (**4**) and 4armPEG10k-azide (**6**) were dissolved in the lysozyme stock solution. For the samples containing linkers, lysozyme was first PEGylated. For this purpose, the linkers **5a**, **5b** or **5c** were incubated with the lysozyme stock solution for 1 h (**5a** and **5b**) or 2 h (**5c**), respectively; the ratio of activated linker groups (SC) to protein amino groups (NH_2) was 14 : 7. After PEGylation, the required amounts of 4armPEG10k-pentyne (**4**) and 4armPEG10k-azide (**6**) were added to achieve a nearly balanced ratio of alkyne to azido groups. Cross-linking was induced by the addition of 0.5 µmol/mL of $CuSO_4$ and 2.5 µmol/mL of ascorbic acid in all cases.

2.2.11. Rheological Characterization

The rheological characterization was performed on a TA Instruments AR 2000 rheometer (TA Instruments, Eschborn, Germany). A parallel plate geometry with 40 mm diameter was used for all experiments.

Hydrogel precursors were prepared as described above (see Chap. 2.2.10). Directly after the addition of $CuSO_4$ and ascorbic acid, 750 µL of the hydrogel precursor were poured on the bottom plate of the rheometer. The upper plate was lowered to a gap size of 500 µm and the measurement was started. Storage modulus (G′) and loss modulus (G″) were recorded as a function of time at 25 °C for 2 h. An oscillatory shear stress with a constant frequency of 1 Hz was applied. A solvent trap was used to minimize water evaporation during the measurement. The cross-over point of loss and storage modulus was regarded as the gel point. The absolute value of the complex shear modulus (|G*|) served as a measure for the gel stiffness. All experiments were done in triplicate. The results are presented as mean ± standard deviation.

2.2.12. Swelling Studies

For swelling studies, 750 µL of each hydrogel precursor (see Chap. 2.2.10) were cast into glass cylinders (10 mm diameter) and allowed to gel for 2 h at room temperature. Afterwards, each gel cylinder was incubated in 10 mL PBS at 37 °C. The gels were weighed before incubation (M_0) and every 24 h (M_t) during swelling. The swelling ratio was calculated using the following equation:

$$\text{Swelling ratio (\%)} = \frac{M_t}{M_0} \text{ x } 100\ \% \qquad (1)$$

The swelling studies were done in triplicate and results are shown as mean ± standard deviations.

2.2.13. Statistical Analysis

The results of the rheological characterization were analyzed ($p < 0.05$) using one-way ANOVA followed by Tukey´s post-hoc test. The testing was performed using GraphPad Prism (Version 5.01, GraphPad Software Inc., La Jolla, CA).

2.3. Results and Discussion

2.3.1. Synthesis

The idea behind this project was the reversible covalent attachment of proteins to the hydrogel backbone in order to control protein release. The reversibility was ensured by using aromatic succinimidyl carbonates (**Table 2.1**) forming hydrolytically cleavable carbamates with protein amino groups.

Table 2.1: Chemical structures of 4armPEG10k-pentyne (compound 4), 4-armPEG10k-linkers (compound 5a, 5b, 5c), and 4armPEG10k-azide (compound 6). The hydrolytically cleavage of the linkers is discussed in the next chapter (Chapter 3).

Compound	Structure
4 / 5	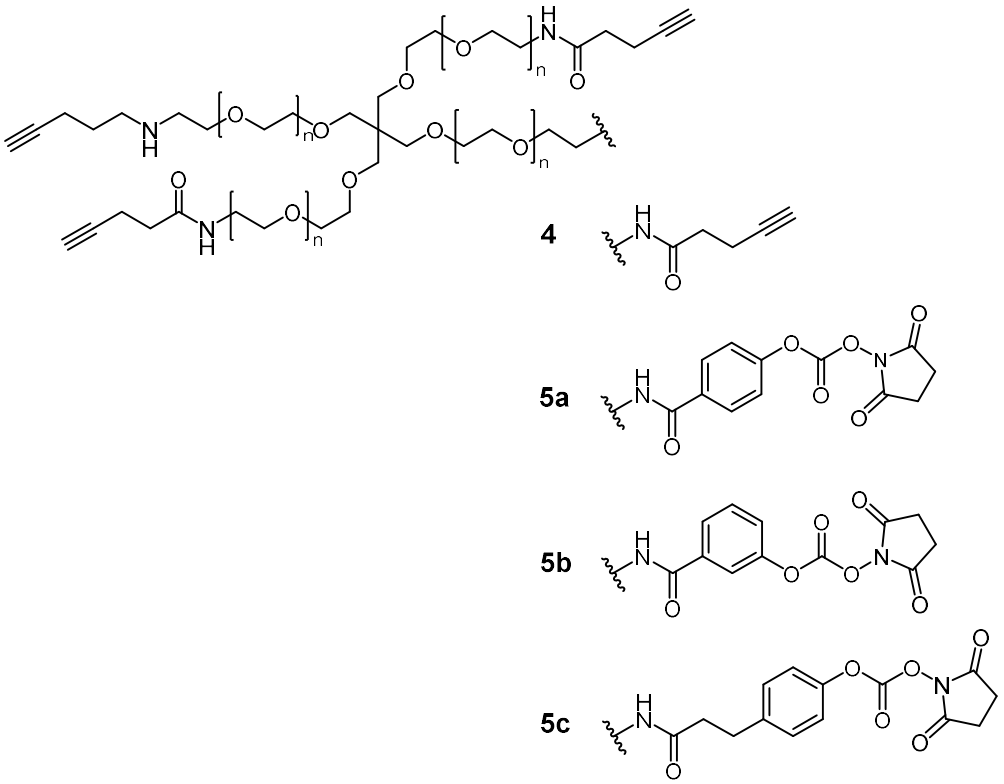
6	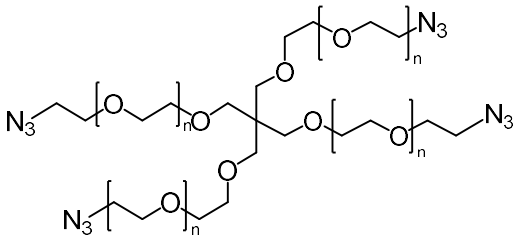

First of all, it was important to integrate the linker into the hydrogel network. This was achieved by using branched PEG with different end-group functionalization. For cross-linking via copper-catalyzed click reaction, four-armed PEG was modified with alkyne or azide groups, respectively (Table 2.1).

The incorporation of the linker into the hydrogel network was realized using four-armed PEG with two different types of functionalization. One arm of these molecules was

modified with the cleavable linker group (**5a – 5c**); the remaining arms were alkyne-functionalized to allow cross-linking with the azide groups.

In the first step, the hydroxyl end groups of four-armed PEG were converted into amine groups in order to prepare the polymer for end-group functionalization. This was achieved using a Mitsunobu reaction and subsequent hydrazinolysis (**Figure 2.2**).

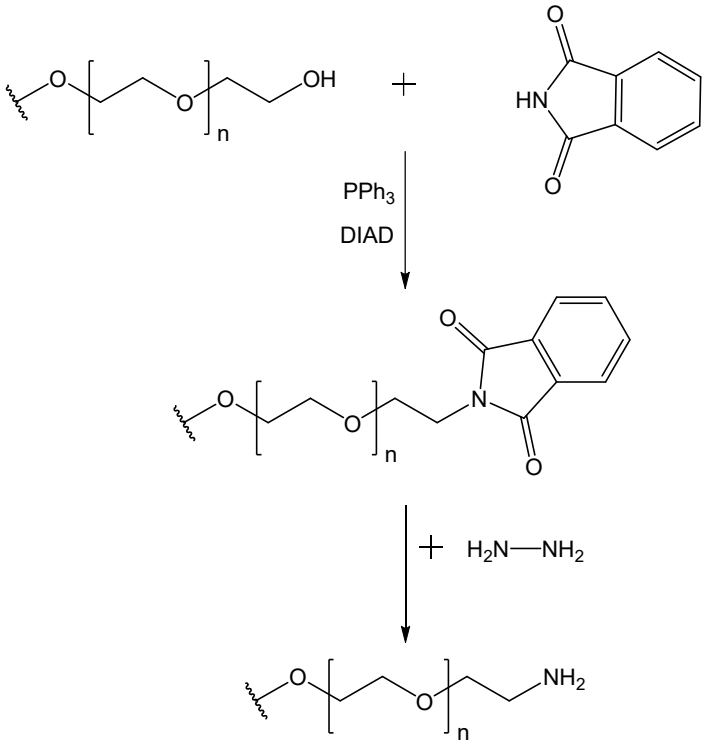

Figure 2.2: Synthesis of compound 3 (4armPEG10k-amine).

The hydrogel precursors and linkers were synthesized starting from the amine. The functionalization with the alkyne group (**Figure 2.3**) and the linker groups (**Figure 2.4**) were obtained in a similar way using DCC/NHS chemistry.

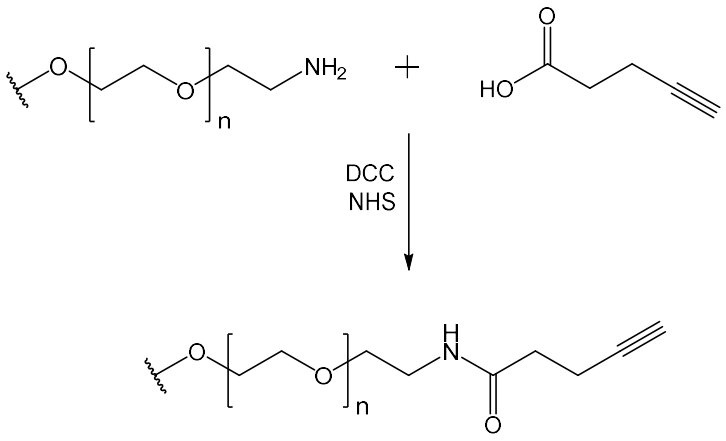

Figure 2.3: Synthesis of compound 4 (4armPEG10k-pentyne).

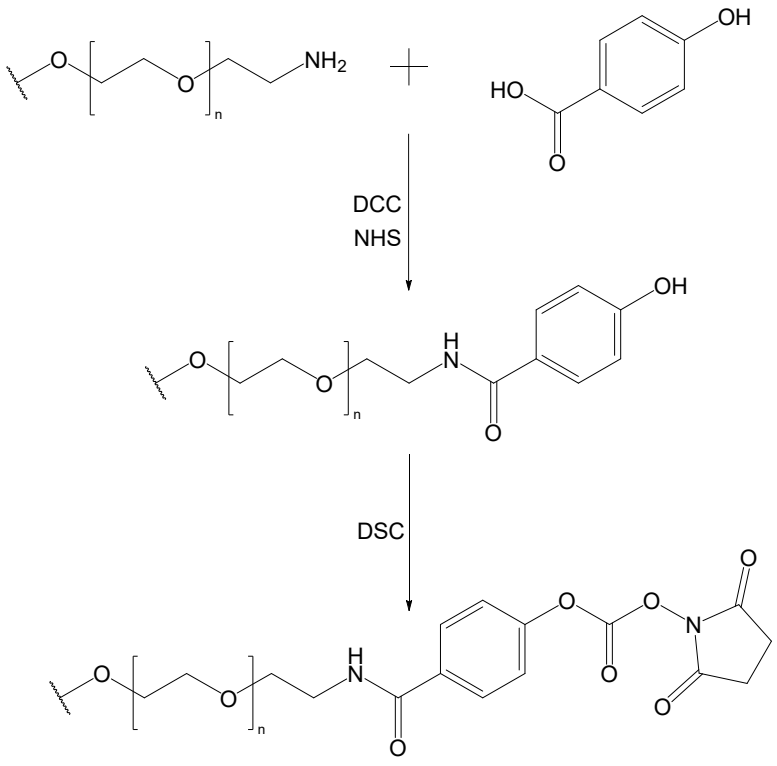

Figure 2.4: Synthesis and activation of the linkers. The synthesis of 5a is shown exemplarily for all linkers.

Using the same reaction mechanism for both modifications allowed for the synthesis of **5c** in one step. Due to the different reactivity of the carboxylic acids, the synthesis of **5a** and **5b** occurred in two steps. First, statistically one arm was modified with the linker group. Using the molar ratios described above, it was possible to modify statically one arm of each linker molecule as verified by 1H-NMR spectroscopy and fluram assay.

This allowed a simple synthesis without additional protection or de-protection reactions. Afterwards, the remaining arms were modified with alkyne groups according to Figure 2.3. The last step in the synthesis of all linkers was the activation using DSC. The resulting succinimidyl functionalization served for protein PEGylation via carbamte formation with protein amine groups. Protein PEGylation and de-PEGylation is discussed in detail in the next chapter (Chapter 3).

For the synthesis of 4armPEG-azide (**6**), the four arms were functionalized using a diazotransfer reaction (**Figure 2.5**).

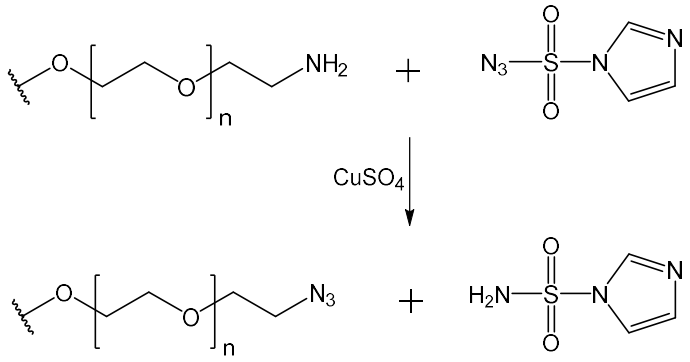

Figure 2.5: Synthesis of compound 6 (4armPEG10k-azide).

The synthesized azide was used to form 1,2,3-triazoles with the alkyne group in a copper-catalyzed click reaction during cross-linking.

2.3.2. Rheological Characterization

To determine the influence of linker incorporation on gel stiffness and gelation time, the different hydrogels with and without linker were analyzed by rheological measurements. In **Figure 2.6**, the rheogram of a reference gel without linker is shown exemplarily. At the beginning of the measurement, cross-linking had not yet occurred and the mixture behaved like a viscous liquid ($G'' > G'$) [37]. With proceeding cross-linking, the stiffness of the mixture increased and the mixture behaved more like an elastic solid ($G' > G''$) [37]. The cross-over point of loss (G'') and storage modulus (G') was defined as gelation time. The absolute value of the complex shear modulus $|G^*|$ ($G^* = G' + i \cdot G''$) is a measure of the stiffness of the hydrogel and was used to compare the stiffness of the different formulations [38].

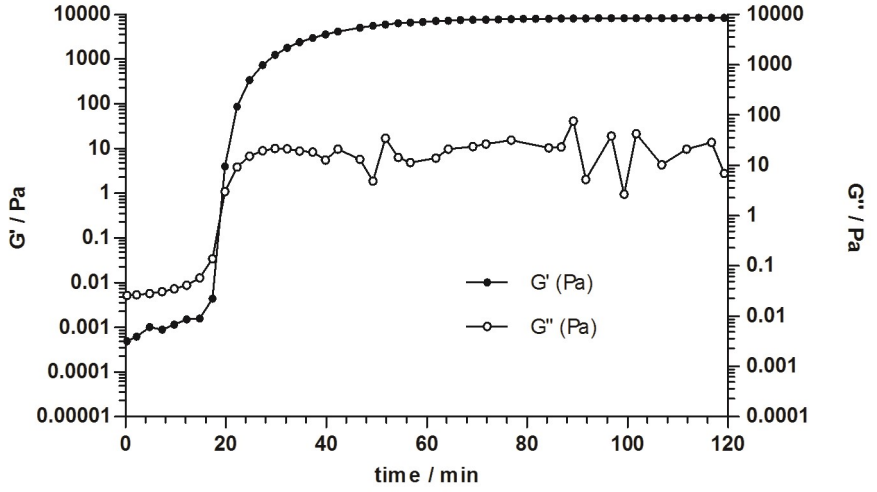

Figure 2.6: Rheogram of a reference gel without linker. The storage modulus G′ is represented by closed circles, the loss modulus G″ is represented by open circles. The measurement was carried out at 25 °C and 1.0 Hz oscillatory frequency with a 40 mm steel plate with 500 µm gap size.

In **Table 2.2** the gelation times and maximal complex shear moduli of all analyzed hydrogel formulations are presented. Gelation occurred between 15.1 ± 0.1 min and 19.4 ± 0.5 min. The Cu(I)-catalyzed cycloaddition of the azide and alkyne functionalities, which was used for cross-linking, is known for its rapid reaction kinetics [39]. In **Figure 2.7** the results are visualized and statistical significant differences are shown. The gelation times of the reference gels without lysozyme (Ctrl) and with lysozyme but without linker (w/o) were nearly the same. This indicates that incorporation of the model protein did not affect the gelation time. The gelation times of the samples with incorporated linker groups were significantly lower. The reason for that behavior is not clear. It can be speculated that cross-linking is completed faster, due to the excess of azide groups. In the hydrogels containing linker groups, about one quarter of the alkyne groups are replaced by a linker group, which is not involved in cross-linking. This results in a lower amount of reactive alkyne groups and consequently an excess of azide groups.

However, no differences in gelation time were detected between the different linker groups. So, the chemical structure of the linker seemed not to affect the gelation time. The gelation times of all analyzed samples matched the requirements of a model hydrogel. The gelation occurred fast enough for timesaving preparation, but still provided enough time for accurate handling. A possible way to tailor the gelation time

would be the variation of the amount of copper-catalyst, which also influences the gelation time of click hydrogels [40].

The maximal detected absolute value of the complex shear modulus ranged between 2897 ± 174 Pa and 7923 ± 506 Pa indicating high stiffness of all samples (Table 2.2). Click reactions are highly efficient and lead to almost quantitative conversion [27, 41]. This results in high homogeneity and low amount of network defects, which is reflected in the strong mechanical properties [42]. These are ideal properties for a model system with regard to sample handling and minimizing interfering effects on drug release studies.

Table 2.2: Characterization of the prepared hydrogels with 5 % total polymer concentration.

Group	Gelation time (min)	$\|G^*\|$ (Pa)
Ctrl.	19.4 ± 0.5	7908 ± 634
w/o	19.1 ± 0.1	7923 ± 506
Linker **5a**	15.9 ± 0.4	3564 ± 57
Linker **5b**	15.5 ± 0.4	2897 ± 174
Linker **5c**	15.1 ± 0.1	4325 ± 114

For the different complex shear moduli, similar results were observed as for the detected gelation times (Figure 2.7). No significant differences existed between the reference gels with or without lysozyme. However, the incorporation of linker groups resulted in significant lower stiffness. The gel stiffness of hydrogels after incorporation of **5c** was significantly higher than after incorporation of **5b**. Between **5a** and **5b**, no significant differences were detected. The stiffness of a hydrogel depends on the cross-linking density [43]. Decreasing the cross-linking density results in decreased mechanical strength [43]. By incorporating the linker into the hydrogel, additional network defects are introduced at each polymer-arm functionalized with the linker group instead of an alkyne group. These defects decrease the cross-linking density of the hydrogel, which is reflected by the lower complex shear modulus. Due to less functional groups and steric hindrance of the incorporated bulky protein, network defects will appear in every model system when working with linker groups and covalent protein attachment. So, this small

drawback of little differences in cross-linking density between the samples was accepted for the investigation of protein release kinetics.

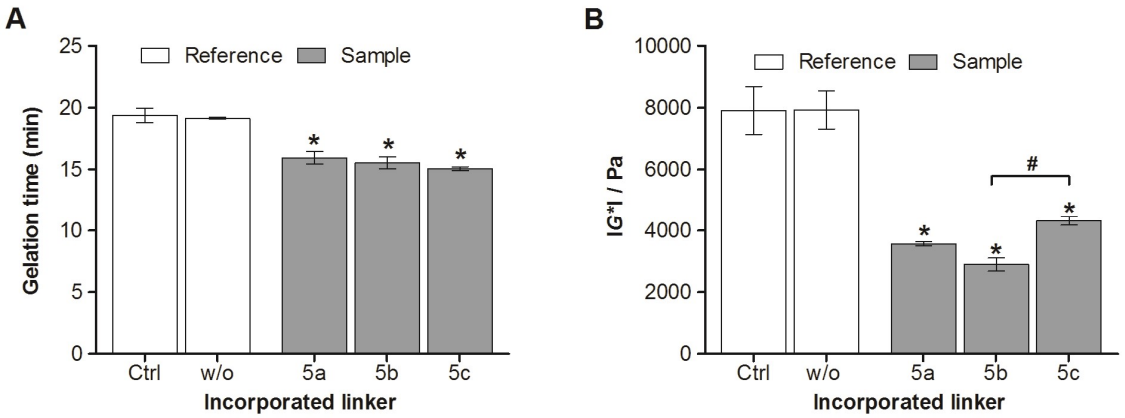

Figure 2.7: Rheological characterization of click hydrogels with regard to gelation time (A) and absolute value of the complex shear modulus |G*| (B). Samples with lysozyme incorporated via linker 5a, 5b, or 5c are shown in comparison to reference hydrogels without lysozyme (Ctrl) and hydrogels with lysozyme but without linker (w/o). The measurements were performed in triplicate and the results are shown as means ± standard deviations. * indicates statistical significance ($p < 0.05$) versus the reference groups. # indicates statistical significant differences between two groups.

The reported changes regarding gelation time and gel stiffness after incorporation of linker molecules should also be kept in mind, when developing hydrogels for clinical applications. Especially for in-situ gelling systems, the gelation time is of great importance. During injection, the gel precursor should preferably show low viscosity to ensure simple application. After injection a fast gelation is required to prevent diffusion of the drug and the gel precursors into the surrounding tissue [44]. The gel strength should be similar to the strength of the tissue at the application site [12].

2.3.3. Hydrogel Swelling

The swelling behavior of the reference hydrogels and the hydrogels with incorporated linkers was determined (**Figure 2.8**). The swelling of the reference hydrogels without linker and with (w/o) or without (Crtl.) model protein was completed after 24 h. The reference hydrogels showed only little mass increase not exceeding 108 % during swelling experiments. This low extent of mass increase can be explained by the high cross-linking density due to almost complete conversion of the used click chemistry [27, 31, 45].

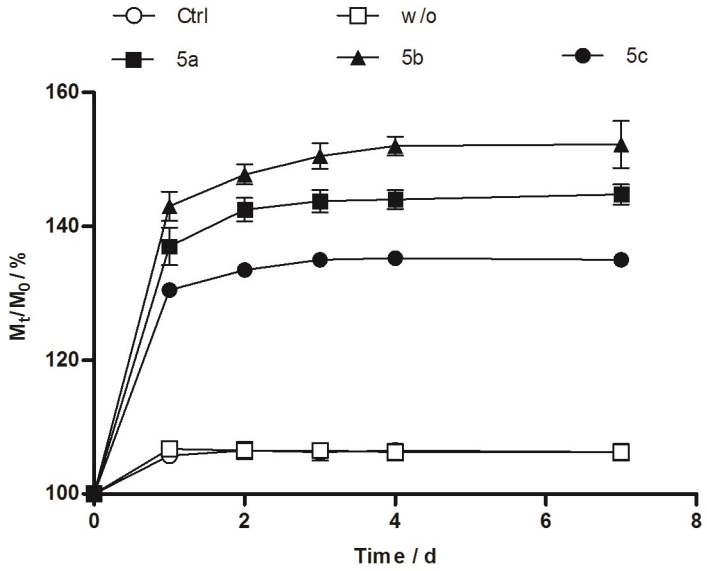

Figure 2.8: Swelling of the prepared hydrogels. Comparison of control group without protein (open circle), hydrogels without linker (open square) and hydrogels containing lysozyme PEGylated by 5a (closed square), 5b (closed triangle) or 5c (closed circle). The experiment was carried out in PBS at 37 °C.

The mass of hydrogels with incorporated linker molecules increased rapidly over 24 h. After about 4 d the mass increase was completed. Swelling behavior of these hydrogels was in line with the complex shear modulus; with decreasing cross-linking density due to the incorporated linker groups, the extent of swelling increased to 135 ± 1 % (**5c**), 145 ± 2 % (**5a**), and 152 ± 3.0 % (**5b**) [43].

However, the degree of swelling of the analyzed hydrogels containing linker groups was still low compared to other hydrogel systems such as Diels-Alder hydrogels for example [46]. This makes these hydrogels excellently suitable to determine protein release. Excluding the influence of swelling, the influence of the cleavage kinetics of the linker on protein release can be analyzed.

The optimal swelling behavior with regard to medical applications depends on the type of application. For hydrogels used as wound dressings, high water absorption may be desired in order to take up the exudate [47]. On the other hand, strong swelling at application sites with sensitive tissue and limited expansibility, such as cartilage trauma sites for example, may damage the surrounding tissue or aggravate the situation [48].

2.4. Conclusion

A simple synthesis allowed the functionalization of one of the cross-linking agents with linker groups for reversible protein attachment. By choosing the adequate molar ratio of the raw materials, the modification of one arm could be realized. This enabled the integration of the linker groups into the hydrogel backbone during cross-linking. The integration of the linker group affected the gelation time, gel stiffness und hydrogel swelling. About the reasons for the lower gelation times after incorporation of linker groups could just be speculated. The significant lower gel stiffness compared to the reference gels resulted from the induced defects in the hydrogel network after incorporation of the linker group. The results of the swelling studies were in good agreement with the rheological characterization. Due to the network defects caused by the incorporation of linker groups, the extent of hydrogel swelling increased. However, using click chemistry, the resulting hydrogels still showed fast gelation, high gel stiffness and low swelling even after incorporation of linker groups. In conclusion, these hydrogels are ideally suitable as model hydrogels to study protein release based on linker cleavage without the influence of swelling or degradation.

Chapter 3

Cleavable Carbamate Linkers for Controlled Protein Delivery from Hydrogels

The content of this chapter has been published in: Nadine Hammer, Ferdinand P. Brandl, Susanne Kirchhof, Achim M. Goepferich. Cleavable carbamate linkers for controlled protein delivery from hydrogels. *Journal of Controlled Release*, 183: 67–76, 2014. doi: 10.1016/j.jconrel.2014.03.031

Author contributions: F.P.B., A.M.G., and N.H. conceived the idea and designed the experiments; N.H. conducted the experiments; F.P.B., A.M.G., N.H., and S.K. interpreted and discussed the data and wrote the manuscript.

Acknowledgements: The authors thank Dr. Helmut Durchschlag and Klaus-Jürgen Tiefenbach for their help with the CD spectroscopy, and Viktoria Messmann, Veronika Scheidler and Theresa Ferstl for their assistance in conducting the experiments. The financial support from the German Research Foundation (DFG), grant number GO 565/16-1 is gratefully acknowledged. The authors thank the sponsorship of the Alexander von Humboldt Foundation and the Max Planck Society under the auspices of Professor Robert Langer's Max Planck Research Award funded by the Federal Ministry of Education and Research.

Abstract

The reversible attachment of proteins to polymers is one potential strategy to control protein release from hydrogels. This chapter reports on the reversible attachment of lysozyme to poly(ethylene glycol) (PEG) by degradable carbamate linkers. Phenyl groups with different substituents were used to control the rate of carbamate hydrolysis and the resulting protein release. Sodium dodecyl sulfate (SDS) polyacrylamide gel electrophoresis (PAGE) showed modification with 1 – 3 PEG chains per lysozyme molecule. Protein PEGylation and PEG chain elimination occurred without changes in secondary protein structure, as demonstrated by circular dichroism (CD) spectroscopy. The lytic activity of lysozyme was restored to 73.4 ± 1.7 % – 92.5 ± 1.2 % during PEG chain elimination. Attached PEG chains were eliminated within 24 h to 28 d, depending on the used linker molecule. When formulated into hydrogels, a maximum of about 60 % of the initial dose was released within 7 d to 21 d. Linker elimination occurs 'traceless', so that the protein is released in its native, unmodified form. Altogether, tethering proteins by degradable carbamate linkers is a promising strategy to control their release from hydrogels.

3.1. Introduction

Even though the significance of therapeutic proteins has increased enormously since the development of recombinant insulin in 1979, several shortcomings still outweigh potential therapeutic benefits in many cases [12, 49]. First and foremost it is often difficult to reach effective protein concentrations at the target tissue due to degradation in the blood stream, unspecific binding to off-target sites or difficulties in crossing endothelial barriers [50]. The necessary injections and the short application intervals often compromise the patient compliance and increase the health care costs. Furthermore, many proteins do not target specific cell types, which limits their use as therapeutics. For example, growth factors may be highly selective *in vitro*, but show a significant number of systemic side effects *in vivo* [50]. One promising approach to solve these problems would be the local release of proteins from injectable hydrogels that serve as a drug carrier and control the release kinetics of their payload. Among the different strategies to control protein release, the reversible binding of proteins to the hydrogel carrier seems most promising; the release rate would then be controlled by the degradation kinetics of the used linker molecules and not only by the fast diffusion of the incorporated protein [12, 50, 51].

This approach has already been successfully applied to control the release of small molecules from hydrogels using hydrolytically [52, 53] or enzymatically cleavable linkers [54]. Similar techniques have been proposed for sustained protein release. Bovine serum albumin was covalently bound to poly(ethylene glycol) (PEG) hydrogels containing labile ester bonds and slowly released while the hydrogels degraded [55]. In another approach, vascular endothelial growth factor was immobilized in enzymatically degradable PEG hydrogels, which would allow cell-demanded protein release [56, 57]. Biotinylated insulin-like growth factor 1 was tethered to biotinylated peptide nanofibers using streptavidin as a cross-linker and proved to be successful in the treatment of myocardial infarction [58]. Reduction-sensitive linkers were investigated as an alternative way for temporary protein immobilization. Upon incubation with glutathione, the immobilized lysozyme was released from dextran hydrogels to the same extent as native lysozyme [59]. And recently, a very interesting concept has been proposed that relies on the formation of thermally reversible covalent bonds. Cell adhesion peptides with furan functionalities were covalently bound to maleimide moieties of the hydrogel and released by retro-Diels-Alder reactions [60]. A common

disadvantage of these approaches is the use of linker molecules that remain bound to the proteins even after their release from the hydrogel. These remaining 'tags' may compromise protein bioactivity or induce immune responses [23, 61, 62].

Our concept, in contrast, relies on the use of aromatic succinimidyl carbonates that react with protein amino groups under formation of degradable carbamates. These linker molecules have been originally developed for the reversible PEGylation of proteins and decompose without leaving any 'tags' on the protein [61, 63]. In an earlier publication, Brandl et al. reported on the synthesis of branched PEG-succinimidyl carbonates that react with branched PEG-amines to form hydrolytically degradable hydrogels. Proteins present in the reaction mixture were reversibly tethered to the hydrogel network and released during gel degradation [64]. A possible drawback of this approach is that protein release is controlled by both the decomposition of the linker molecules and the degradation of the hydrogel carrier. In this chapter, the entire focus was set on the carbamate linkers and the investigation of the influence of their chemical structure on the release kinetics of tethered proteins. Three different linker molecules were studied; lysozyme was used as a model protein. Linear methoxy poly(ethylene glycol) (mPEG) was used to study lysozyme PEGylation and PEG chain elimination kinetics. Non-degradable hydrogels were prepared by cross-linking branched PEG molecules using the copper(I)-catalyzed azide-alkyne cycloaddition (CuAAC). For lysozyme immobilization, branched carbamate linkers with two different types of reactive groups were synthesized and subsequently used for hydrogel preparation. Release studies were performed to demonstrate the feasibility of our approach.

3.2. Materials and Methods

3.2.1. Materials

3-Hydroxybenzoic acid, 3-(4-hydroxyphenyl)propionic acid, phthalimide and toluene were purchased from Acros Organics (Geel, Belgium). Tetramethylethylenediamine (TEMED) was purchased from Carl Roth GmbH & Co. KG (Karlsruhe, Germany). 2-Amino-2-hydroxymethyl-propane-1,3-diol (TRIS) was obtained from GE Healthcare Europe GmbH (Freiburg, Germany). Deuterated Chloroform ($CDCl_3$) was purchased from Deutero GmbH (Kastellaun, Germany). Phosphate-buffered saline (PBS) was purchased from Invitrogen GmbH (Karlsruhe, Germany). Four-armed poly(ethylene

glycol) with a molecular weight of 10 kDa was purchased from JenKem Technology (Allen, TX, USA). Iodine was purchased from Riedel-de Haën AG (Seelze, Germany). Acrylamide/bisacrylamide solution (37.5 : 1) and sodium dodecylsulfate were obtained from Serva Electrophoresis GmbH (Heidelberg, Germany). Acetonitril, Coomassie brilliant blue G-250, *N*,*N'*-dicyclohexylcarbodiimide (DCC), *N*-hydroxysuccinimide (HOSu), diisopropyl azodicarboxylate, *N*,*N'*-discuccinimidyl carbonate (DSC), fluorescamine, 4-hydroxybenzoic acid, lysozyme (from chicken egg white), magnesium sulfate, micrococcus lysodeikticus, sodium tetraborate decahydrate, 4-pentynoic acid, methoxy poly(ethylene glycol) with a molecular weight of 5 kDa and tetrahydrofuran were purchased from Sigma-Aldrich (Taufkirchen, Germany). Acetone, methylene chloride (DCM), diethyl ether and ethanol were from CSC Jäcklechemie (Nürnberg, Germany). All other chemicals were purchased from Merck KGaA (Darmstadt, Germany). Deionized water was obtained using a Milli-Q water purification system from Millipore (Schwalbach, Germany).

3.2.2. General Procedures

^{1}H-NMR spectra were recorded in $CDCl_3$ at room temperature on a Bruker Avance 300 spectrometer (Bruker BioSpin GmbH, Rheinstetten, Germany).

The number of free amino groups was determined as described by Udenfriend et al. [33]. The sample was dissolved in 50 mM borate buffer, pH 8.5 and diluted to a concentration of 0.2 µmol/mL. Then, 100 µL of the sample were mixed with 1300 µL of borate buffer and 600 µL of a fluorescamine solution in acetone (0.3 mg/mL). The fluorescence intensity (λ_{ex} = 390 nm, λ_{em} = 480 nm) was measured on a PerkinElmer LS 55 Fluorescence spectrometer (Perkin-Elmer, Wiesbaden, Germany). Compound **1** (**Table 3.1**) was used to prepare a calibration curve and the number of free amino groups was calculated.

Sodium dodecyl sulfate (SDS) polyacrylamide gel electrophoresis (PAGE) was conducted using polyacrylamide gels of 14 % cross-linking. The gels were loaded with 26.25 µg of protein per lane; native lysozyme was used as a reference. The running buffer consisted of 25 mM TRIS, 192 mM glycine and 0.1 % SDS. The system was programmed to apply a constant voltage of 120 V and decreasing current starting at 68 mA over 1.5 h. Afterwards the gels were stained with Coomassie brilliant blue G-250 and scanned. The conjugated PEG was detected by placing the gels into barium chloride and iodine solutions as described by Natarajan et al. [65]. For quantification,

the band areas and densities of the Coomassie brilliant blue-stained gels were measured using the NIH software ImageJ [66].

For circular dichroism (CD) spectroscopy, protein samples were diluted to a concentration of approx. 0.25 mg/mL; the exact concentration was determined spectrophotometrically at 280 nm. CD spectra were recorded on a Jasco J-815 CD spectrometer (Jasco Germany GmbH, Groß-Umstadt, Germany) from 260 to 190 nm at room temperature using cuvettes with a path length of 0.5 mm. Secondary structure fractions were quantified as described by Böhm et al. [67].

3.2.3. Synthesis of Compounds 1 and 3

Compounds **1** (Table 3.1) and 3 (**Table 3.2**) were synthesized in 95 % and 93 % yield as described by Brandl et al. [34].

3.2.4. Synthesis of Compound 2a

For the synthesis of compound **2a** (Table 3.1), a previously published procedure was modified as follows [64]. First, 0.11 g of 4-hydroxybenzoic acid (0.8 mmol), 0.09 g of HOSu (0.8 mmol) and 0.17 g of DCC (0.8 mmol) were dissolved in 10 mL of 1,4-dioxane and stirred for 4 – 6 h at room temperature. The *N*,*N'*-dicyclohexylurea (DCU) byproduct was filtered off; 2.0 g of compound **1** (0.40 mmol) and 0.04 g (0.48 mmol) of $NaHCO_3$ were then dissolved in 10 mL of water and mixed with the filtrate. The reaction mixture was stirred overnight at 50 °C. The next day, the solvent was evaporated and the residue was taken up in water. The raw product was extracted with DCM and the combined organic phases were dried over anhydrous $MgSO_4$. The solution was concentrated under reduced pressure and the product was crystallized at 0 °C by dropwise addition of diethyl ether. The precipitate was washed with cold diethyl ether and dried under vacuum to yield 1.9 g (93 %).

^{1}H-NMR ($CDCl_3$, 300 MHz): δ 3.40 ppm (s, 3 H, H_3CO–), 3.66 ppm (s, –OCH_2CH_2–), 6.90 ppm (d, 2 H, –C_6H_4OH), 7.33 ppm (d, 2 H, –C_6H_4OH). The degree of end-group conversion was 98 %, as calculated from the number of free amino groups.

The product from above (0.37 mmol) and 0.380 g of DSC (1.48 mmol) were dissolved in 7 mL of dried acetonitrile; 238 µL of pyridine were then added. The mixture was stirred overnight at room temperature. The next day, the solvent was evaporated under reduced pressure and the residue was taken up in DCM. The insoluble residue was filtered off. The solution was concentrated under reduced pressure and the product was

crystallized at 0 °C by dropwise addition of diethyl ether. The precipitate was washed with cold diethyl ether and dried under vacuum to yield 1.8 g (97 %) of compound **2a**.
^{1}H-NMR ($CDCl_3$, 300 MHz): δ 2.92 ppm (s, 4 H, –C(O)CH_2CH_2C(O)–), 3.40 ppm (s, 3 H, H_3CO–), 3.66 ppm (s, –OCH_2CH_2–), 7.38 ppm (d, 2 H, –C_6H_4OSu), 7.93 ppm (d, 2 H, –C_6H_4OSu).

3.2.5. Synthesis of Compound 2b

The precursor of compound **2b** was synthesized from compound **1** and 3-hydroxybenzoic acid in 90 % yield (1.83 g) as described above.
^{1}H-NMR ($CDCl_3$, 300 MHz): δ 3.40 ppm (s, 3 H, H_3CO–), 3.66 ppm (m, –OCH_2CH_2–), 7.00 ppm (d, 1 H, –C_6H_4OH), 7.26 ppm (d, 1 H, –C_6H_4OH), 7.39 ppm (d, 1 H, –C_6H_4-OH), 7.68 ppm (d, 1 H, –C_6H_4OH). The degree of end-group conversion was almost quantitative, as calculated from the number of free amino groups.
Compound **2b** (Table 3.1) was synthesized in 82 % yield (0.56 g) as described above.
^{1}H-NMR ($CDCl_3$, 300 MHz): δ 2.91 ppm (s, 4 H, –C(O)CH_2CH_2C(O)–), 3.40 ppm (s, 3 H, H_3CO–), 3.66 ppm (s, –OCH_2CH_2–), 7.26 ppm (d, 1 H, –C_6H_4OSu), 7.38 ppm (d, 1 H, –C_6H_4OSu), 7.52 ppm (d, 1 H, –C_6H_4OSu), 7.80 ppm (d, 1 H, –C_6H_4OSu).

3.2.6. Synthesis of Compound 2c

The precursor of compound **2c** was synthesized from compound **1** and 3-(4-hydroxyphenyl)propionic acid in 92 % yield (1.9 g) as described above.
^{1}H-NMR ($CDCl_3$, 300 MHz): δ 2.45 ppm (t, 2 H, –C(O)$CH_2$$CH_2$–), 3.89 ppm (t, 2 H, –C(O)CH_2CH_2–), 3.40 ppm (s, 3 H, H_3CO–), 3.66 ppm (s, –OCH_2CH_2–), 6.80 ppm (d, 2 H, –C_6H_4OH), 7.03 ppm (d, 2 H, –C_6H_4OH). The degree of end-group conversion was almost quantitative, as calculated from the number of free amino groups.
Compound **2c** (Table 3.1) was synthesized in 93 % yield (1.42 g) as described above.
^{1}H-NMR ($CDCl_3$, 300 MHz): δ 2.53 ppm (t, 2 H, –C(O)$CH_2$$CH_2$–), 2.90 ppm (s, 4 H, –C(O)CH_2CH_2C(O)–), 3.01 ppm (t, 2 H, –C(O)CH_2CH_2–), 3.40 ppm (s, 3 H, H_3CO–), 3.66 ppm (s, –OCH_2CH_2–), 7.21 ppm (d, 2 H, –C_6H_4OSu), 7.27 ppm (d, 2 H, –C_6H_4-OSu).

Table 3.1: Linear poly(ethylene glycol) derivatives (molecular weight 5 kDa)

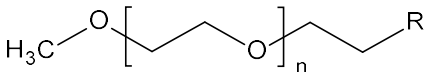

Compound	R
1	NH_2
2a	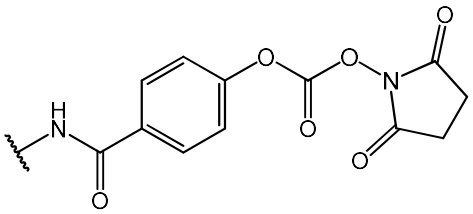
2b	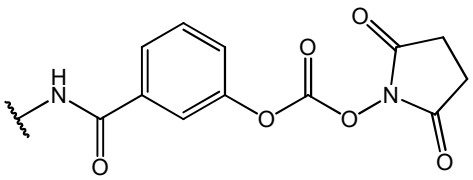
2c	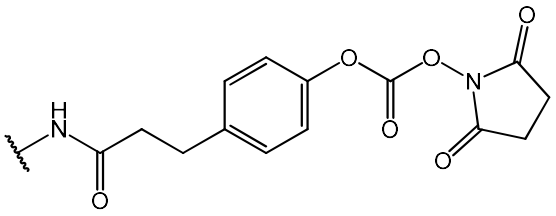

3.2.7. Synthesis of Compound 4

0.24 g of 4-pentynoic acid (2.4 mmol), 0.28 g of HOSu (2.4 mmol) and 0.50 g of DCC (2.4 mmol) were dissolved in 10 mL of 1,4-dioxane. The reaction mixture was stirred for 6 h at room temperature and the precipitated DCU was filtered off. Then, 3.0 g (0.3 mmol) of compound **3** and 0.20 g (2.4 mmol) of $NaHCO_3$ were dissolved in 10 mL of water and combined with the filtrate. The mixture was stirred overnight at 50 °C. The next day, the solvent was evaporated and the residue was taken up in 20 mL of water. The raw product was extracted with DCM and the combined organic phases were dried over anhydrous $MgSO_4$. The solution was concentrated under reduced pressure and the product was crystallized at 0 °C by dropwise addition of diethyl ether. The precipitate

was washed with cold diethyl ether and dried under vacuum to yield 2.9 g (95 %) of compound **4** (Table 3.2).

^{1}H-NMR ($CDCl_3$, 300 MHz): δ 2.05 ppm (t, 4 H, *HC*≡C–), 2.44 ppm (t, 8 H, –C(O)-*CH$_2$*CH$_2$–), 2.55 ppm (t, 8 H, –C(O)CH$_2$*CH$_2$*–), 3.66 ppm (s, –O*CH$_2$CH$_2$*–).

3.2.8. Synthesis of Compound 5a

The precursor of compound **5a** was synthesized in a similar manner to that of compound **2a**. In brief, 0.03 g of 4-hydroxybenzoic acid (0.2 mmol), 0.02 g of HOSu (0.2 mmol), 0.04 g of DCC (0.2 mmol), 2.0 g of compound **3** (0.2 mmol) and 0.02 g of $NaHCO_3$ (0.22 mmol) were allowed to react as described above to yield 1.82 g (90 %).

^{1}H-NMR ($CDCl_3$, 300 MHz): δ 2.94 ppm (t, 6 H, –*CH$_2$*-NH$_2$), 3.66 ppm (s, –O*CH$_2$*-*CH$_2$*–), 6.93 ppm (d, 2 H, –C$_6$H$_4$OH), 7.74 ppm (d, 2 H, –C$_6$H$_4$OH). The degree of end-group conversion was 27 % as calculated from the number of free amino groups.

In the next step, the remaining amino groups were modified with 4-pentynoic acid as described for compound **4** to yield 1.6 g (88 %).

^{1}H-NMR ($CDCl_3$, 300 MHz): δ 2.04 ppm (t, 3 H, *HC*≡C–), 2.44 ppm (t, 6 H, –C(O)-*CH$_2$*CH$_2$–), 2.55 ppm (t, 6 H, –C(O)CH$_2$*CH$_2$*–), 3.66 ppm (s, –O*CH$_2$CH$_2$*–), 6.93 ppm (d, 2 H, –C$_6$H$_4$OH), 7.76 ppm (d, 2 H, –C$_6$H$_4$OH). The degree of end-group conversion was almost quantitative. In the last step, the phenolic hydroxyl groups were activated using DSC to yield 1.39 g (86 %) of compound **5a** (Table 3.2).

^{1}H-NMR ($CDCl_3$, 300 MHz): δ 2.05 ppm (t, 3 H, HC≡C–), 2.44 ppm (t, 6 H, –C(O)-*CH$_2$*CH$_2$–), 2.55 ppm (t, 6 H, –C(O)CH$_2$*CH$_2$*–), 2.92 ppm (s, 4 H, –C(O)*CH$_2$CH$_2$*-C(O)–), 3.66 ppm (s, –O*CH$_2$CH$_2$*–), 7.38 ppm (d, 2 H, –C$_6$H$_4$OH), 7.94 ppm (d, 2 H, –C$_6$H$_4$OH).

3.2.9. Synthesis of Compound 5b

The precursor of compound **5b** was synthesized in 93 % yield (2.8 g) as described for compound **5a**.

^{1}H-NMR ($CDCl_3$, 300 MHz): δ 2.97 ppm (t, 6 H, –*CH$_2$*-NH$_2$), 3.66 ppm (s, –O*CH$_2$*-*CH$_2$*–), 6.98 ppm (d, 1 H, –C$_6$H$_4$OH), 7.28 ppm (d, 1 H, –C$_6$H$_4$OH), 7.39 ppm (d, 1 H, –C$_6$H$_4$OH). The degree of end-group conversion after the first coupling step was 33 %, as calculated from the number of free amino groups.

The second intermediate was synthesized in 82 % yield (2.53 g) as described above.

^{1}H-NMR ($CDCl_3$, 300MHz): δ 2.04 ppm (t, 3 H, *HC*≡C–), 2.44 ppm (t, 6 H, –C(O)*CH$_2$*-CH$_2$–), 2.55 ppm (t, 6 H, –C(O)CH$_2$*CH$_2$*–), 3.66 ppm (s, –O*CH$_2$CH$_2$*–), 7.00 ppm (d, 1 H, C_6H_4OH), 7.28 ppm (d, 1 H, –C_6H_4OH), 7.39 ppm (d, 1 H, –C_6H_4OH).

Compound **5b** (Table 3.2) was synthesized in 72 % yield (2.28 g) as described above.

^{1}H-NMR ($CDCl_3$, 300 MHz): δ 2.05 ppm (t, 3 H, HC≡C–), 2.44 ppm (t, 6 H, –C(O)-*CH$_2$*-CH$_2$–), 2.55 ppm (t, 6 H, –C(O)CH$_2$*CH$_2$*–), 2.91 ppm (s, 4 H, –C(O)*CH$_2$CH$_2$*-C(O)–), 3.66 ppm (m, –O*CH$_2$CH$_2$*–), 7.44 ppm (d, 1 H, –C_6H_4OH), 7.52 ppm (d, 1 H, –C_6H_4OH), 7.81 ppm (d, 1 H, –C_6H_4OH).

3.2.10. Synthesis of Compound 5c

Compound **5c** was synthesized in a slightly different manner. First, 0.12 g of 4-pentynoic acid (1.2 mmol), 0.06 g of 3-(4-hydroxyphenyl)propionic acid (0.4 mmol), 0.15 g of HOSu (1.6 mmol) and 0.33 g of DCC (1.6 mmol) were dissolved in 7 mL of 1,4-dioxane. The mixture was stirred for 6 h at room temperature and the precipitated DCU was filtered off. Then, 2 g of compound **3** (0.2 mmol) and 0.13 g of $NaHCO_3$ were dissolved in water and combined with the filtrate. The mixture was stirred overnight at 50 °C. The next day, the solvent was evaporated; the residue was taken up in water and extracted with DCM. The combined organic phases were dried over anhydrous $MgSO_4$. The solution was concentrated under reduced pressure and the product was crystallized at 0 °C by dropwise addition of diethyl ether. The precipitate was washed with cold diethyl ether and dried under vacuum to yield 1.65 g (79 %).

^{1}H-NMR ($CDCl_3$, 300 MHz): δ 2.05 ppm (t, 3 H, *HC*≡C–), 2.42 ppm (t, 2 H, C(O)*CH$_2$*CH$_2$–), 2.44 ppm (t, 6 H, –C(O*)CH$_2$*CH$_2$–), 2.55 ppm (t, 6 H, –C(O)CH$_2$-*CH$_2$*–), 2.90 ppm (t, 2 H, –C(O)CH$_2$*CH$_2$*–), 3.66 ppm (s, –O*CH$_2$CH$_2$*–), 6.80 ppm (d, 2 H, –C_6H_4OH), 7.04 ppm (d, 2 H, –C_6H_4OH). The degree of end-group conversion was 97 %, as determined by ^{1}H-NMR.

The product from above was activated using DSC to yield 1.06 g (56 %) of compound **5c** (Table 3.2).

^{1}H-NMR ($CDCl_3$, 300 MHz): δ 2.05 ppm (t, 3 H, HC≡C–), 2.44 ppm (t, 6 H, –C(O)-*CH$_2$*CH$_2$–), 2.55 ppm (t, 6 H, –C(O)CH$_2$*CH$_2$*–), 2.86 ppm (s, 4 H, –C(O)*CH$_2$CH$_2$*-C(O)–), 2.91 ppm (t, 2 H, –C(O)CH$_2$*CH$_2$*–), 3.66 ppm (s, –O*CH$_2$CH$_2$*–), 6.95 ppm (d, 2 H, –C_6H_4OH), 7.21 ppm (d, 2 H, –C_6H_4OH).

3.2.11. Synthesis of Compound 6

Imidazole-1-sulfonyl azide hydrochloride was synthesized as described by Goddard-Borger et al. [36]. In the next step, 3.0 g of compound **3** (0.3 mmol), 292 µL of triethylamine and 3.0 mg of copper(II) sulfate were dissolved in 10 mL of methanol. Imidazole-1-sulfonyl azide hydrochloride was added subsequently. The mixture was allowed to react overnight at room temperature. The next day, the mixture was concentrated under reduced pressure, diluted with 40 mL of water and acidified with HCl. The raw product was extracted with DCM and the combined organic phases were dried over anhydrous $MgSO_4$. The solution was concentrated under reduced pressure and the product was crystallized at 0 °C by dropwise addition of diethyl ether. The precipitate was washed with cold diethyl ether and dried under vacuum to yield 2.85 g (95 %) of compound **6** (Table 3.2).

^{1}H-NMR ($CDCl_3$, 300 MHz): δ 3.66 ppm (s, –O*C*H_2*C*H_2–).

Table 3.2: Branched poly(ethylene glycol) derivatives (molecular weight 10 kDa)

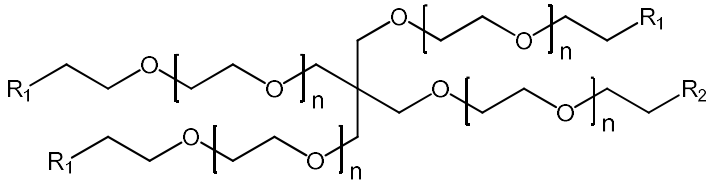

Compound	R_1	R_2
3	NH_2	NH_2
4	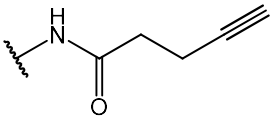	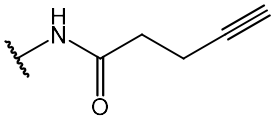
5a	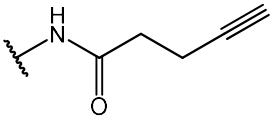	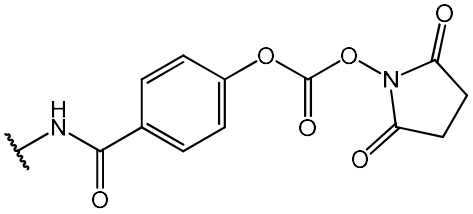
5b	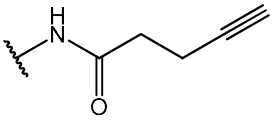	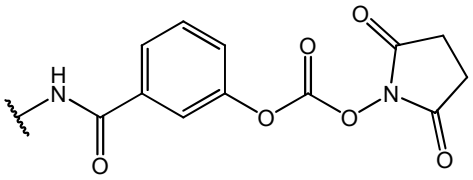
5c	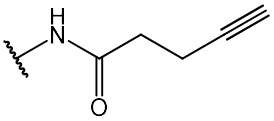	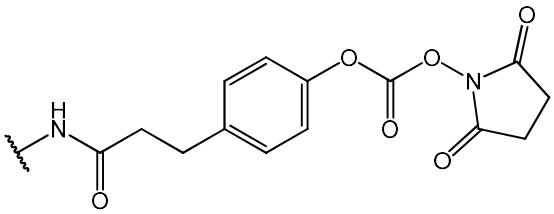
6	N_3	N_3

3.2.12. PEGylation of Lysozyme

A lysozyme stock solution (concentration of amino groups 6.10 µmol/mL) was prepared in 25 mM phosphate buffer pH 7.4 For PEGylation, specified amounts of compound **2a**, **2b** and **2c** were dissolved in the lysozyme stock solution and allowed to react for 1 h at room temperature. Different PEG concentrations were used (0.087 µmol/mL, 0.3 µmol/mL, 0.61 µmol/mL, 1.22 µmol/mL, 2.44 µmol/mL and 3.66 µmol/mL); the ratio of reactive succinimidyl (SC) : protein amino groups (NH_2) varied between 1 : 7 and 42 : 7. The protein conjugates were analyzed by SDS-PAGE to determine the degree of PEGylation. CD spectroscopy was used to estimate the secondary structure fractions of native and PEGylated lysozyme. The PEGylation studies were done in triplicate and the results are presented as means ± standard deviations.

3.2.13. Enzymatic Activity of Lysozyme

Lysozyme (protein concentration 1mg/mL) was PEGylated with compound **2a**, **2b** and **2c** as described above; the ratio of SC : NH_2 groups was 7 : 7. A lysozyme solution containing an equivalent amount of compound **1** served as reference. All samples were diluted to a protein concentration of 0.01 mg/mL. The enzymatic activity of lysozyme was determined directly after PEGylation, and after incubation at 37 °C using a method described by Shugar with the following modifications [68]. In a cuvette, 2.5 mL of a 0.015 % Micrococcus lysodeikticus cell suspension in 66 mM phosphate buffer pH 6.2 were added to 100 µL protein sample. The decrease in the absorption at 450 nm was measured over 4.8 min in 0.8 min intervals. The enzymatic activity was calculated from the slope of the linear part of the curve. All measurements were done in triplicate and the results are presented as means ± standard deviations.

3.2.14. Elimination Kinetics of PEG Chains

Lysozyme (concentration of amine groups 6.10 µmol/mL) was PEGylated with compound **2a**, **2b** and **2c** as described above. The molar ratio of SC : NH_2 groups was 7 : 7. To follow the elimination of PEG chains, 250 µl aliquots of the samples were incubated in a shaking water bath at 37 °C. The samples were removed at defined time points and stored at –20 °C for further analysis by SDS-PAGE. The experiment was done in triplicate and the results are presented as means ± standard deviations.

3.2.15. Preparation of Lysozyme Loaded Hydrogels and Release Studies

Hydrogels were prepared from PEG macromonomers substituted with alkyne (compound **4**) and azido groups (compound **6**). A lysozyme stock solution (protein concentration 1.33 mg/mL) was prepared in 25 mM phosphate buffer pH 7.4. PEGylation with compound **5a**, **5b** and **5c** was carried out as described above with the exception that **5c** was allowed to react for 2 h. The ratio of SC : NH_2 groups was 14 : 7 in all cases. The successful PEGylation of lysozyme was verified by SDS-PAGE. After PEGylation, the required amounts of compound **4** and **6** were dissolved in the protein solution. The stoichiometric ratio between alkyne and azido groups was nearly balanced and the total polymer content was 5 % (w/v). Cross-linking was started by the addition of 0.5 µmol/mL $CuSO_4$ and 2.5 µmol/mL ascorbic acid. Samples of 750 µL were cast into glass cylinders with a diameter of 10 mm and allowed to gel for 2 h at room temperature. As control, hydrogels containing physically entrapped, non-PEGylated lysozyme were prepared in a similar manner. For the release studies, the hydrogel cylinders were immersed in 10 mL of PBS containing 0.1 % NaN_3 and incubated in shaking water bath at 37 °C. Samples were withdrawn at regular time intervals and replaced by fresh buffer. The samples were stored at 4 °C until the completion of the release experiment. Protein quantification was carried out as described by Bradford [69]. The released protein amount was normalized to the initial dose (1 mg per gel cylinder). For better comparability, all release profiles were additionally scaled to their maximum values, which were taken as 100 %. At least three repetitions were done and the results are presented as means ± standard deviations.

3.3. Results and Discussion

3.3.1. Synthesis of Degradable Carbamate Linkers for Protein PEGylation

Different types of linkers, such as aromatic linkers employing the 1,4- or 1,6-benzyl elimination [63, 70, 71], linkers based on the trimethyl lock lactonization [72], or aliphatic bicin linkers [73], have been developed for the reversible PEGylation of proteins. Although these linkers have been successfully used for the generation of PEGylated protein prodrugs [74, 75], this approach of using phenyl carbamates for

protein conjugation offers several advantages. First of all, the here described PEG linkers can be readily synthesized from commercially available reagents. The synthesis involves a condensation reaction between an amine and a carboxylic acid function followed by an activation step, and does not require any chromatographic purification steps. The desired polymers were obtained in satisfactory yields and acceptable purity, as calculated from the number of free amino groups and ^{1}H-NMR spectra. Second, different to the above-mentioned elimination reactions, the hydrolysis of phenyl carbamates does not involve the departure of potentially toxic leaving groups [76–80]. For example, the generation of reactive quinone methides during the 1,6-benzyl elimination reaction may result in the alkylation of proteins with important biochemical and toxicological consequences [81]. Apart from that, most of the existing linkers were designed to release the attached PEG chains within a few hours after protein administration [74, 75], whereas the aim of this investigation was the development of hydrogels that release their tethered proteins over days to weeks. To achieve this goal, linkers employing the 1,4- or 1,6-benzyl elimination reaction would have required the introduction of enzymatically cleavable groups [74, 75], which could have made the resulting release rates less predictable and controllable. In contrast to that, the decomposition rate of phenyl carbamates can be modulated over a wide range by changing the substitution pattern of the phenolic leaving group [76–79].

3.3.2. PEGylation of Lysozyme

The first experiment was aimed at investigating the reactivity of the synthesized PEG linkers and establishing optimal conditions for lysozyme PEGylation. Lysozyme has seven amino groups, namely six lysine residues and one amino terminus. Three lysine amino groups are located on the protein surface and can be easily PEGylated by amine-reactive reagents. PEGylation of the three other lysine residues that are hidden within the protein is associated with structural breakdown and irreversible denaturation [82]. To find optimal reaction conditions, lysozyme was PEGylated at different SC : NH_2 ratios and the degree of PEGylation was determined by SDS-PAGE. After Coomassie brilliant blue staining, SDS-PAGE showed PEGylation with 1 – 3 PEG chains per lysozyme molecule (**Figure 3.1**). This is in good agreement with previously published studies, which also showed PEGylation with 1 – 3 PEG chains under similar reaction conditions [63, 71, 73, 83]. The low degree of PEGylation and the mild reaction conditions (25 mM phosphate buffer pH 7.4, room temperature) suggest that

PEGylation with linker **2a**, **2b** and **2c** most likely does not affect the protein structure. For all tested PEG linkers, the number of attached PEG chains per lysozyme molecule increased with increasing $SC : NH_2$ ratio. At the same time, the fraction of free lysozyme decreased to a minimum of 4 – 10 %, depending on the used linker molecule and $SC : NH_2$ ratio. Linker **2b** and **2c** both gave a similar PEGylation pattern; at higher $SC : NH_2$ ratios, however, linker **2b** favored the formation of highly PEGylated lysozyme derivatives (Figure 3.1 B and C). Linker **2a**, in contrast, generally yielded less PEGylated derivatives. In particular at low $SC : NH_2$ ratios, the amount of free lysozyme was considerably higher when linker **2a** was used for PEGylation (Figure 3.1 A). This can be explained by different reactivity of the synthesized succcinimidyl carbonates. Faster hydrolysis of linker **2a**, which decreases the amount of amine-reactive succinimidyl carbonates, would be another explanation for the observed differences. Last, once attached PEG chains could be cleaved off faster compared to the other linkers, which would also increase the amount of free lysozyme.

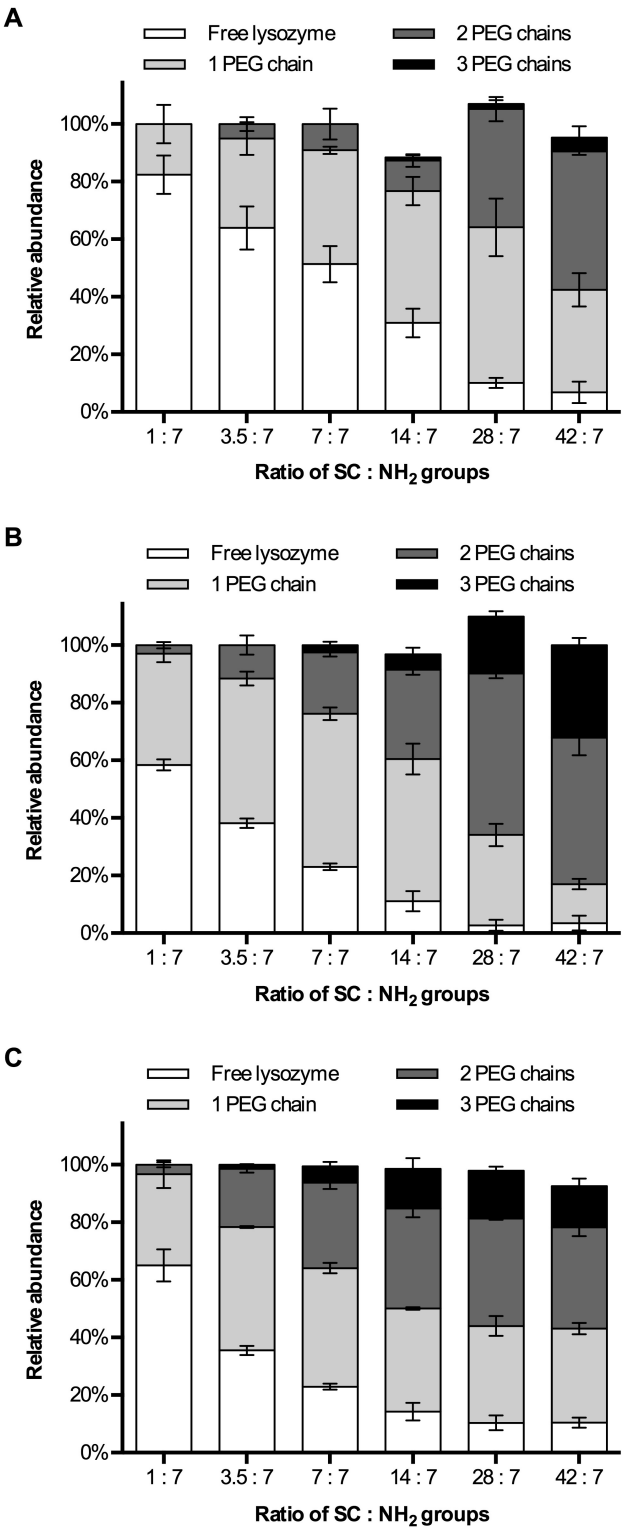

Figure 3.1: PEGylation of lysozyme with 2a (A), 2b (B) and 2c (C). The ratio of SC : NH_2 groups varied between 1 : 7 and 42 : 7. The relative abundance of the different protein species was determined by SDS-PAGE and the results are presented as means ± standard deviations (n = 3).

CD spectroscopy was used to check if PEGylation affects the secondary structure of lysozyme. This method has previously been used to investigate the effects of acylation with succinimidyl-S-acetylthioacetate on the secondary structure of lysozyme [83]. The recorded CD spectra did not show any changes due to PEGylation compared to native lysozyme (**Figure 3.2** A).

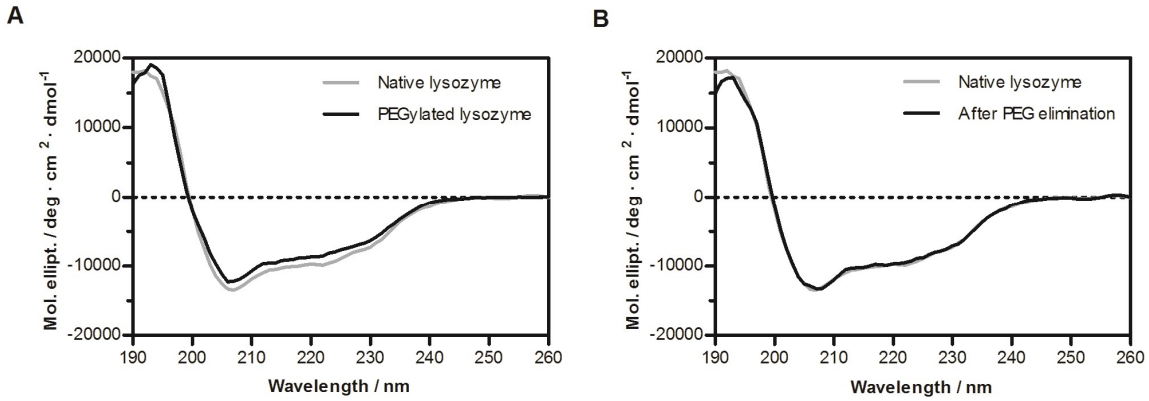

Figure 3.2: CD spectra of native and PEGylated lysozyme. Lysozyme was PEGylated with linker 2a; the ratio of SC : NH_2 groups was 7 : 7. CD spectra were recorded directly after PEGylation (A) and after 48 h of incubation at 37 °C (B). The measurements were done in triplicate and representative curves are shown.

The secondary structure fractions of native and PEGylated lysozyme are listed in **Table 3.3**. In both samples, the secondary structure consisted of 34.0 – 34.8 % α-helix, 7.6 – 7.8 % antiparallel β-sheet, 8.6 – 8.8 % parallel β-sheet, 16.5 – 16.7 % β-turn and 32.1 – 32.7 % random coil. The differences between the two samples were all within the experimental error. Therefore, it can be concluded that PEGylation with up to three PEG chains does not affect the secondary structure of lysozyme. This is consistent with previously published results, which showed that up to three amino groups of lysozyme could be acylated while maintaining the secondary protein structure [83].

Table 3.3: Secondary structure fractions of native and PEGylated lysozyme. Lysozyme was PEGylated with compound 2a at a SC : NH_2 ratio of 7 : 7. The CD measurements were done in triplicate and the results are presented as means ± standard deviations.

Secondary structure	Native lysozyme	PEGylated lysozyme
α-Helix	34.0 % ± 0.6 %	34.8 % ± 1.3 %
Antiparallel β-sheet	7.8 % ± 0.2 %	7.6 % ± 0.3 %
Parallel β-sheet	8.8 % ± 0.2 %	8.6 % ± 0.4 %
β-Turn	16.7 % ± 0.0 %	16.5 % ± 0.2 %
Random coil	32.7 % ± 0.4 %	32.1 % ± 1.0 %

3.3.3. Enzymatic Activity of Lysozyme

The enzymatic activity of PEGylated lysozyme was measured before and after PEG chain elimination. Although none of the possible PEGylation sites are within its active center, lysozyme shows decreased activity due to PEGylation, partly from the exclusion of the substrate from the binding site [82, 84]. Therefore, lysozyme is an excellent model protein to study reversible PEGylation. After PEGylation, the enzymatic activity of lysozyme decreased to 50.3 ± 0.4 % (linker 2a), 29.4 ± 1.1 % (linker 2b) and 28.3 ± 1.4 % (linker 2c) of the activity of the non-PEGylated reference (**Figure 3.3**). This confirms the results of the SDS-PAGE, which also showed incomplete PEGylation at SC : NH_2 ratios of 7 : 7 (Figure 3.1). To test if the conjugated PEG chains can be cleaved off and the enzymatic activity of lysozyme is restored, the samples were incubated at 37 °C and reanalyzed at predetermined time points. After 24 h of incubation, the enzymatic activity of lysozyme PEGylated with linker 2a had increased to 90.7 ± 1.0 % of the activity of the unmodified protein. Lysozyme PEGylated with linker 2b completely regained its activity after 7 d of incubation. The activity of lysozyme PEGylated with linker **2c** increased to 73.9 ± 1.7 % within 28 d of incubation (Figure 3.3).

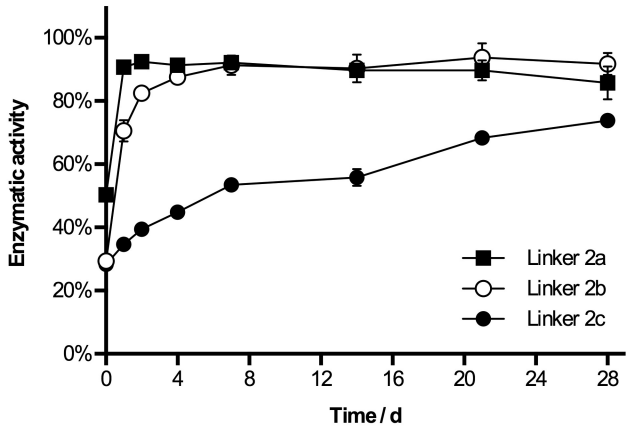

Figure 3.3: Effect of PEG attachment and elimination on the enzymatic activity of lysozyme. The experiment was done in triplicate and the results are expressed as percent of the activity of native lysozyme (means ± standard deviations).

These findings are consistent with previously published results, which showed recovery of the lysozyme activity after release from PEG conjugates [63, 71, 73, 84]. Therefore, it can be concluded that the synthesized linkers are hydrolyzed in aqueous media at 37 °C and conjugated PEG chains are cleaved off. The obtained results also demonstrate that the kinetics of PEG chain elimination depends on the nature of the linker molecules used for PEGylation. However, it has been shown in previous studies on releasable PEGylation reagents that the activity increase is not strictly dependent on the amount of free lysozyme but also includes conjugates where PEG chains have been released near the active center [84]. Consequently, measuring the enzymatic activity overestimates the amount of free lysozyme, due to that reason it was decided to follow the kinetics of PEG chain elimination by SDS-PAGE. To complement the activity measurements, the secondary structure of the recovered lysozyme was additionally analyzed by CD spectroscopy. As shown in Figure 3.2 B, the recorded CD spectra did not show any significant differences to native lysozyme. Therefore, it can be concluded that neither PEGylation nor the elimination of the conjugated PEG chains affects the secondary structure of lysozyme.

3.3.4. Elimination Kinetics of PEG Chains

Lysozyme was PEGylated and the subsequent PEG chain elimination was followed by SDS-PAGE. The different protein species were identified by a combination of Coomassie brilliant blue and barium iodide staining in which PEGylated proteins appear

as brown spots and non-PEGylated proteins give a dark-blue staining. In the experiment shown in **Figure 3.4**, lysozyme was PEGylated using linker **2a** and the elimination of PEG chains was followed over time.

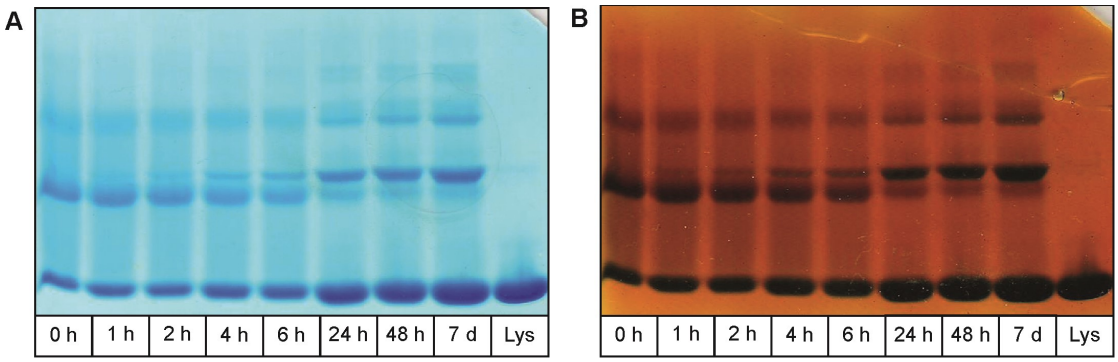

Figure 3.4: Elimination of conjugated PEG chains over time followed by SDS-PAGE. Lysozyme was PEGylated with linker 2a; the molar ratio of SC : NH_2 groups was 7 : 7. A combination of Coomassie brilliant blue (A) and barium iodide staining (B) was used to identify the different protein species. Free lysozyme ("Lys") served as a reference.

SDS-PAGE showed an increase for unmodified lysozyme over time while the amount of PEGylated lysozyme decreased at the same time. The relative amounts of PEGylated and free lysozyme were measured using ImageJ and the results are presented in **Figure 3.5**.

Linker **2a** was hydrolyzed very rapidly; after 24 h, a maximum amount of 63 % of free lysozyme could be detected. No further increase was observed between 24 h and 7 d (Figure 3.5 A). The hydrolysis of linker **2b** was slower compared to **2a** and continued over at least 7 d; the amount of free lysozyme was determined to be 56 % after 7 d of incubation (Figure 3.5 B). The elimination of PEG chains was slowest when linker **2c** was used for PEGylation. The hydrolysis of the carbamate group proceeded very slowly and only 44 % of the introduced lysozyme was in its free form after 28 d (Figure 3.5 C). This is different from previously reported studies. Lysozyme was almost completely released from conjugates with PEGylation reagents employing the 1,6-benzyl elimination reaction [63, 71] or bicin linkers [73] after 24 h of incubation at 37 °C. However, these experiments were carried out at pH 8.0 – pH 9.2, whereas our elimination studies were done at pH 7.4.

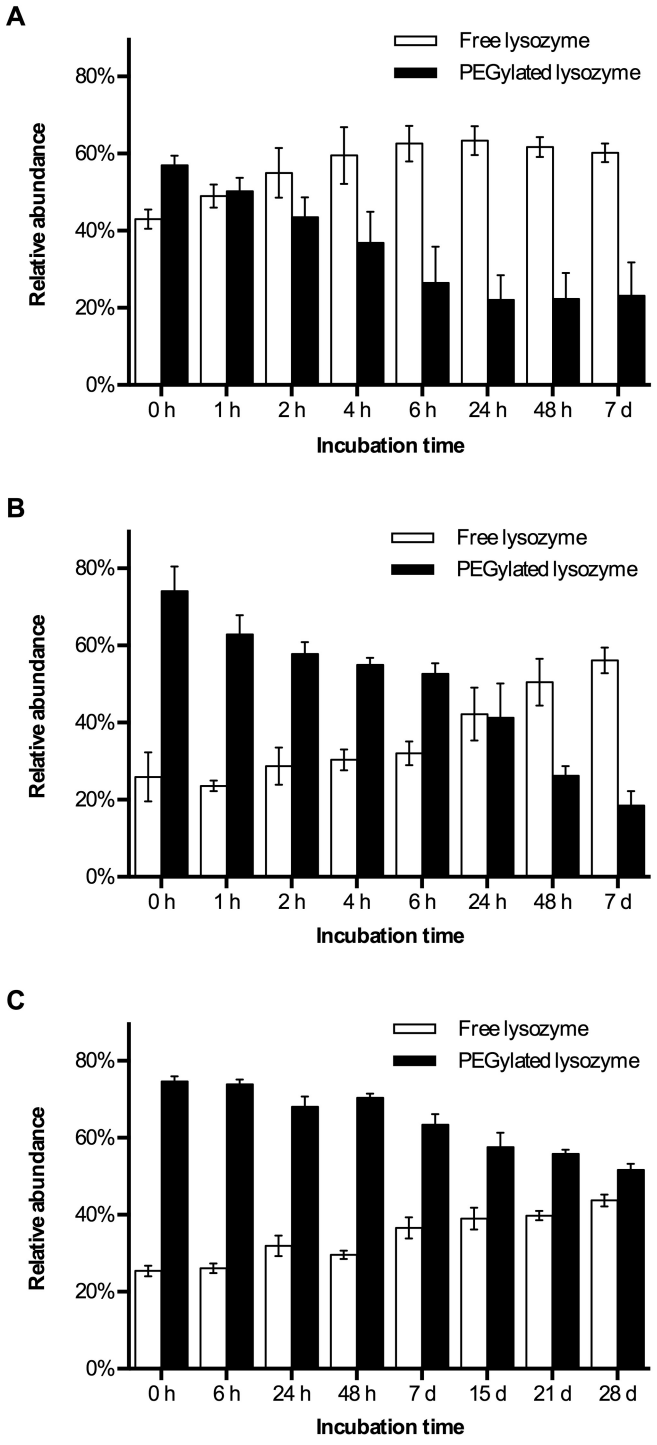

Figure 3.5: Elimination of PEG chains over time. Lysozyme was PEGylated with 2a (A), 2b (B) or 2c (C); the molar ratio of SC : NH_2 groups was 7 : 7. The relative abundance of the different protein species was determined by SDS-PAGE and the results are presented as means ± standard deviations (n = 3).

The hydrolysis of phenyl carbamtes in neutral and basic solutions proceeds by an E1cB elimination reaction involving the intermediate formation of an unstable isocyante, which then disintegrates into a primary amine and carbon dioxide [76–80]. Substituents in the phenolic leaving group have a great effect on the rate of carbamate hydrolysis (**Table 3.4**). Electron withdrawing groups in the ortho or para-position stabilize the phenolate ion by resonance and accelerate hydrolysis compared to the unsubstituted compound [76–79]. In compound **2a**, the electron withdrawing carbamoyl group is in the para-position to the carbamate group and able to stabilize the phenolate ion by resonance. In compound **2b**, on the other hand, the carbamoyl group is located in the meta-position and, therefore, unable to stabilize the phenolate ion. The substitution pattern of compound **2c** is different; unlike the other linker molecules, **2c** is substituted with an electron releasing alkyl group in the para-position to the carbamate group, which destabilizes the phenolate ion. Based on these theoretical considerations, linker **2a** should hydrolyze more rapidly than **2b** and **2c**. This was fully reflected by the experimental data. The electron releasing alkyl group in para-position to the carbamate group (linker **2c**) dramatically slows down hydrolysis, whereas shifting the electron withdrawing carbamoyl group from the para (linker **2a**) into the meta-position (linker **2b**) only has a minor influence on the hydrolysis rate.

Table 3.4: Chemical structures of the formed carbamates

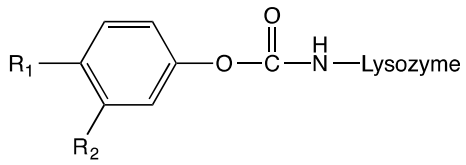

Linker	R_1	R_2
2a	$C(O)NH[CH_2CH_2O]_nCH_3$	H
2b	H	$C(O)NH[CH_2CH_2O]_nCH_3$
2c	$CH_2CH_2C(O)NH[CH_2CH_2O]_nCH_3$	H

Although PEGylation with aromatic succinimidyl carbonates should be completely reversible [61, 63], a maximum of 63 % of the PEGylated lysozyme could be recovered in its free form. There are two possible explanations for this incomplete elimination of

PEG chains. First, **1** may contain residual hydroxyl groups that will react with DSC to aliphatic succinimidyl carbonates, which in turn form stable carbamates with protein amino groups. Additionally, incomplete substitution of **1** with 4-hydroxybenzoic acid, 3-hydroxybenzoic acid or 3-(4-hydroxyphenyl)propionic acid and subsequent reaction with DSC will yield aliphatic succinimidyl carbamates that can react with protein amino groups to stable ureas [85]. And second, nucleophilic groups (e.g. amino or hydroxyl groups) might attack the isocyanate formed during the hydrolysis of phenyl carbamates and produce stable protein conjugates [86, 87].

The intermediate isocyanate could also be attacked by nucleophilic groups of other proteins (e.g. hydroxyl, sulfhydryl, imidazole or amino groups) [88], which would result in the formation of protein aggregates. In fact, lysozyme dimers were identified after Coomassie brilliant blue and barium iodide staining by their dark-blue color. When using linker **2a** or **2b** for PEGylation, first lysozyme dimers were detected after 1 h of incubation. The tendency to form oligomers further increased during the experiment; after 7 d of incubation, lysozyme dimers accounted for approx. 10 % of the total protein amount (Figure 3.4). After PEGylation with linker **2c**, only few aggregates were observed after 15 d of incubation (data not shown). Self-association of lysozyme in aqueous solution would be another explanation for the observed aggregation [89]. PEGylation can prevent the aggregation of proteins by steric shielding [90], which might explain why less lysozyme dimers were observed when linker **2c** was used for PEGylation.

3.3.5. Release of Lysozyme from Hydrogels

In the final experiment, the release of lysozyme from PEG based hydrogels was investigated. For this purpose, four-armed PEG was functionalized with alkyne (compound **4**, Table 3.2) and azide groups (compound **6**, Table 3.2), respectively. To enable lysozyme immobilization, branched PEG linkers with two different types of reactive groups were synthesized. In the first synthetic step, compound **3** (Table 3.2) was partially functionalized with 4-hydroxybenzoic acid (linker **5a**, Table 3.2), 3-hydroxybenzoic acid (linker **5b**, Table 3.2) or 3-(4-hydroxyphenyl)propionic acid (linker **5c**, Table 3.2). The remaining amino groups were then acylated with 4-pentynoic acid to allow cross-linking with **6**. In the last step, the phenolic hydroxyl groups were activated with DSC to yield amine-reactive succinimidyl carbonates. (For more details see Chapter 2.) For hydrogel preparation, lysozyme was first PEGylated with **5a**, **5b** or

5c and subsequently mixed with the required amounts of **4** and **6**. Gel formation and protein immobilization occurred within a few minutes by azide-alkyne cyclodaddition in the presence of $CuSO_4$ and ascorbic acid (CuAAC). As a control, non-PEGylated lysozyme was physically entrapped in PEG hydrogels.

The successful PEGylation with linker **5a**, **5b** and **5c** was verified by SDS-PAGE (**Figure 3.6**). The results are in good agreement with the data obtained from PEGylation with linker **2a**, **2b** and **2c** (Figure 3.1). The amount of free, non-PEGylated lysozyme was comparable for the three different linkers and varied between 16 % and 27 %.

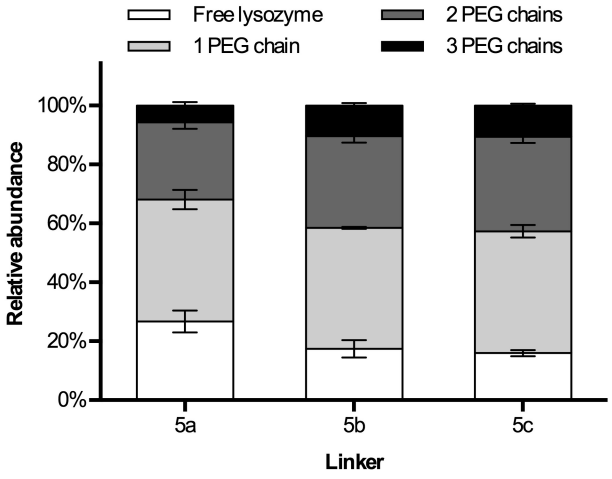

Figure 3.6: PEGylation of lysozyme with linker 5a, 5b and 5c. The ratio of SC : NH_2 groups was 14 : 7. The relative abundance of the different protein species was determined by SDS-PAGE and the results are presented as means ± standard deviations (n = 3).

The results of the release experiments are presented in **Figure 3.7**. As expected, physically entrapped lysozyme was released very fast; 83 % of the initial dose was released within the first 24 h. The protein release reached a plateau after 3 d; by that time, 92 % of the initial dose had been released into solution (Figure 3.7 A). This is explained by the high water content (> 95 %) and low cross-linking density of the hydrogels, which both lead to a high diffusivity of the incorporated lysozyme. When the incorporated lysozyme was tethered to the hydrogel network, a maximum of about 60 % of the initial dose was released (Figure 3.7 B). The release rate was dependent on the used linker; the maximum values were reached after 7 d (linker **5a**), 10 d (linker **5b**) and 21 d (linker **5c**). These results are in good agreement with those obtained by SDS-

PAGE (Figure 3.5). The incomplete protein release is most likely due to irreversible binding to the hydrogel network, as outlined in the previous section.

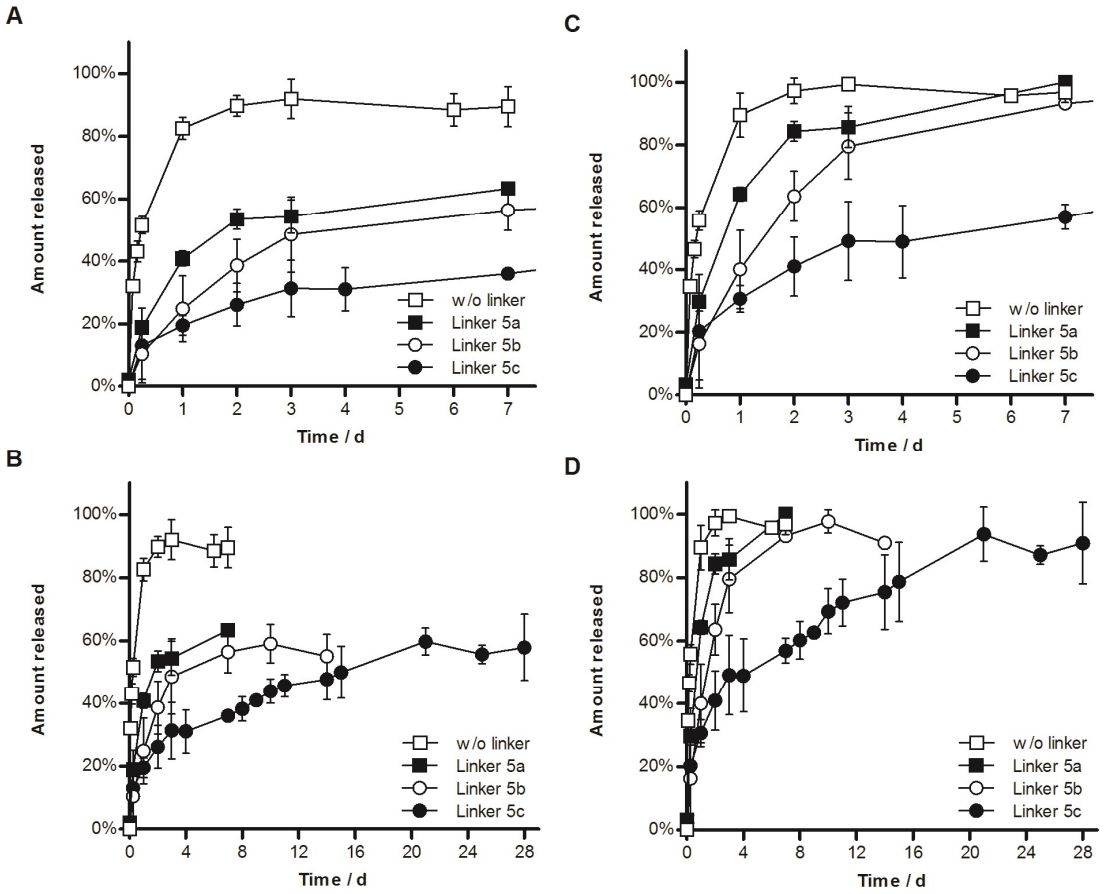

Figure 3.7: Release of lysozyme from PEG hydrogels. The released protein amounts were calculated in percent of the initial dose (A and B). For better comparability, the release profiles were additionally scaled to their maximum values (C and D). All experiments were done in triplicate and the results are presented as means ± standard deviations.

For better comparability, all release profiles were scaled to their maximum values, which were taken as 100 % (Figure 3.7 C and D). As already discussed above, the release from hydrogels loaded with physically entrapped lysozyme was very fast. After 5 h, already 50 % of the total amount had been released into solution; 75 % of the total amount was released after 16 h. Tethering lysozyme to the hydrogel network considerably slowed down the release kinetics. The release rates were found to depend on the used linker molecules; 50 % of the total amount was released after 17 h (linker **5a**), 34 h (linker **5b**) and 105 h (linker **5c**). The effect of the different linker molecules becomes even more distinct when looking at later time points of the release profiles; 75 % of the total amount was released after 1.5 d (linker **5a**), 2.7 d (linker **5b**) and

13.6 d (linker **5c**). In addition, the initial release rate could have been dominated by the presence of free, non-tethered lysozyme in the hydrogels. As shown in Figure 3.6, however, the amount of non-PEGylated lysozyme was similarly low for all three linkers. Therefore, the observed differences in the release kinetics are most likely not due to different sized fractions of free lysozyme. The measured release profiles match the kinetics of PEG chain elimination very well (Figure 3.5). As already discussed in the previous section, linker **5a** and **5b** both hydrolyze much faster than linker **5c** because of their different aromatic substitution patterns [76–79]. Therefore, linker **5a** and **5b** both retard protein release to a much lesser extent than linker **5c**. It can be concluded from the SDS-PAGE that tethered lysozyme will be released in its free, unmodified form. This is an advantage over previous approaches since the absence of any remaining 'tags' helps to preserve protein bioactivity and reduces the risk of generating immune reactions [23, 61, 62].

Although it was shown that the synthesized linker molecules, in particular linker **5c**, can control the release of tethered proteins, the used hydrogels will require further modification before they can be applied as a protein delivery system. First of all, using the CuAAC as cross-linking reaction could be problematic because of the toxicity of the copper(I) catalyst [91]. Second, the hydrogels used in this study are non-degradable, which would require their surgical removal after complete protein release. From a research perspective, however, the prepared hydrogels offer several advantages. The CuAAC is an orthogonal reaction, which avoids unwanted side reactions with proteins during the cross-linking process. Furthermore, the use of stable hydrogels allows studying the effects of the different linker molecules on protein release without having to consider hydrogel swelling and degradation. For *in vivo* application, the hydrogels could be cross-linked, for example, by strain-promoted azide-alkyne cycloadditions, thiolene reactions or Michael additions [92]. Gel degradation could be achieved by introducing hydrolytically or enzymatically cleavable groups. Alternatively, PEG macromonomers could be cross-linked by Diels-Alder reactions. The resulting hydrogels were recently shown to dissolve after several weeks of incubation at body temperature [46].

3.4. Conclusion

The use of aromatic succinimidyl carbonate linkers is a promising strategy for the reversible PEGylation of proteins. Succinimidyl carbonates react with lysine residues of proteins to generate degradable carbamate groups. The kinetics of PEG chain elimination can be controlled by the substitution pattern of the generated carbamates. These linker groups were integrated into star-shaped, cross-linkable PEG macromonomers. When formulated into hydrogels, present proteins are reversibly tethered to the polymer network and immobilized. Such systems could serve the localized delivery of therapeutic proteins in certain applications, where controlled protein release over days to weeks is required. The release of the tethered proteins is then controlled by the decomposition of the linker molecules rather than protein diffusion. Most importantly, linker decomposition is ‘traceless’, which helps to preserve protein bioactivity and reduces the risk of immunological reactions. One remaining problem is the incomplete and comparatively fast protein release over a maximum of three weeks. This could be addressed by further modifying the chemical structure of the linker molecules, for example by introducing additional electron donating groups or shielding the carbamates with bulky side groups. Altogether, tethering proteins by degradable carbamate groups is a promising strategy to control their release from hydrogels independent from diffusion, swelling or degradation.

Chapter 4

Cleavable Carbamate Linkers: Determination of Elimination by SEC

Abstract

A method to separate free lysozyme and PEGylated derivatives by size exclusion chromatography (SEC) was established. The measurements were performed on a TSKgel G3000SW$_{XL}$ column using 0.3 M NaCl in 0.05 M phosphate buffer pH 6.9 containing 20 % ethanol as mobile phase. A special device allowed for holding the samples at 37 °C during the experiment. The method enabled to follow PEG chain elimination over time. Quantification of the recorded chromatograms showed complete elimination after about 26 h with a maximum amount of 73.6 % (sample 1) and 75.9 % (sample 2) of free lysozyme, respectively.

4.1. Introduction

Different methods, like high-performance liquid chromatography (HPLC), Sodium dodecyl sulfate (SDS) polyacrylamide gel electrophoresis (PAGE), matrix-assisted laser desorption ionization mass spectrometry (MALDI MS) or capillary electrophoresis (CE), are commonly used to analyze PEGylated proteins with regard to the number of attached PEG chains, the extent of PEGylation, and the kinetics of PEGylation and De-PEGylation [84, 93–96]. In Chap. 3, the investigation of PEGylation and PEG chain elimination by SDS-PAGE was introduced. Although the method worked reliably, SDS-PAGE has some drawbacks such as a protein stressing sample preparation and a time consuming experimental procedure. Samples for SDS-PAGE had to be frozen at defined time points to stop the elimination process, stored at –20 °C until measurement, and thawed just before gel electrophoresis. During this process of freezing and thawing the risk of protein aggregation is increased due to the intermediate presence of an ice-water interface stimulating nucleation of aggregates [7]. To avoid this, real-time measurements at each defined time point would be the optimal way of sample handling. Furthermore, gel preparation, running and staining is time consuming and must be carried out manually. Moreover, the gel precursor, acrylamide, is toxic in its un-polymerized form. It may cause cancer and genetic defects, and it is suspected to be harmful to human fertility. Using HPLC, the whole measurement process can be automated avoiding time consuming and toxic gel preparation and allowing real-time measurements.

Generally, HPLC is a frequently used method in the entire field of protein analysis and purification [97]. Different HPLC techniques are available to analyze proteins in general and PEGylated proteins in particular. One common technique is reversed phase HPLC (RP-HPLC). Here, separation is based on hydrophobic interactions between the protein, the stationary phase, and the mobile phase [97]. Zalipsky et al. used RP-HPLC to follow elimination of thiolytically cleavable PEG linkers [93]. However, gradients containing organic solvents as mobile phase limit its use for preparative applications due to protein denaturation [98]. Separation by charge, ion-exchange chromatography, is another frequently used chromatographic technique to separate PEGylated proteins [97]. The separation is based on analyte binding to the charged stationary phase by exchange reactions with the counterions of the functional group of the column. Afterwards, an excess of counterions in the eluent or a pH gradient initiate displacement of the analyte

[26, 98]. In the case of PEGylated proteins, ion-exchange chromatography can be used to separate PEGylated proteins depending on the site of PEGylation [99]. Isoforms differ in protein areas shielded by the attached PEG groups and therefore, in surface charge distribution [99]. This makes ion-exchange chromatography suitable for determining the sites of PEGylation of different isoforms [100]. Furthermore, ion-exchange chromatography is often used to separate PEGylated and unreacted components for purification purposes [93, 94, 101].

Furthermore, separation by size is used in protein analytics. In size exclusion chromatography (SEC) separation is based on interaction with a porous stationary phase consisting of porous dextran, agarose, polyacrylamide or silica particles [97, 98]. During elution, the solutes diffuse into and out of the pores and are, thereby, sorted by size; the solutes too big to enter the pores are eluted first, followed by smaller components with longer pore residence time [98]. In case of PEGylated proteins, the hydrodynamic radius is markedly increased compared to native proteins [8]. Due to the absence of intramolecular interactions (e.g., disulfide bonds, hydrogen bonds, van der Waals interactions) and the ability to bind approximately 16 water molecules per ethoxy group, PEG is shaped as a coil with large hydrodynamic radius in aqueous media [8]. This makes SEC ideally suited to follow the PEGylation process and quantify the degree of PEGylation [26, 95, 102]. The eluent does not directly influence the separation process. For natural polymers, such as proteins, aqueous buffers are useful to control the pH during the experiment and to prevent denaturation in preparative separation (gel filtration chromatography (GFC)) [97, 103]. Further techniques like normal-phase chromatography, hydrophobic interaction chromatography, or immunoaffinity chromatography are less common for separating PEGylated proteins [104, 105].

In the following experiments, SEC was used to analyze PEGylated lysozyme. SEC operates with non-toxic aqueous buffer systems [106]. Furthermore, the method is simple and reproducible, and all required components are commercially available [106, 107]. A method was established to separate free lysozyme from PEGylated derivatives. For method development, lysozyme was irreversibly PEGylated by linker **2d** (**Table 4.1**). For elimination experiments, lysozyme was PEGylated using the rapidly hydrolyzing linker **2a** (Table 4.1). The recorded SEC chromatograms were used to quantify the increasing amounts of free lysozyme during PEG chain elimination.

4.2. Materials and Methods

4.2.1. Materials

Narrow opening screw caps (black) with septa and 2 mL screw vial (amber) were purchased from BGB Analytik Vertrieb (Schlossboekelheim, Germany). Deuterated chloroform ($CDCl_3$) was purchased from Deutero GmbH (Kastellaun, Germany). Acetonitril, N,N'-discuccinimidyl carbonate (DSC), lysozyme (from chicken egg white) and methoxy poly(ethylene glycol) with a molecular weight of 5 kDa were purchased from Sigma-Aldrich (Taufkirchen, Germany). GHP Acrodisc® 13 mm syringe filters (0.2 µm pore size) were purchased from Pall GmbH (Dreieich, Germany). Sodium chloride was purchased from VWR International GmbH (Darmstadt, Germany). Spartan 30 / 0.2 RC syringe filters were purchased from Whatman GmbH (Dassel, Germany). Methylene chloride (DCM), diethyl ether and ethanol were from CSC Jäcklechemie (Nürnberg, Germany). All other chemicals were purchased from Merck KGaA (Darmstadt, Germany). Purified water was freshly prepared each day using a Milli-Q water purification system from Millipore (Schwalbach, Germany).

4.2.2. ^{1}H-NMR Spectra

^{1}H-NMR spectra were recorded in $CDCl_3$ at room temperature using a Bruker Avance 300 spectrometer (Bruker BioSpin GmbH, Rheinstetten, Germany).

4.2.3. Synthesis of Linker 2a

Linker **2a** (Table 4.1) was synthesized as described in Chap. 3 [35].

4.2.4. Synthesis of Linker 2d

Linker **2d** (Table 4.1) was synthesized according to a procedure described by Brandl et al. [64]. In brief, 5.0 g (1 mmol) of dried mPEG5k-OH and 1.3 g (5 mmol) of DSC were dissolved in 50 mL of acetonitrile; 645 µL of pyridine were added and the reaction mixture was stirred over night at room temperature. The next day, the acetonitrile was evaporated under reduced pressure. Afterwards, the residue was dissolved in dichloromethane and the insoluble residue was filtered off. The solution was concentrated under reduced pressure and precipitated at 0 °C by dropwise addition of diethyl ether. The precipitate was dried under vacuum to yield 4.55 g (88.5 %) of linker 2d.

^{1}H-NMR ($CDCl_3$, 300 MHz): δ 2.86 ppm (s, 4 H, –C(O)CH_2CH_2C(O)–), 3.40 ppm (s, 3 H, H_3CO–), 3.66 ppm (s, –OCH_2CH_2–), 4.46 ppm (t, 2 H, –OCH$_2$CH_2OC(O)O–).

Table 4.1: Linear poly(ethylene glycol) linkers (molecular weight 5 kDa)

Linker	Chemical structure
2a	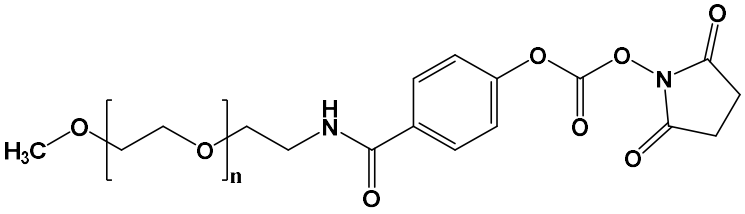
2d	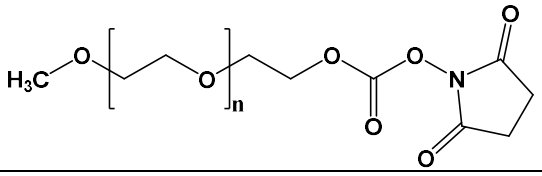

4.2.5. Size Exclusion Chromatography

SEC experiments were performed using a Shimadzu HPLC system (Shimadzu Europa GmbH, Duisburg, Germany). The HPLC installation consisted of a SCL–10A VP controller, an auto injector SIL–10AD VP, a pump LC–10AT and a column oven CTO–6A. The fluorescence detector RF-551 was used for protein detection (λ_{ex} 295 nm, λ_{em} 360 nm). Furthermore, the degasser WellChrom K-5004 was used to prevent air bubbles in the system (Wissenschaftliche Gerätebau Dr. Ing. Herbert Knauer GmbH, Berlin, Germany).

For separation of free and PEGylated lysozyme, a TSKgel G3000SW$_{XL}$ column (7.8 mm x 30 cm; 5 µm particle size; 250 Å pore size) (Tosoh Bioscience GmbH, Stuttgart, Germany) was used at a flow rate of 1 mL/min and 25 °C. The mobile phase consisted of 0.3 M NaCl in 0.05 M phosphate buffer pH 6.9 containing 20 % ethanol. The mobile phase was filtered through a cellulose membrane syringe filter (Spartan 30 / 0.2 RC syringe filter) before use.

4.2.6. SEC Method Establishment

A lysozyme stock solution (conc. 1 mg/mL) was prepared in 25 mM phosphate buffer pH 7.4. For PEGylation, 50.0 mg (9.8 µmol) or 12.5 mg (2.4 µmol) of linker **2d** were dissolved in 5 mL of the lysozyme stock solution (2.4 µmol amino groups) and incubated for 1 h at room temperature. The ratio of reactive succinimidyl groups

(SC) : amino groups of lysozyme (NH_2) was 28:7 and 7:7, respectively. The lysozyme stock solution and PEGylated lysozyme were diluted to a protein concentration of 0.1 mg/mL. All samples were filtered through a hydrophilic propylene membrane syringe filter (GHP Acrodisc® 13 mm syringe filter). For SEC, 10 µL of each sample were injected automatically. Chromatograms of all samples were recorded using the method described above.

4.2.7. Determination of Linker Elimination

A lysozyme stock solution (conc. 1 mg/mL) was prepared in 25 mM phosphate buffer pH 7.4. For PEGylation, 12.5 mg of linker **2a (**2.4 µmol) were incubated in 5 mL of the lysozyme stock solution (2.4 µmol amino groups) for 1 h at room temperature. The ratio of SC: NH_2 groups was 7 : 7. The experiment was done in duplicate; PEGylation of the second sample was started with a time delay of 1 h.

Directly after PEGylation, the determination of the elimination kinetics of the first sample via SEC was started; the second sample was started one hour later. To this end, the samples were diluted to a protein concentration of 0.1 mg/mL and filtered through a hydrophilic propylene membrane syringe filter (GHP Acrodisc® 13 mm syringe filter). The sample vials were put in the auto injector rack and heated to 37 °C using a special device (**Figure 4.1**).

To determine the elimination kinetics, 10 µL of the sample were injected at defined time points. Every 58 min, a new measurement run was started. Sample 1 and sample 2 were injected alternating; this resulted in a measurement interval of 2 h for each sample. The elution of protein derivatives from the column was recorded by a fluorescence detector over 20 min (λ_{ex} 295 nm, λ_{em} 360 nm) for each sample. The chromatograms were analyzed by the Class VP software (Shimadzu Europa GmbH, Duisburg). For quantification, the amount of free lysozyme was calculated from the area under the curve using a calibration curve (see below) and normalized to the total initial amount of lysozyme (1 mg/mL). Furthermore, the peak areas of free and PEGylated lysozyme were normalized to the total peak area.

4.2.8. Sample Heating during PEG Chain Elimination

Using the temperature regulator of the auto injector, room temperature could be reached at the most because the auto injector is not designed for heating. Therefore, a way had to be found to hold the samples at body temperature (37 °C) during the experiment. To this

end, a special device (Figure 4.1) was manufactured to heat samples to 37 °C during the experiment.

The heating device consisted of a metal block equipped with round boreholes on the top to provide the vials for sample injection. Connections to a water bath at both ends ensured water circulation inside the metal block and sample heating during the experiment.

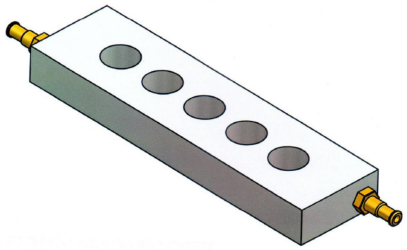

Figure 4.1: Device for sample heating during determination of PEG chain elimination. (Schematic drawings and manufacturing of the device were kindly realized by Stefan Kolb and Herbert Tischhoefer.)

4.2.9. Calibration

For calibration, the lysozyme stock solution was diluted to concentrations between 0.02 mg/mL and 0.1 mg/mL. The samples were filtered through a hydrophilic propylene membrane syringe filter (GHP Acrodisc® 13 mm syringe filter). For quantification, 10 µL of each concentration were injected. The chromatograms were recorded using the fluorescence detector RF-551 (λ_{ex} 295 nm, λ_{em} 360 nm) and the areas under the curve were determined using the Class VP software (Shimadzu Europa GmbH, Duisburg).

4.3. Results and Discussion

4.3.1. Method Establishment

Stationary and Mobile Phase

SEC experiments were performed using a column containing a silica-based, hydrophilic bonded phase packing and a mobile phase composed of ethanol and 0.3 M NaCl in 0.05 M phosphate buffer pH 6.9. Silica-based packings are less compressible compared to other packings, like agarose or dextran based packings, and suitable for higher pressure due to their mechanical robustness [98]. The non-derivatized surface silanol groups of the packing show a pK_a of 3.5 to 4.0 and are, therefore, deprotonated at

neutral conditions [98, 109]. Lysozyme (pI 11) is positively charged under these conditions and would be adsorbed on the stationary phase [109, 110]. To prevent the overlaying of size exclusion effects by ionic interactions between lysozyme and the column packing, the mobile phase was adjusted to intermediate ionic strength with NaCl [97, 98, 107, 109, 111]. A drawback of SEC is the short life time of the column, especially in the presence of PEG. Ethanol was added to the mobile phase to prevent PEG induced degradation of the column [112]. Hydrogen bonding or dipolar interactions between the ether functions of PEG and the diol functionalized silica surface are assumed to be the reason for column degradation [112]. The addition of ethanol prevents those interactions between PEG and the stationary phase [112].

For the same column, Conze et al. and Christel et al. suggested another mobile phase composed of 0.1 M Na_2SO_4 in 0.1 M phosphate buffer pH 6.7 for the separation of free lysozyme, mono-PEGylated and di-PEGylated species [99, 113]. However, this method could not be successfully applied. Peak separation of free and PEGylated lysozyme was insufficient using the respective mobile phase. Furthermore, the eliminated PEG chain of linker **2a** was eluted at the same time as free lysozyme interfering with qualitative and quantitative analysis.

Retention of Lysozyme Derivatives

For method establishment, the individual components were characterized first. An overlay of the detected chromatograms is shown in **Figure 4.2**.

Free lysozyme was eluted from the column after about 11.4 min. PEGylated lysozyme was eluted faster compared to unmodified lysozyme. The increased size due to the attached PEG chains led to less interaction with the stationary phase and faster elution from the column. To prevent PEG chain elimination during development of the method, lysozyme was irreversible PEGylated with linker **2d.** Linker **2d** forms aliphatic carbamates with primary amines [64]. Due to the absence of an aromatic spacer, the carbamate bond is not degradable under the used conditions [64]. Two different ratios of reactive succinimidyl (SC) to protein amino groups (7 : 7 and 28 : 7) were used for PEGylation to create different degrees of protein modification as determined by SDS-PAGE [35]. Lysozyme PEGylated with an excess of linker **2d** (28 : 7) was eluted after about 7.9 min. No free lysozyme was detected in this case. After incubation with less linker **2d** (SC : NH_2 7 : 7) a small amount of free lysozyme was detected at about 11.4 min. Different derivatives of PEGylated lysozyme were eluted after about

10.8 min, 9.5 min, and 8.5 min. However, a clear separation of mono-, di-, and tri-PEGylated lysozyme derivatives was not possible. Maybe PEGylation with a higher molecular weight PEG would improve resolution. Nevertheless, the overlay of the individual chromatograms clearly demonstrated that the method is suitable to separate free and PEGylated lysozyme and to follow PEG chain elimination.

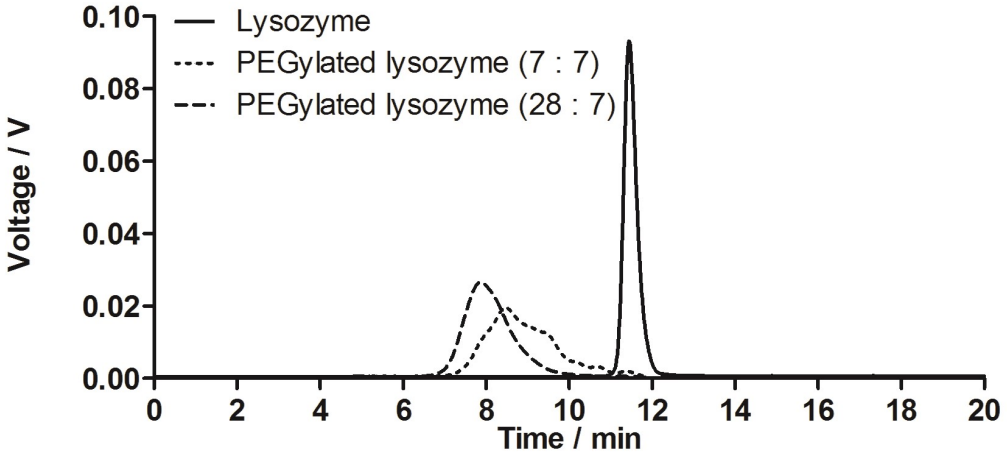

Figure 4.2: Chromatograms of lysozyme and irreversible PEGylated lysozyme. The ratio of SC : NH_2 groups during irreversible PEGylation was 7 : 7 and 28 : 7. Samples were detected by a fluorescence detector (λex 295nm, λem 360nm).

4.3.2. PEG Chain Elimination

Retention of Lysozyme Derivatives

For SDS-PAGE experiments (see Chap. 3), samples taken during elimination process were stored at -20 °C until measurement to stop hydrolysis. To circumvent protein denaturation and changes within the sample by freezing and thawing, the elimination samples for SEC were incubated in HPLC vials and directly injected at defined time points.

Figure 4.3 exemplarily shows an overlay of two chromatograms detected during PEG chain elimination. At the beginning of the experiment (0 h), lysozyme was freshly PEGylated with linker **2a.** PEGylated lysozyme was eluted first (11.3 min) because of its increased size compared to free lysozyme. A small amount of lysozyme remained unmodified and was eluted after about 12.6 min. During incubation, linker **2a** was hydrolyzed and, thereby, the amount of free lysozyme increased. After 24 h of incubation, the peak of free lysozyme was clearly enlarged. At this time, free lysozyme was eluted after about 12.5 min, while the PEGylated lysozyme was already eluted after

about 10.7 min. The peak shift of PEGylated lysozyme might be a first indicator for column degradation during the sequence.

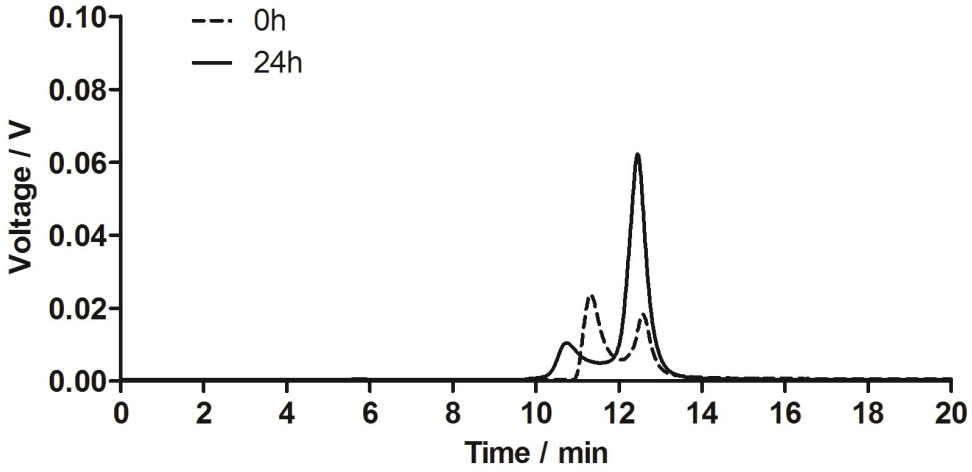

Figure 4.3: Elimination of linker 2a from lysozyme. Chromatograms after 0 h and 24 h detected by a fluorescence detector (λex 295nm, λem 360nm).

Problems, which could be traced back to column degradation, manifested after about 160 injections. The peak for PEGylated lysozyme disappeared from the chromatograms, probably meaning that PEGylated lysozyme was no longer eluted from the column. Furthermore, the maximum pressure was exceeded a couple of times, indicating clogging of the column. After another 75 injections, the broadness of the lysozyme peak increased to a time span of about 20 min. Several cleaning steps could not improve the resolution, indicating final column degradation. In the future, column life time could be possibly extended by purifying the samples from unreacted PEG by ion-exchange chromatography, for example [94].

Besides monitoring PEG chain elimination, SEC can be used as an indicator for the stability of protein formulations [98]. Dimerization and aggregation, as a consequence of instability, are detectable due to the increased protein size [98]. The appearance of lysozyme in only one peak without shifts in the retention time indicates protein stability during PEGylation and PEG chain elimination. This is in good agreement with the data already obtained by CD spectroscopy and Micrococcus assay (see Chap. 3). The different retention times determined during method establishment and elimination experiments can be explained by the use of two different columns of the same type with different age and small variations in column packing.

Quantification

For quantification, lysozyme calibration solutions of different concentrations were injected at the end of the sequence (**Figure 4.4**). As expected, the peak area increased with increasing lysozyme concentration. The retention time (12.5 min) corresponded to the retention time of the unmodified lysozyme fraction during PEG chain elimination.

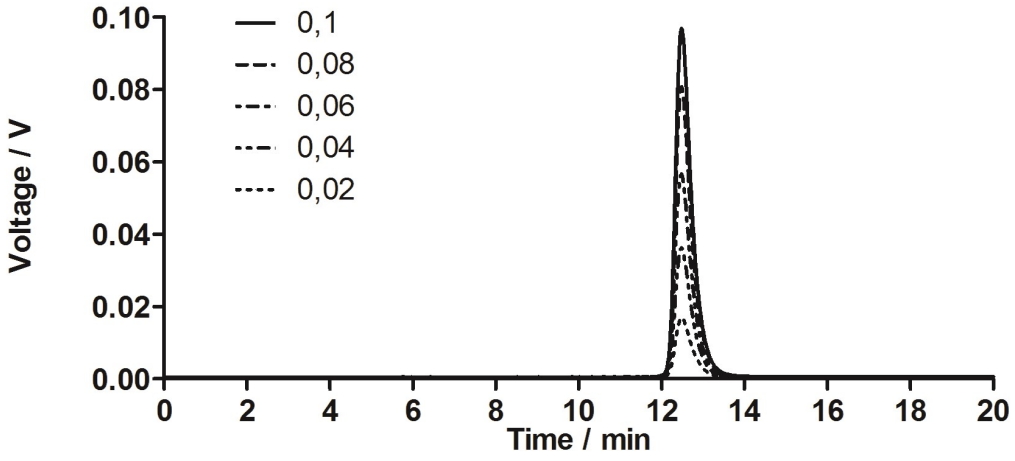

Figure 4.4: Chromatograms of different lysozyme concentrations from 0.02 mg/mL to 0.1 mg/mL were detected using a fluorescence detector (λex 295nm, λem 360nm) for lysozyme calibration.

The resulting calibration curve was used to quantify the increasing amount of free lysozyme during PEG chain elimination (**Figure 4.5** A). Directly after PEGylation, only 24.5 % (sample 1) and 28.1 % (sample 2) of the protein, respectively, remained unmodified. Over time, the amount of free lysozyme increased due to linker hydrolysis. After about 26 h, with a maximum amount of 73.6 % (sample 1) and 75.9 % (sample 2) of free lysozyme, respectively, PEG chain elimination was completed. Quantification of the PEGylated lysozyme using the calibration shown in Figure 4.4 was not possible, because the fluorescence of the aromatic linker groups might interfere with the fluorescence of the protein. For further information about the kinetics of PEG chain elimination, the peak areas of free and PEGylated lysozyme were normalized to the total peak area as shown in Figure 4.5 B. Due to the possibly interfered fluorescence described above the obtained data must be understood as an indication of the order of magnitude not as absolute values. The fraction of free lysozyme increased from 44.8 % (sample 2: 39.3 %) to 82.4 % (sample 2: 82.9 %) within 24 h, while the fraction of PEGylated lysozyme decreased from 55.2 % (sample 2: 60.7 %) to 17.6 % (sample 2: 17.1 %). This is in good agreement with the data obtained by SDS-PAGE (see Chap. 3).

When normalizing the lysozyme band to the sum of all bands per lane, an increase of free lysozyme from 43.0 % ± 2.5 % to 63.4 % ± 3.7 % after 24 h was detected [35].

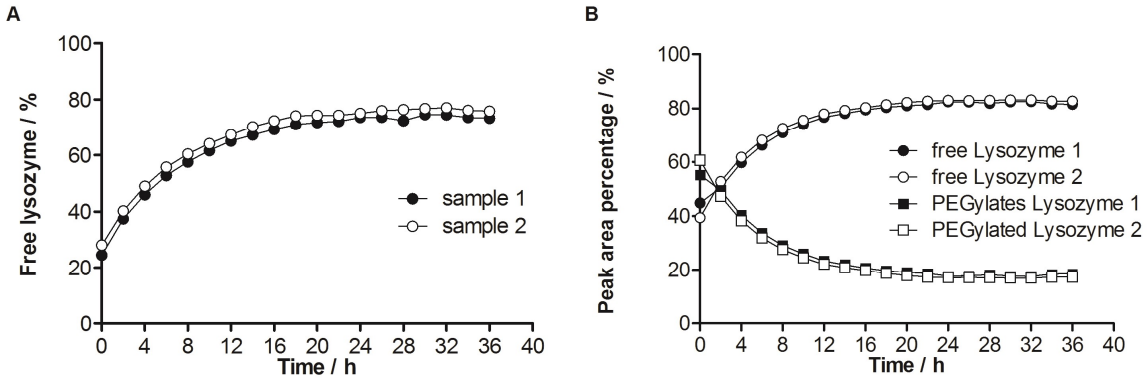

Figure 4.5: Elimination of linker 2a from lysozyme. The amount of free lysozyme as determined by SEC. Concentration of free lysozyme calculated using calibration curve (A). Peak area percentage of free and PEGylated lysozyme (B).

These results prove that SEC is an adequate alternative to SDS-PAGE for the purpose of following PEG chain elimination and quantification of released lysozyme. Investigation of PEG chain elimination using linker **2b** or **2c** (see Chap. 3) should also be possible with the introduced method. However, a new column has to be used in each experiment.

4.4. Conclusion

A SEC method to separate PEGylated and non-PEGylated lysozyme was established. A TSKgel G3000SWXL column and a mobile phase containing 0.3 M NaCl in 0.05 M phosphate buffer pH 6.9 and 20 % ethanol proved to be appropriate to follow PEG chain elimination over time. After about 26 h, no further increase of lysozyme was detected indicating that PEG chain elimination was completed. No shift or double peak of lysozyme was observed during the experiments. This indicates structural integrity and the absence of aggregates during PEGylation and PEG chain elimination. Data regarding elimination kinetics as well as structural integrity was in good agreement with the results described in Chap. 3. SEC proved as an adequate alternative to SDS-PAGE for the determination of elimination kinetics.

Chapter 5

Protein Compatibility of Selected Cross-linking Reactions for Hydrogels

The content of this chapter has been published in: Nadine Hammer, Ferdinand P. Brandl, Susanne Kirchhof, Viktoria Messmann, Achim M. Goepferich. Protein compatibility of selected cross-linking reactions for hydrogels. *Macromolecular Bioscience*, 15 (3): 405–413, 2015. doi:10.1002/mabi.201400379.

Author contributions: F.P.B., A.M.G., and N.H. designed the concept and the experiments; N.H., S.K., and V.M. performed the experiments; F.P.B., A.M.G., and N.H. interpreted and discussed the data and wrote the manuscript.

Acknowledgements: The authors thank Prof. Dr. Jens Schlossmann and the Department of Pharmacology and Toxicology at the University of Regensburg for providing access to the ChemiDoc™ MP gel imaging system. The authors thank the German Research Foundation (DFG), grant number GO 565/16-1 for financial support.

Abstract

The protein compatibility of selected cross-linking reactions was investigated. Lysozyme was incubated with methoxy poly(ethylene glycol) (mPEG5k) derivatives. Formed protein-polymer conjugates were analyzed by gel electrophoresis. Michael-type addition reactions of nucleophilic amino acids, especially lysine residues, to maleimide, vinyl sulfone and acrylamide groups were detected. The degree of modification depended on the polymer species and the pH. Complete modification with more than five PEG chains was observed after incubation with mPEG5k-vinyl sulfone at pH 9, whereas 96 % of the introduced protein remained unmodified after incubation with mPEG5k-acrylamide at pH 4. Incubation with mPEG5k-thiol resulted in thiol-disulfide exchange reactions; 83 % to 93 % of the introduced lysozyme remained unaffected. Hydrogel preparation was simulated by using mixtures of mPEG5k-maleimide and mPEG5k-furan, mPEG5k-vinyl sulfone and mPEG6k-thiol, mPEG5k-acrylamide and mPEG6k-thiol, or mPEG5k-acrylamide and a radical initiator. Protein modifications were detected, which may affect the protein structure, decrease activity and bioavailability, and increase the risk for immune responses.

5.1. Introduction

Hydrogels are attractive for biomedical applications because of their chemical versatility and favorable properties. For example, hydrogels are considered biocompatible, they exhibit mechanical properties similar to those of the natural extracellular matrix, they can be made biodegradable, and they can be injected by minimally invasive techniques [12, 114, 115]. Among the many possible applications, the use of hydrogels as delivery system for therapeutic peptides and proteins seems especially promising [12, 115]. As a consequence of this, different strategies of hydrogel preparation have been proposed and investigated over the past decades. Compared to physical cross-linking (e.g., by hydrophobic or ionic interactions), chemical or covalent cross-linking has the benefit of forming more stable hydrogels and allows fine-tuning of the resulting release rates [12, 51, 115]. Several cross-linking reactions are frequently used for hydrogel preparation. One prominent example is radical polymerization of acrylate, methacrylate or acrylamide groups, which can be triggered by various initiators (e.g., peroxides or persulfates) or irradiation with light [116–120]. Michael-type addition reactions between thiol groups and acrylate groups [121, 122], vinyl sulfone groups [56, 115, 123, 124], or maleimide groups [125–127] are another possibility to prepare hydrogels at physiological conditions. Besides acting as electrophiles in Michael-type addition reactions, maleimides can react with conjugated dienes by means of Diels-Alder reactions. Thanks to its high efficiency and selectivity, the Diels-Alder reaction has been investigated as a cross-linking mechanism for hydrogels [128, 129]. For example, Kirchhof et al. functionalized star-shaped poly(ethylene glycol) (PEG) with furyl and maleimide groups. Step-growth polymerization of the two macromonomers yielded covalently cross-linked hydrogels that might be suitable for the controlled release of therapeutic proteins [46].

If hydrogels are used for controlled protein delivery, the stability and availability of the incorporated proteins must be ensured. Proteins can be loaded into hydrogels by incubating cross-linked gels in concentrated protein solutions (post-fabrication partitioning) or by *in situ* encapsulation during cross-linking. The former technique has the advantage of preserving protein stability; however, it offers less control over the amount of protein loading [51]. Furthermore, injection of pre-formed hydrogels might not always be possible [130]. On the other hand, *in situ* encapsulation permits the preparation of hydrogels loaded with large quantities of proteins in a fast and

reproducible manner. However, side reactions during cross-linking can affect the bioactivity of proteins, decrease their availability, and trigger undesired immune responses [12, 51]. This chapter reports on the protein compatibility of cross-linking reactions that are frequently used for the preparation of hydrogel-based protein delivery systems. As a model polymer, methoxy poly(ethylene glycol) functionalized with maleimide, vinyl sulfone, acrylamide, furyl, and thiol groups was investigated; lysozyme served as a model protein to determine occurring side reactions. Protein modifications, like Michael-type addition reactions of nucleophilic amino acids or thiol-disulfide exchange reactions were detected by sodium dodecyl sulfate (SDS) polyacrylamide gel electrophoresis (PAGE). Although possible side reactions between proteins and cross-linking agents are discussed in the literature, no in-depth analysis of the protein compatibility of common cross-linking mechanisms has been done so far. To the best of our knowledge, this is the first study comparing the protein compatibility of cross-linking reactions under standardized conditions.

5.2. Materials and Methods

5.2.1. Materials

Tetramethylethylenediamine (TEMED) was obtained from Carl Roth GmbH & Co. KG (Karlsruhe, Germany). 2-Amino-2-hydroxymethyl-propane-1,3-diol (TRIS) was purchased from GE Healthcare Europe GmbH (Freiburg, Germany). Dulbecco's phosphate-buffered saline (PBS) was obtained from Invitrogen GmbH (Karlsruhe, Germany). Methoxy poly(ethylene glycol) vinyl sulfone with a molecular weight of 5 kDa (mPEG5k-vinyl sulfone, **Table 5.1**) was puchased from JenKem Technology (Allen, TX, USA). Iodine was obtained from Riedel-de Haën AG (Seelze, Germany). Acrylamide/bisacrylamide solution (37.5 : 1), bromphenol blue sodium salt and sodium dodecylsulfate were purchased from Serva Electrophoresis GmbH (Heidelberg, Germany). Coomassie brilliant blue G-250, lysozyme (from chicken egg white), methoxy poly(ethylene glycol) with a molecular weight of 5 kDa, poly(ethylene glycol) methyl ether thiol with a molecular weight of 6 kDa (mPEG6k-thiol, Table 5.1) and sodium tetraborate decahydrate were obtained from Sigma-Aldrich (Taufkirchen, Germany). All other chemicals were purchased from Merck

KGaA (Darmstadt, Germany). Deionized water was obtained by using a Milli-Q water purification system from Millipore (Schwalbach, Germany).

5.2.2. Synthesis of PEG Derivatives

Methoxy poly(ethylene glycol) maleimide, molecular weight 5 kDa (mPEG5k-maleimide, Table 5.1) and methoxy poly(ethylene glycol) 3-(furan-2-yl)propanamide, molecular weight 5 kDa (mPEG5k-furan, Table 5.1) were synthesized according to previously published protocols [46]. Methoxy poly(ethylene glycol) acrylamide, molecular weight 5 kDa (mPEG5k-acrylamide, Table 5.1) was synthesized from methoxy poly(ethylene glycol) amine as described by Browning et al. [34, 120].

Table 5.1: Linear poly(ethylene glycol) derivatives

Name	Chemical structure
mPEG5k-maleimide	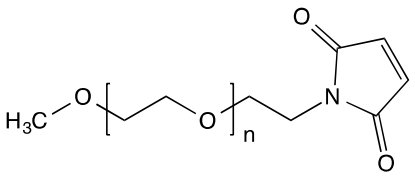
mPEG5k-furan	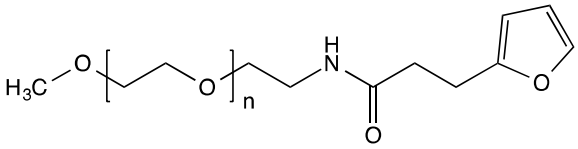
mPEG5k-vinyl sulfone	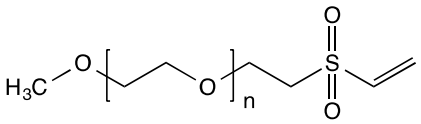
mPEG5k-acrylamide	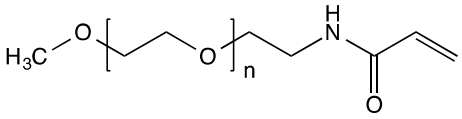
mPEG6k-thiol	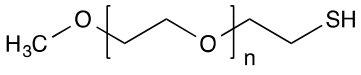

5.2.3. Protein Reactivity of Different PEG Derivatives

Lysozyme stock solutions (c = 1.33 mg/mL) were prepared in water, 25 mM acetate buffer pH 4.0, 25 mM acetate buffer pH 5.0, 25 mM phosphate buffer pH 6.0, PBS (pH 7.0 – 7.2) and 50 mM borate buffer pH 9.0. To determine the protein reactivity, 1.83 µmol of each polymer (Table 5.1) were dissolved in 400 µL of the prepared lysozyme stock solutions and incubated for 24 h at 37 °C. Additionally, stoichiometric mixtures of mPEG5k-maleimide and mPEG5k-furan, mPEG5k-vinyl sulfone and mPEG6k-thiol, and mPEG5k-acrylamide and mPEG6k-thiol in 400 µL of lysozyme stock solution were investigated; 1.83 µmol of each polymer were used. In a further experiment, 1.83 µmol of mPEG5k-acrylamide in 400 µl of lysozyme stock solution were combined with a radical initiator consisting of 4 % (m/m) ammonium persulfate and 2 % (m/m) TEMED based on the polymer mass. SDS-PAGE was used to analyze the resulting protein-polymer conjugates [35]. In brief, polyacrylamide gels of 14 % cross-linking were run for about 1.5 h at a constant voltage of 120 V and a decreasing current starting at 68 mA. The protein amount was 27.93 µg per lane. The gels were stained with Coomassie brilliant blue G-250 and imaged with a ChemiDoc™ MP gel imaging system (Bio-Rad Laboratories GmbH, München, Germany). The relative abundance of the different protein species was determined by using the software Image Lab™ (Bio-Rad Laboratories GmbH, München, Germany). Afterwards, the conjugated PEG chains were visualized by iodine staining as described by Natarajan [65]. All conjugation studies were done in triplicate and the results are presented as means ± standard deviations.

5.3. Results and Discussion

5.3.1. Results

The protein-polymer conjugates that formed during incubation with hydrogel cross-linking agents were analyzed by SDS-PAGE. **Figure 5.1** exemplarily shows the modification of lysozyme with mPEG5k-maleimide at different pH-values.

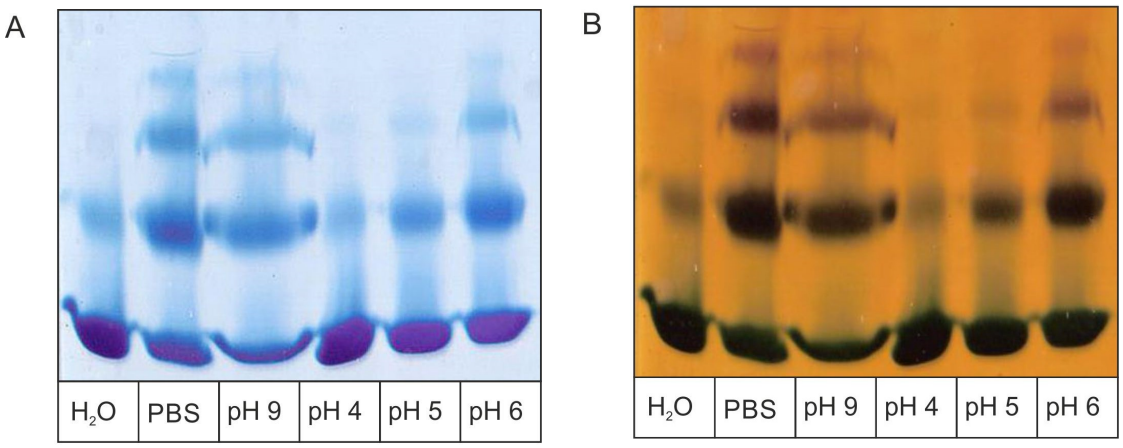

Figure 5.1: Modification of lysozyme with mPEG5k-maleimide analyzed by SDS-PAGE. Gels were stained with Coomassie brilliant blue (A) and barium iodide (B). Lysozyme was incubated with the polymer at different pH values at 37 °C for 24 h.

After protein staining with Coomassie brilliant blue, the conjugated PEG chains were visualized by an iodine staining. In this way, protein species with attached PEG chains appeared as brown spots, while free lysozyme was detected by its dark blue staining. The relative abundance of free and modified lysozyme was determined and the results are presented in **Figure 5.2**.

Lysozyme incubated with mPEG5k-maleimide was modified with one to three PEG chains. Depending on the pH of the incubation medium, the amount of unmodified lysozyme decreased from 79 ± 1.1 % (pH 4) to 36 ± 1.8 % (pH 9); 76 ± 4.3 % of the total protein amount were unmodified after incubation with mPEG5k-maleimide in water (Figure 5.2 A). When lysozyme was incubated with mPEG5k-vinyl sulfone, the degree of modification increased with increasing pH (Figure 5.2 B). In water and at pH 4, lysozyme was modified with one PEG chain, at pH 5 with two PEG chains, at pH 6 with three PEG chains and in PBS with four PEG chains. At pH 9, lysozyme was completely modified with more than five PEG chains; the highest amount of free lysozyme (87 ± 3.2 %) was detected at pH 4. Incubation with mPEG5k-acrylamide caused conjugation of one or two PEG chains per protein molecule at pH 9 (Figure 5.2 C). With increasing pH, the relative abundance of free lysozyme decreased from 96 ± 1.2 % (pH 4) to 64 ± 1.2 % (pH 9).

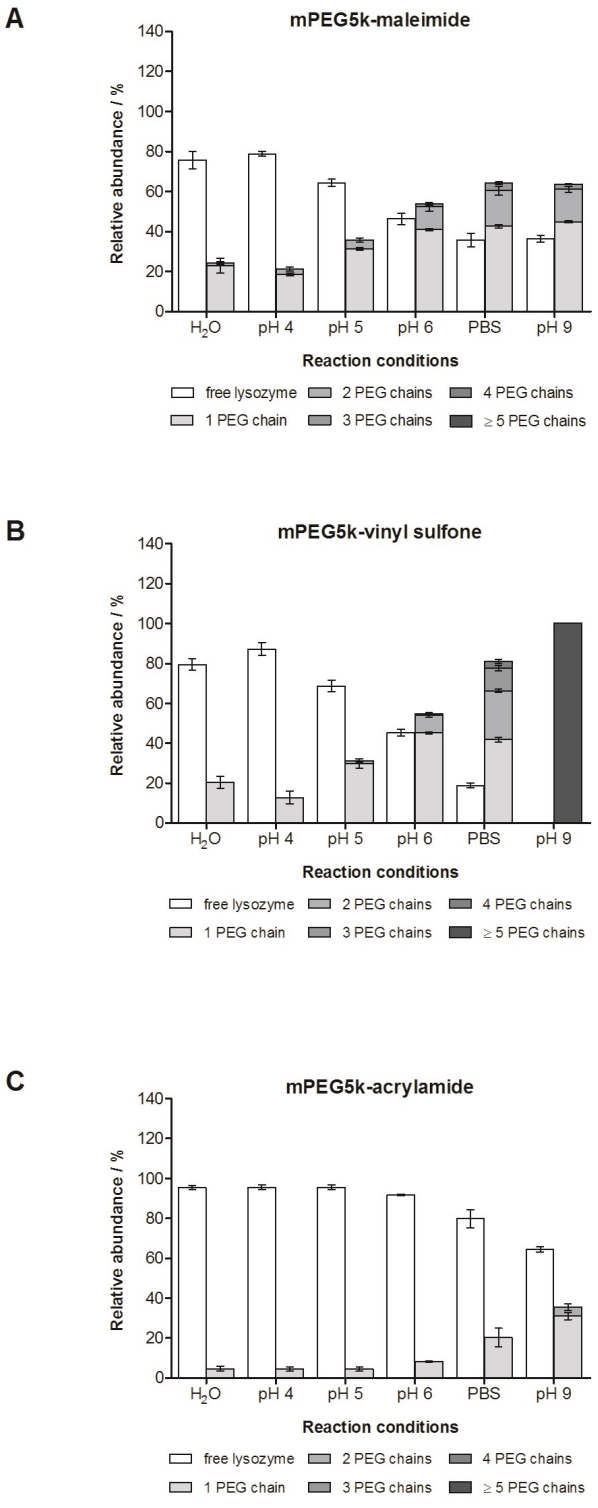

Figure 5.2: Modification of lysozyme with mPEG5k-maleimide (A), mPEG5k-vinyl sulfone (B), and mPEG5k-acrylamide (C) at different pH-values. The relative abundance of the different lysozyme species was determined by SDS-PAGE. The gray scale indicates the number of attached PEG chains. The experiments were done in triplicate and the results are shown as means ± standard deviations.

After incubation with mPEG6k-thiol, lysozyme was modified with one to two PEG chains (**Figure 5.3**). The degree of modification did not depend on the pH; 83 ± 0.9 % (water) to 93 ± 0.8 % (pH 6) of the total lysozyme amount remained unmodified.

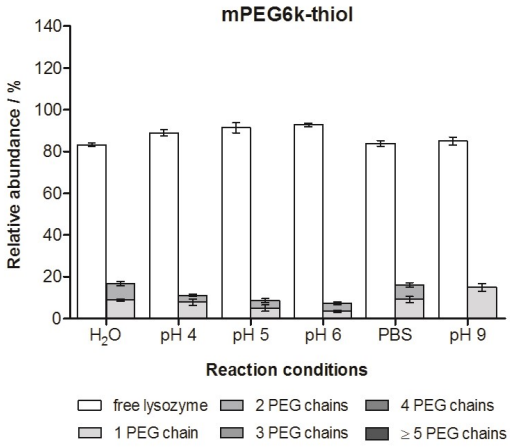

Figure 5.3: Incubation of lysozyme with mPEG6k-thiol for 24 h at 37 °C. The relative abundance of lysozyme species was analyzed by SDS-PAGE. The gray scale indicates the number of attached PEG chains. Results are shown as means ± standard deviations (n = 3).

After incubation with the stoichiometric mixture of mPEG5k-maleimide and mPEG5k-furan, pH-dependent modification of lysozyme was observed **(Figure 5.4** A); the amount of free lysozyme decreased with increasing pH form 75 ± 0.4 % (pH 4) to 33 ± 1.9 % (pH 9). Incubation with mPEG5k-furan alone also resulted in modification of 2 ± 0.7 % to 7 ± 1.7 % of the total lysozyme amount (data not shown). Upon incubation with mPEG5k-vinyl sulfone and mPEG6k-thiol, the degree of modification slightly increased at low pH-values and decreased at high pH-values (Figure 5.4 B). At pH 4, 73 ± 4.8 % of the total lysozyme amount remained unmodified; however, lysozyme was completely modified with two to seven PEG chains at pH 9. The incubation of lysozyme with mPEG5k-acrylamide and mPEG6k-thiol resulted in the conjugation of two PEG chains (Figure 5.4 C). The degree of modification increased at basic pH. At pH 4, 88 ± 1.9 % of the introduced lysozyme were unmodified, whereas only 72 ± 1.7 % remained unmodified at pH 9. The addition of a radical initiator to mPEG5k-acrylamide resulted in heavily modified protein species, with up to five PEG chains being attached in water (Figure 5.4 D). The amount of unmodified lysozyme varied between 82 ± 2.5 % (pH 4) and 72 ± 1.8 % (pH 9).

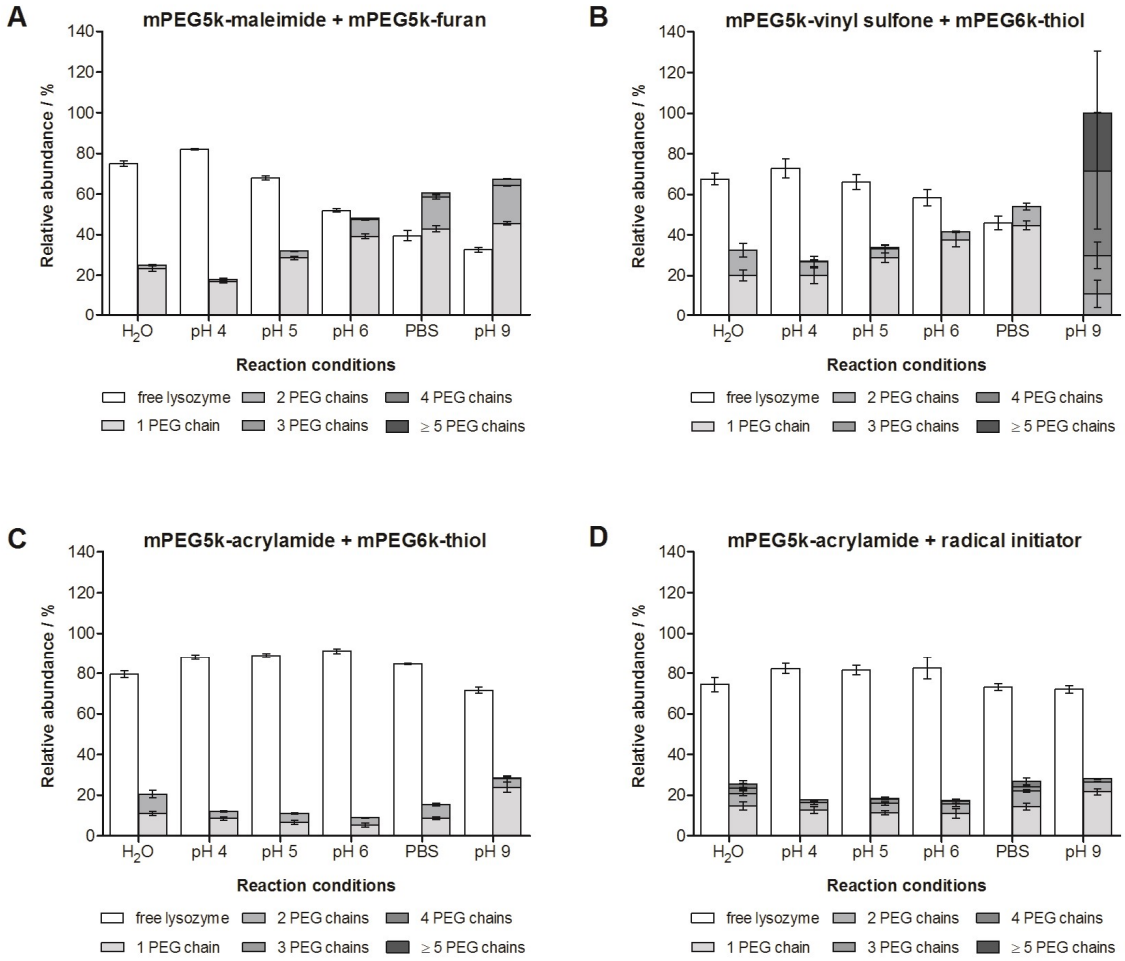

Figure 5.4: Modification of lysozyme after incubation with mixtures of mPEG5k-maleimide and mPEG5k-furan (A), mPEG5k-vinyl sulfone and mPEG6k-thiol (B), mPEG5k-acrylamide and mPEG6k-thiol (C), and mPEG5k-acrylamide with a radical initiator (D) at different pH-values. The gray scale indicates the number of attached PEG chains. Results are shown as means ± standard deviations (n = 3).

5.3.2. Discussion

Protein Structure and Reactivity of Amino Acid Side Chains

Several amino acids of proteins are prone to side reactions during cross-linking of hydrogels. Nucleophilic amino acids (e.g., arginine, cysteine, histidine, lysine and tryptophan) can react with α,β-unsaturated carbonyl compounds in Michael-type addition reactions. Sulfhydryl groups of cysteine residues are strong nucleophiles, especially in the ionized form. These are followed by primary and secondary amino groups; the α-amino group of the N-terminus, ε-amino groups of lysine residues, secondary amines of histidine and tryptophan, and the guanidino group of arginine exhibit moderate nucleophilicity. The α-carboxyl group of the C-terminus, ß-carboxyl

groups of aspartic acid, γ-carboxyl groups of glutamic acid, and hydroxyl groups of tyrosine residues are weak nucleophiles [131]. As nucleophilicity depends on the ionization of the involved functional groups, nucleophilic addition reactions of proteins are pH-dependent. Generally speaking, nucleophilicity is increased near or above the pK_a of the functional group. However, the actual pK_a-values within the three-dimensional protein structure differ from the theoretical values due to strong effects of the existing microenvironment [131]. The reactivity of amino acid residues further depends on their position in the protein structure. Nucleophiles on the protein surface can react more easily than those located in the core of the protein. For example, hydrophilic amino acids, in particular lysine residues, are mostly located on the protein surface, while hydrophobic amino acids are usually buried inside the protein structure [131]. Most cysteine residues are located in the protein core and covalently bound to other cysteine residues to form disulfide bonds [132]. Therefore, their reactivity in Michael-type addition reactions is low despite the high nucleophilicity of the free thiol group. Possible side reactions occurring at cysteine residues of proteins also include thiol-disulfide exchange reactions between thiol groups of polymers and disulfide bonds.

In our experiments, lysozyme served as a model protein to determine possible side reactions with polymers commonly used for hydrogel preparation (**Figure 5.5**). The amino acid sequence of lysozyme contains eight cysteine residues (Cys 6, 30, 64, 76, 80, 94, 115, and 127) bound in four disulfide bonds, which can be attacked during cross-linking [133]. Besides, lysozyme has six lysine residues and one N-terminus. Three of the lysine residues are located on the protein surface (Lys 1, 33, and 97), while the others are buried inside the three-dimensional protein structure [82, 133–136]. Furthermore, four out of eleven arginine residues are located on the protein surface (Arg 14, 21, 73, 128) [134, 135, 137]. However, the guanidino of arginine is less nucleophilic than the ε-amino group of lysine and, therefore, less susceptible to side reactions [137]. Lysozyme additionally contains one histidine residue (His 15), which is located on the protein surface [133, 138]; but secondary amines are generally less reactive in Michael-type addition reactions than primary amines [139]. The same applies to the five tryptophan residues on the protein surface (Trp 62, 63, 108, 111, and 123) [140]. Consequently, lysine residues mainly react in Michael-type addition reactions, while cysteine residues are sensitive to thiol-disulfide exchange reactions.

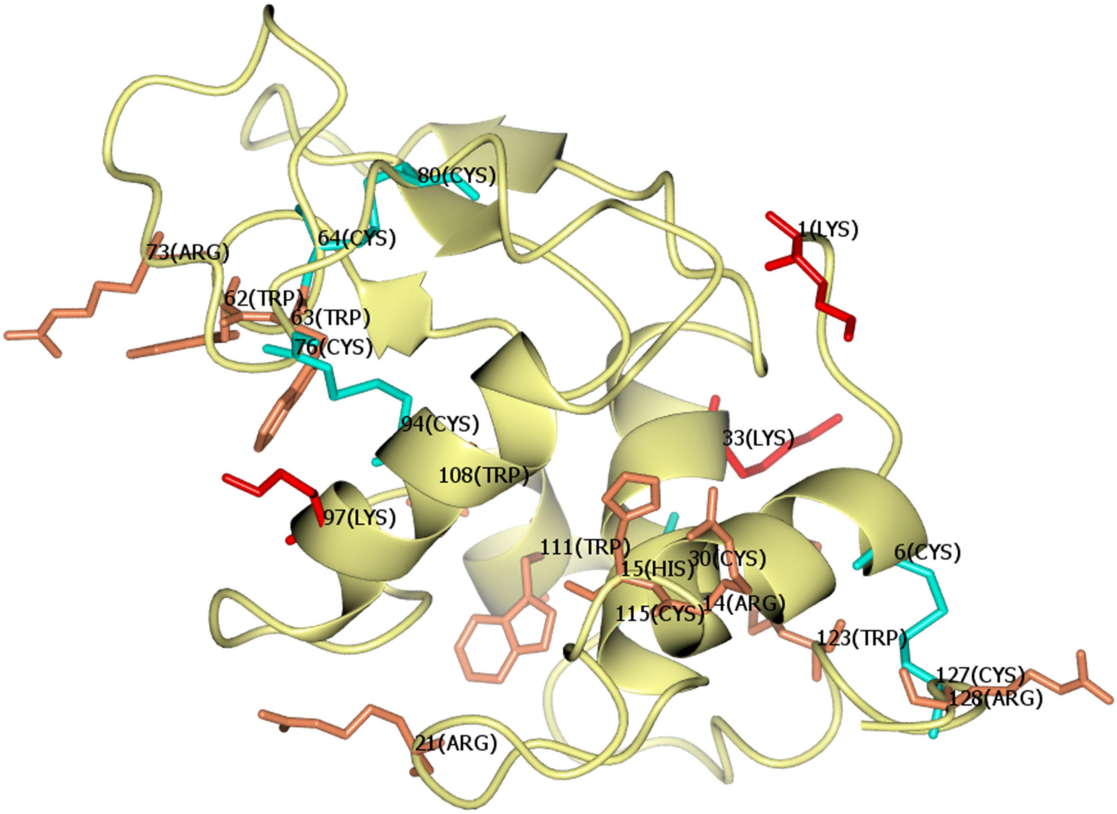

Figure 5.5: Three-dimensional structure of lysozyme with highlighted nucleophilic amino acids (red: lysine; cyan: cysteine; coral: arginine, histidine, and tryptophan). The structure model was created using the CCP4 Moleclar Graphics software [5]. Structural information is based on results from Diamond (PDB ID: 2 LYZ) [6].

Side Reactions between Proteins and Selected Cross-linking Agents

To study potential side reactions with lysozyme, mono-functional PEG derivatives were used to prevent gelation of the protein solutions during incubation and electrophoresis. The used polymer amounts corresponded to the typical concentrations of cross-linking agents in common hydrogel formulations [46, 120, 127]. It should be pointed out that low molecular weight cross-linkers, such as *N*,*N'*-methylenebisacrylamide, are also commonly used in hydrogel formations. In comparison to polymers, these cross-linkers may lead to even higher degrees of protein modification due to less steric hindrance and easier approach to reactive amino acids. Michael-type additions of nucleophilic side chains to vinyl groups were observed after incubation of lysozyme with mPEG5k-maleimide, mPEG5k-vinyl sulfone, and mPEG5k-acrylamide (Figure 5.2). This type of reaction has already been exploited for site-specific protein PEGylation [61, 141]. As already discussed above, Michael-type addition reactions are pH-dependent due to ionization of the involved functional groups [131, 142]. As a result of this, the extent of

protein modification and the number of attached PEG chains increased with increasing pH of the incubation medium. Interestingly, incubation of lysozyme with mPEG5k-maleimide, mPEG5k-vinyl sulfone, or mPEG5k-acrylamide in ultrapure water resulted in low degrees of modification comparable to those at pH 4 or pH 5. This is explained by protonation of amino groups in ultrapure water, which has a slightly acidic pH due to dissolved carbon dioxide. The degree of modification was similar after incubation of lysozyme with mPEG5k-maleimide and mPEG5k-vinyl sulfone (Figure 5.2 A and B). Incubation with mPEG5k-maleimide resulted in a slightly increased degree of modification at acidic pH, while incubation with mPEG5k-vinyl sulfone caused heavy protein modification at neutral and basic pH. In comparison to mPEG5k-maleimide and mPEG5k-vinyl sulfone, only moderate protein modification was detected after incubation with mPEG5k-acrylamide (Figure 5.2 C). Especially at neutral and basic pH, the degree of modification was much lower compared to the two other Michael acceptors. The reactivity of Michael acceptors mostly depends on the electron deficiency of the vinyl group. Therefore, maleimide and vinyl sulfone groups are more reactive in Michael-type addition reactions than acrylamides [139, 143]. Furthermore, maleimide is obviously a stronger electrophile than vinyl sulfone; Michael-type additions to vinyl sulfone groups are slower, with the reaction rate increasing with the pH of the incubation medium [61, 141]. Besides Michael-type addition reactions, thiol-disulfide exchange reactions were observed after incubation of lysozyme with mPEG6k-thiol (Figure 5.3). Thiol groups of the polymer can reduce disulfide bonds of the protein independent from the pH of the incubation medium [51].

Potential Side Reactions with Proteins during Hydrogel Formation

To mimic the conditions during hydrogel formation, mPEG5k-maleimide, mPEG5k-vinyl sulfone, and mPEG5k-acrylamide were incubated together with suitable reaction partners and lysozyme. For example, branched PEG-maleimides can be polymerized with furan substituted PEG derivatives by means of Diels-Alder reactions to form covalently cross-linked hydrogels [46]. The addition of stoichiometric amounts of mPEG5k-furan should, therefore, suppress side reactions between mPEG5k-maleimide and lysozyme. However, Tang et al. found that the Michael addition of methanethiol to *N*-methylmaleimide has a much lower energy barrier than the Diels-Alder reaction [144]. This is in good agreement with our experimental data showing only slightly decreased levels of protein modification in the presence of both mPEG5k-maleimide

and mPEG5k-furan (Figure 5.4 A). Obviously, Michael-type additions of primary amino groups to maleimides are generally favored over Diels-Alder reactions.

Besides Diels-Alder reactions, Michael-type additions of nucleophiles to α,β-unsaturated carbonyl compounds have been frequently exploited for hydrogel preparation. For example, thiol-maleimide coupling [51, 92, 127] and Michael-type additions of thiol groups to vinyl sulfone or acrylate groups [56, 121–124] were used as cross-linking reactions for hydrogels. Lutolf et al. used PEG-acrylates and cysteine-containing oligopeptides for the preparation of covalently cross-linked hydrogels [123]. They postulated selectivity of PEG-acrylates for thiols over biological amines at physiological conditions [131, 142]. Elbert et al. reported that the reaction rates of amino groups in Michael-type addition reactions were lower than those of thiol groups [121]. The half-lives of *N*-actyl-L-cysteine and α-*N*-acetyl-L-lysine in Michael-type additions to PEG-monoacrylates at physiological conditions were approx. 7 min and 21 h, respectively. Albumin remained almost unmodified after 1 h of incubation with PEG-diacrylate. However, the expected selectivity of mPEG5k-vinyl sulfone and mPEG5k-acrylamide for thiol groups was not fully confirmed in our experiments. Incubation of lysozyme with both mPEG5k-vinyl sulfone and stoichiometric amounts of mPEG6k-thiol resulted in slightly increased levels of protein modification in water and at pH 4, most likely due to thiol-disulfide exchange reactions (Figure 5.4 B). Above pH 5, however, the extent of protein modification and the number of attached PEG chains clearly decreased. The addition of stoichiometric amounts of mPEG6k-thiol to mPEG5k-acrylamide slightly increased the degree of polymer conjugation under all tested conditions except for pH 9 (Figure 5.4 C). Side reactions between proteins and polymers during hydrogel formation have also been reported in the literature. For example, van de Wetering et al. described modification of human growth hormone (hGH) during cross-linking of PEG-acrylates with dithiothreitol [122]. Hiemstra et al. observed incomplete protein release and precipitation due to reactions of amino groups and disulfide bonds with vinyl sulfone and thiol groups of the gel-forming polymers [124].

Radical polymerization of acrylate or acrylamide derivatives is another frequently applied cross-linking chemistry. The addition of a radical initiator increased the degree of protein modification compared to mPEG5k-acrylamide alone (Figure 5.4 D). Side reactions between proteins and acrylate-containing polymers during radical polymerization of hydrogels have been described by several groups [59, 119, 145]. For

example, incomplete protein release and loss of activity were observed, most likely due to covalent binding of proteins through radical chain transfer to thiols or other susceptible groups. Modification of proteins by Michael-type addition reactions may be less pronounced in radical polymerizations. Furthermore, protein denaturation and aggregation can be triggered by the presence of free radicals [146].

Consequences for the Preparation of Hydrogel-based Protein Delivery Systems

When cross-linking of hydrogels is performed in the presence of proteins, side reactions between the incorporated proteins and the gel-forming polymers are likely to occur. This may affect the three-dimensional protein structure, which is often associated with loss of activity, decreased availability and increased risk for immune responses. The number of the attached polymer chains and the site of modification play an important role for the extent of structural damage and the observed loss of activity. In our experiments, the number of conjugated PEG chains was dependent on the cross-linking reagent and the reaction conditions. In several instances, more than three PEG chains were attached to the protein. Lysozyme can be modified with one to three polymer chains at the three lysine residues on the protein surface without causing structural damage [35, 83]; however, a higher degree of modification may lead to structural breakdown [82, 83]. Incubation of lysozyme with mPEG5k-vinyl sulfone in PBS resulted in modification with more than three PEG chains; at pH 9, more than five PEG chains had been attached to the protein (Figure 5.2 B). The addition of mPEG6k-thiol increased the amount of unmodified lysozyme and decreased the number of attached PEG chains (Figure 5.4 B). Nevertheless, protein species with more than three conjugated PEG chains were still detectable at pH 9. Likewise, incubation with mPEG5k-acrylamide and a radical initiator resulted in protein species with more than three conjugated PEG chains (Figure 5.4 D). Although it is not possible to determine the exact site of protein modification by SDS-PAGE, structural damage of lysozyme is very likely.

Several strategies can be applied to protect proteins against side reactions during cross-linking of hydrogels. For example, cross-linking can be performed in slightly acidic solutions below pH 5. This decreases the nucleophilicity of amino groups by protonation and reduces their reactivity in Michael-type addition reactions. Cross-linking by Diels-Alder reactions is, on the other hand, unaffected by acidic pH-values as

this reaction is basically pH-independent. It should be pointed out that lowering the pH may induce protein degradation and aggregation [18, 147]. The majority of antibodies, however, seem to be stabilized in slightly acidic solution [147]. Nevertheless, the stability of each individual protein must be carefully evaluated for all cross-linking conditions in question. In hydrogels formed by Michael-type addition reactions, protein modification can be prevented by precipitation with PEG or Zn^{2+} [122]. The incorporation of solid protein particles effectively protected hGH during hydrogel formation, and complete protein release was observed. To protect proteins during radical polymerizations, Lin et al. proposed the addition of transition metal chelators during hydrogel formation. Iminodiacetic acid and Cu^{2+} were used as protein binding ligands to minimize the exposure of reactive amino acid residues to free radicals [146]. In a different approach, Censi et al. succeeded in retaining protein activity during photopolymerization of methacrylate groups by separating hydrophobic polymerization sites from more hydrophilic protein-containing areas [118].

5.4. Conclusion

In this chapter, potential side reactions of selected cross-linking agents with proteins were investigated. The conjugation of polymer chains by Michael-type addition reactions, thiol-disulfide exchange reactions or radical reactions was determined by SDS-PAGE. Incubation of lysozyme with mPEG5k-maleimide, mPEG5k-vinyl sulfone or mPEG5k-acrylamide resulted in pH-dependent Michael-type additions of nucleophilic amino acid residues to the vinyl group. The addition of suitable reaction partners (e.g., mPEG5k-furan or mPEG6k-thiol) did not noticeably reduce the degree of protein modification. Protein-polymer conjugates detected after incubation with mPEG6k-thiol were attributed to thiol-disulfide exchange reactions. Incubation of lysozyme with mPEG5k-acrylamide and a radical initiator caused radical-induced protein modifications, with a large number of PEG chains being attached. Although many cross-linking reactions (e.g., Diels-Alder reactions and Michael-type addition reactions) are considered selective, caution should be used when hydrogels are cross-linked in the presence of proteins. Proteins contain a large number of nucleophilic amino acid residues and are, therefore, prone to side reactions with cross-linking agents. The occurring protein modifications are often accompanied by incomplete release, structural damage, loss of bioactivity, or increased risk for immune responses [12, 51].

Therefore, side reactions between proteins and polymers, and possible strategies to prevent these should always be considered when developing new hydrogels for protein delivery.

Chapter 6

Protein Delivery from Diels-Alder Hydrogels

Abstract

In this chapter, the suitability of Diels-Alder hydrogels for controlled protein release was investigated. For this purpose, three model proteins (lysozyme, α-chymotrypsin (α-CT), γ-globulin) were used. α-CT and γ-globulin were incubated with linear derivatives of the gel precursor in order to detect side reactions. The extent of modification detected by SDS-PAGE varied between 0 % (incubation of γ-globulin with mPEG5k-maleimide at pH 4 and incubation of α-CT with mPEG5k-furan at pH 9) and 89 ± 5.5 % (incubation of γ-globulin with a mixture of mPEG5k-maleimide and mPEG5k-furan at pH 9) depending on the protein, the pH during incubation and the functionalization of the polymer. The mobile fraction of the three proteins incorporated in Diels-Alder hydrogels decreased with increasing pH due to covalent protein binding to the hydrogel network at pH 7.4 as detected by fluorescence recovery after photobleaching (FRAP). The diffusion coefficients depended on the hydrodynamic diameter of the protein and mesh size of the hydrogel. Likewise protein release depended on both parameters and the pH during cross-linking. After cross-linking in water 94.2 ± 3.4 % of lysozyme and 54.2 ± 6.2 % of α-CT was released over 24 h. After cross-linking in PBS (pH 7.0 - 7.2), protein release occurred along with hydrogel degradation. γ-Globulin was released along with hydrogel degradation in all cases due to its large hydrodynamic diameter. Protein activity could be almost retained (lysozyme) or even improved (α-CT) compared to reference solution by incorporating the protein in Diels-Alder hydrogels and cross-linking at pH 4.

6.1. Introduction

For many diseases controlled delivery of therapeutic proteins directly to the site of action over a longer period of time is the best way of application for an efficient treatment [50]. In the field of bone regeneration, for example, Jeon et al. reported on an enhanced therapeutic benefit of prolonged delivery of bone morphogenetic protein compared to rapid release of the same protein [148]. Especially tissues, which are hard to target systemically, can be treated more effectively by an application directly to the site of action. The retina, for example, is hard to reach via systemic applications due to the blood retina barrier [9, 149]. To overcome this problem, intravitreous injections proved to be an effective treatment of retinal diseases and offer the advantage of minimal systemic side effects [9, 149]. Hydrogels are suitable protein carrier to meet both requirements: local application and long-time release. In form of in-situ gelling systems, hydrogels can be minimally invasively injected directly to the diseased site [124, 150, 151]. Furthermore, hydrogels offer a broad range of technological opportunities to tailor the release profiles [12]. These methods include polymer-protein interactions, such as reversible covalent protein attachment to the hydrogel backbone, or non-covalent interactions, such as electrostatic interactions [12, 35]. Furthermore, encapsulation in secondary carriers, such as micro- or nanoparticles, has been reported [12]. A simple and mild strategy to control the release is to tailor drug diffusion inside the hydrogel and to optimize swelling and degradation behavior of the hydrogel via structural properties, such as the cross-linking density [12]. Diffusion controlled release is associated with protein mobility inside the hydrogel, which depends on the hydrogel mesh size and the hydrodynamic radius of the protein [118]. For proteins with a hydrodynamic diameter larger than the mesh size, diffusion out of the hydrogel is limited; protein release is only possible with increasing mesh size during degradation or at least swelling of the hydrogel [12, 124].

Besides others, Diels-Alder hydrogels developed by Kirchhof et al. are promising formulations to control protein release via hydrogel mesh size, swelling and degradation [46]. These hydrogels consist of star-shaped 8armed poly(ethylene glycol) (PEG) resulting in well-defined networks [46]. The network mesh-size can be tailored by varying the molecular weight of the PEG derivatives [46]. The PEG functionalization with furyl and maleimide groups allows cross-linking by Diels-Alder reaction. Diels-Alder reactions are part of the “click” chemistry and occur without catalyst or initiator

[128, 129]. Due to the reported biodegradability by retro-Diels-Alder reaction, the formulations are promising for degradation controlled release [46]. However, besides these advantages, side reactions of the gel precursor with proteins have been observed (see Chap. 5) [152]. Especially at basic pH, Michael-type addition reactions of nucleophilic amino acids with the maleimide group occur (see Chap. 5) [152].
In this chapter, the suitability of Diels-Alder hydrogels as protein depot formulations for controlled delivery was investigated. A special focus was on optimizing hydrogel preparations in order to prevent side reactions of the gel precursors with the incorporated proteins and to retain protein activity. For this purpose, alpha chymotrypsin (α-CT) and γ-globulin were incubated with linear, mono-functionalized PEG derivatives (mPEG5k-maleimide, mPEG5k-furan) at different pH values and analyzed by SDS-PAGE in order to detect side reactions as already described for lysozyme (see Chap. 5). Additionally, the three model proteins (lysozyme, α-CT, γ-globulin) were incorporated in Diels-Alder hydrogels in order to determine their mobility inside the hydrogel using fluorescence recovery after photobleaching (FRAP) and classical release studies. Finally, the enzymatic activity of lysozyme and α-CT after incubation with mPEG5k-maleimide, and after release from Diels-Alder hydrogels was analyzed.

6.2. Materials and Methods

6.2.1. Materials

Mini-Protean TGX Precast Gels Any kD were purchased from Bio-Rad Laboratories GmbH (München, Germany). Tetramethylethylenediamine (TEMED) was purchased from Carl Roth GmbH & Co. KG (Karlsruhe, Germany). 2-Amino-2-hydroxymethyl-propane-1,3-diol (TRIS) was obtained from GE Healthcare Europe GmbH (Freiburg, Germany). Dulbecco's phosphate-buffered saline (PBS) (pH 7.0 – 7.2) was purchased from Invitrogen GmbH (Karlsruhe, Germany). Ethanol was from CSC Jäcklechemie (Nürnberg, Germany). Eight-armed poly(ethylene glycol) with a molecular weight of 10 kDa and 20 kDa was purchased from JenKem Technology (Allen, TX, USA). Acrylamide/bisacrylamide solution (37.5 : 1), bromphenol blue sodium salt, and sodium dodecylsulfate were obtained from Serva Electrophoresis GmbH (Heidelberg, Germany). α-Chymotrypsin (α-CT) (from bovine pancreas), γ-globulins (from bovine

blood), Coomassie brilliant blue G-250, lysozyme (from chicken egg white), micrococcus lysodeikticus, sodium tetraborate decahydrate, N-succinyl-Ala-Ala-Pro-Phe p-nitroanilide, and methoxy poly(ethylene glycol) with a molecular weight of 5 kDa were purchased from Sigma Aldrich (Taufkirchen, Germany). Lab-Tek™ II chambered cover glass slides were purchased form Thermo Fisher Scientific (Langenselbold, Germany). GHP Acrodisc®13 mm syringe filters (0.2 µm pore size) were purchased from Pall GmbH (Dreieich, Germany). All other chemicals were purchased from Merck KGaA (Darmstadt, Germany). Deionized water was freshly prepared using a Milli-Q water purification system from Millipore (Schwalbach, Germany). Py1-labeled proteins (Py1-lysozyme, Py1-α-Ct, Py1-γ-globulin) were kindly provided by Dr. Robert Meier, Institute of Analytical Chemistry, Chemo- and Biosensors, University of Regensburg.

6.2.2. Synthesis of Linear PEG Derivatives

Methoxy poly(ethylene glycol) amine (mPEG5k-NH_2), methoxy poly(ethylene glycol) maleimide (mPEG5k-maleimide), and methoxy poly(ethylene glycol) 3-(furan-2-yl)propanamide (mPEG5k-furan) with a molecular weight of 5 kDa were synthesized according previously published procedures [34, 46].

6.2.3. Synthesis of Gel Precursors

Eight-armed poly(ethylene glycol) maleimide (8armPEG10k-maleimide, 8armPEG20k-maleimide) and eight-armed poly(ethylene glycol) 3-(furan-2-yl)propanamide (8armPEG10k-furan, 8armPEG20k-furan) with molecular weights of 10 kDa or 20 kDa were synthesized as described by Kirchhof et al. [46].

6.2.4. Protein Reactivity of Hydrogel Precursors: α-CT

Side reactions of the hydrogel precursors with α-CT were detected by SDS-PAGE. α-CT stock solutions with concentrations of 2.66 mg/mL were prepared in water and different buffers (25 mM acetate buffer pH 4.0, 25 mM acetate buffer pH 5.0, 25 mM phosphate buffer pH 6.0, PBS (pH 7.0 – 7.2) and 50 mM borate buffer pH 9.0). To determine protein modifications, 400 µL of each stock solution were incubated with 3.66 µmol of mPEG5k-furan, mPEG5k-maleimide, or stoichiometric mixtures of both polymers at 37 °C for 24 h. Afterwards all samples were analyzed by SDS-PAGE. For comparison, stock solutions were handled the same way and loaded next to the corresponding

protein-polymer mixtures on the stacking gel. SDS-PAGE was conducted on Mini-Protean TGX Precast Gel Any kD at a constant voltage of 120 V and a decreasing current starting at 68 mA. For all samples, 55.86 µg of α-CT were loaded per lane. Afterwards, the gels were stained with Coomassie brilliant blue G-250. For documentation and quantification, the gels were imaged with a ChemiDoc™ MP gel imaging system (Bio-Rad Laboratories GmbH, München, Germany). The software Image Lab™ (Bio-Rad Laboratories GmbH, München, Germany) was used to determine the relative abundance of protein-polymer conjugates. The experiments were performed in triplicate and the results are presented as means ± standard deviations.

6.2.5. Protein Reactivity of Hydrogel Precursors: γ-Globulin

Side reactions of the gel precursors with γ-globulin were detected by SDS-PAGE. γ-Globulin stock solutions (c = 1.33 mg/mL) were prepared in water and different buffers (25 mM acetate buffer pH 4.0, 25 mM acetate buffer pH 5.0, 25 mM phosphate buffer pH 6.0, PBS (pH 7.0 – 7.2) and 50 mM borate buffer pH 9.0). To detect possible side reactions, 1.83 µmol of mPEG5k-furan, mPEG5k-maleimide or stoichiometric mixtures of both polymers were incubated with 400 µL of each stock solution at 37 °C for 24 h. Protein-polymer conjugates were analyzed by SDS-PAGE using polyacrylamide gels of 5 % cross-linking. Stock solutions treated the same way were loaded next to the corresponding protein-polymer mixtures for comparison. The amount of γ-globulin per lane was 27.93µg. Electrophoresis and quantification were carried out as described for α-CT in 6.2.4.

6.2.6. Fluorescence Recovery after Photobleaching (FRAP)

FRAP experiments were performed following a method described by Brandl et al. [153]. 3.0 mg/mL stock solutions of Py1-labeled proteins (Py1-lysozyme, Py1-α-CT, Py1-γ-globulin) were prepared in 50 mM acetate buffer pH 4 or 50 mM phosphate buffer pH 7.4, respectively. 8armPEG-furan with molecular weights of 10 kDa or 20 kDa were dissolved in 50 mM acetate buffer pH 4 or 50 mM phosphate buffer pH 7.4, respectively, to a final concentration of 156.3 mg/mL. Afterwards, the solution was filtered through a hydrophilic propylene membrane syringe filter (GHP Acrodisc®13 mm syringe filter).

8armPEG-maleimide (10 kDa / 20kDa) (c = 143.7mg/mL) was dissolved in 50 mM acetate buffer pH 4 or 50 mM phosphate buffer pH 7.4, respectively. For hydrogel preparation, equal amounts of protein stock solution, filtered 8armPEG-furan solution, and 8armPEG-maleimide solution were combined. 250 µL of the mixture were cast into a Lab-Tek™ II Chambered Cover glass and allowed to gel for 24 h at 37 °C. The final composition for all hydrogels (8armPEG10k-hydrogels / 8armPEG20k-hydrogels) was 10 % total polymer content and 1 mg/mL Py1-labeld protein.

FRAP experiments were conducted using a LSM 510 META scanning device installed on a Zeiss Axiovert 200 M microscope (Carl Zeiss MicroImaging GmbH, Jena, Germany) equipped with a Plan-Neofluar 10x objective lens (numerical aperture 0.30). Imaging and bleaching was performed with an argon laser (488 nm, 30 mW) at 25 % output power with completely opened confocal pinhole. For the measurement, a homogenous area inside the gel was brought into focus. Digital images were recorded every 8 s using 0.5 % transmission. After the first five intervals, a defined area with a diameter of 36 µm was bleached at 100 % transmission with 30 iterations. Afterwards, 75 further images of fluorescence recovery were recorded.

To analyze the obtained data, fluorescence intensities in the bleached area (I_{roi}) and in the reference region (I_{ref}) were calculated for each time point t using the NIH software ImageJ. The intensity of the bleached area $I_{roi}(t)$ was normalized to the mean intensity detected before bleaching $I_{roi}(pre)$. A correction factor for any bleaching effect occurring during image recording was included.

$$f(t) = \frac{I_{ref}(pre)}{I_{ref}(t)} \cdot \frac{I_{roi}(t)}{I_{roi}(pre)} \tag{7.1}$$

$f(t)$ is the corrected and normalized intensity of the bleached region of interest.

$I_{ref}(pre)$ is the fluorescence intensity of the reference region before bleaching.

$I_{ref}(t)$ is the fluorescence intensity of the reference region at each time point t.

$I_{roi}(pre)$ is the fluorescence intensity of the region of interest before bleaching.

$I_{roi}(t)$ is the fluorescence intensity of the region of interest at each time point t.

In the next step, *f(t)* was normalized to full scale using the following equation (7.2).

$$F(t) = \frac{f(t)-f(0)}{f(pre)-f(0)} \tag{7.2}$$

F(t) is the fluorescence intensity of the region of interest normalized to full scale.

f(t) is the normalized intensity of the bleached region of interest.

f(0) is the normalized intensity of the region of interest directly after bleaching.

f(pre) is the normalized intensity of the region of interest before bleaching.

The last step was a least-squares fit of the following equation to the experimental recovery data to determine the diffusion time T_D and mobile fraction *k*.

$$F(t) = k \cdot e^{-\frac{T_D}{2t}} \left[I_0\left(\frac{T_D}{2t}\right) + I_1\left(\frac{T_D}{2t}\right) \right] \tag{7.3}$$

k is the mobile fraction.

T_D is the diffusion time.

I_0 is the modified Bessel function of the first kind zero order.

I_1 is the modified Bessel function of the first kind first order.

The diffusion time was used to calculate the diffusion coefficient D:

$$D = \frac{w^2}{T_D}$$

w is the radius of the bleached region of interest (18 µm in all experiments).

6.2.7. Protein Release from Diels-Alder Hydrogels

Protein stock solutions of lysozyme, α-CT, or γ-globulin with a concentration of 1.33 mg/mL were prepared in water and PBS. Stoichiometric amounts of 8armPEG-furan and 8armPEG-maleimide were dissolved in the protein stock solution. The molecular weight of the polymer was either 10 kDa or 20 kDa (8armPEG10k-hydrogel / 8armPEG20k-hydrogels). Aliquots of the prepared protein-polymer mixture (375 µL) were cast into glass cylinders (Ø 7 mm) and allowed to gel for 24 h at 37 °C. The total

polymer content was 10 % (w/v) in all experiments. For protein release, each gel cylinder was incubated in 5 mL of PBS in a shaking water bath at 37 °C. At defined time points, samples of 500 µL in volume were drawn and replaced by fresh PBS. The samples were stored at 4 °C until quantification. For calibration, stock solutions were diluted with PBS, and stored at 4 °C until measurement. Protein concentrations were determined using a method described by Bradford [69]. The measurements were performed on a Kontron UVIKON® 941 spectrophotometer (Kontron Instruments S.p.A, Milan, Italy). The obtained data was normalized to the initial protein amount (0.5 mg) per gel cylinder. All release experiments were done in triplicate and the results are presented as means ± standard deviations.

6.2.8. Enzymatic Activity of Lysozyme

The enzymatic activity of lysozyme was determined as described in Chap. 3 [35]. In brief: all samples were diluted to a protein concentration of maximal 0.01 mg/mL. 100 µL of each protein sample were mixed with 2.5 mL of a 0.015 % Micrococcus lysodeikticus cell suspension in 66 mM phosphate buffer pH 6.2. The measurement was immediately started and the decrease in the absorption was recorded over 4.8 min at 450 nm on a Kontron UVIKON® 941 spectrophotometer (Kontron Instruments S.p.A, Milan, Italy). During the measurement, all solutions were kept at a constant temperature of 25 °C. The slope of the linear part of the curve was used to determine the lytic activity of lysozyme.

6.2.9. Enzymatic Activity of α-CT

The enzymatic activity of α-CT was determined following a procedure published by Solá and Griebenow [154]. For this purpose, a substrate solution of 0.4 mM N-succinyl-Ala-Ala-Pro-Phe-p-nitroanilide was prepared in PBS (pH 7.0 – 7.2) and diluted 1 : 3.9 with PBS before measurement. All protein samples were diluted to a protein concentration of maximal 0.02 mg/mL. In a cuvette, 25 µL of the protein sample and 975 µL of the substrate dilution were mixed and the increasing amount of p-nitroaniline was followed over 4.8 min in 0.8 min intervals at 410 nm on a Kontron UVIKON® 941 spectrophotometer (Kontron Instruments S.p.A, Milan, Italy). The lytic activity of α-CT was determined from the slope of the curve.

6.2.10. Effect of Maleimide on Enzymatic Activity of Lysozyme and α-CT

Protein stock solutions of lysozyme and α-CT, respectively, with a concentration of 1.33 mg/mL were prepared in water and different buffers (25 mM acetate buffer pH 4.0, 25 mM acetate buffer pH 5.0, 25 mM phosphate buffer pH 6.0, PBS (pH 7.0 – 7.2), 50 mM borate buffer pH 9.0). To determine the effect of maleimide on the enzymatic activity, the stock solutions were incubated with 0.91 µmol, 1.83 µmol and 3.66 µmol of mPEG5k-maleimide at 37 °C for 24 h in a shaking water bath. Afterwards, the enzymatic activity of each sample was determined as described above. In case of lysozyme, reference solutions were prepared for comparison. For this purpose, non-reactive mPEG5k-NH_2 (0.91 µmol, 1.83 µmol, 3.66 µmol) was dissolved in each stock solution and incubated at 37 °C for 24 h. Due to the influence of PEG on the lytic activity each sample activity was normalized to the corresponding activity of the reference. In case of α-CT, all stock solutions were incubated at 37 °C for 24 h for comparison. Due to the pH dependence of α-CT activity, the obtained sample activities were normalized to the stock solution showing the highest activity after incubation (stock solution prepared at pH 4). All activities were determined in triplicate. The results are presented as means ± standard deviation.

6.2.11. Protein Activity after Release

Protein stock solutions of lysozyme and α-CT, respectively, with a concentration of 1.33 mg/mL were prepared in 25 mM acetate buffer pH 4. Hydrogel cylinders were prepared in the same way as described for the release experiments. After cross-linking the gels were incubated in 5 mL of PBS (pH 7.0 – 7.2) at 37 °C. After 24 h, the activity of the proteins released in the incubation medium was determined as described above. For this, all lysozyme samples were diluted 1:10 and all α-CT samples were diluted 1:5 with PBS. Stock solutions were diluted with PBS and incubated at 37 °C for 24 h to serve as a reference. Additionally, the protein amount released in the incubation medium and the protein amount of the reference was quantified using the Bradford assay [69]. This allowed standardization of the obtained protein activities to activity per mg protein. The standardized sample activities were normalized to the standardized reference activity. All release experiments were performed in triplicate. The results are presented as means ± standard deviation.

6.3. Results and Discussion

In the previous chapters, lysozyme was used as a model protein to determine PEGylation and PEG chain elimination of carbamate linkers, or side reactions during cross-linking of different, selected gel precursors. Lysozyme consists of 129 amino acids arranged in a three-dimensional structure with a molecular weight (MW) of about 14 kDa and a hydrodynamic radius (R_h) of about 2.1 nm [124, 155]. It is found in body fluids, tissues and macrophages of humans, and in many further vertebrate and invertebrate animals [156]. Due to its antibacterial activity, lysozyme is part of the innate immune defense of many species [156]. In different fields, such as protein chemistry, enzymology, crystallography, or molecular biology, lysozyme is used as a model system [156]. In this chapter, two further model proteins, α-chymotrypsin (α-CT) and γ-globulin, were used in addition to lysozyme.

6.3.1. Protein Reactivity of Diels-Alder Precursors

In Chap. 5, side reactions of Diels-Alder hydrogel precursors with surface exposed nucleophilic amino acids of lysozyme were reported. In case of lysozyme, Michael-type addition reactions of nucleophilic amino acids to the maleimide group were observed. Especially amino acid residues located on the protein surface are susceptible for side reactions. The highest nucleophilicity is described for cysteine residues [131]. However, cysteine residues are mostly bound in disulfide bonds inside the secondary protein structure and show, therefore, low accessibility for modifications by macromolecules [131, 132]. The next lower nucleophilicity is exhibited by lysine residues and the N-terminus. The lowest reactivity in this series is described for secondary amines (histidine, tryptophan) and the guanidino group of arginine [131]. Here, side reactions of the cross-linking agents with two further model proteins, α-CT and γ-globulin, were investigated. In line with the published data obtained for lysozyme, the extent of protein modification with maleimide and furan groups and mixtures of both polymers was determined by SDS-PAGE using linear mono-functionalized PEG derivatives (mPEG5k-maleimide, mPEG5k-furan).

α-CT

α-Chymotrypsin (α-CT) has a MW of 25 kDa and an R_h of about 2.9 nm [157]. α-CT is a serine protease formed in the digestive tract from the inactive pancreas storage form, chymotrypsinogen, in order to hydrolyze polypeptides [158, 159]. It is used as a

biocatalyst in organic synthesis [158, 160]. α-CT has a number of nucleophilic amino acid residues exposed to the protein surface which are vulnerable to side reactions during cross-linking. These are 14 of the 28 lysine residues, both histidine residues, 6 of the 8 tryptophan residues, and all three arginine residues [158, 159, 161, 162]. The 10 cysteine residues are bound in disulfide bridges and are, therefore, less accessible for modifications [158].

Figure 6.1 exemplarily shows the modification of α-CT after incubation with mPEG5k-maleimide, mPEG5k-furan, and mixtures of both polymers in water and PBS in comparison to the corresponding stock solution. α-CT stock solutions were separated in more than one band per lane by electrophoresis, indicating the existence of different α-CT derivatives. α-CT is known for autolysis as well as self-association which might explain the appearance of different molecular weight species in the stock solution [163, 164]. This complicates the interpretation of the SDS-PAGE data compared to lysozyme.

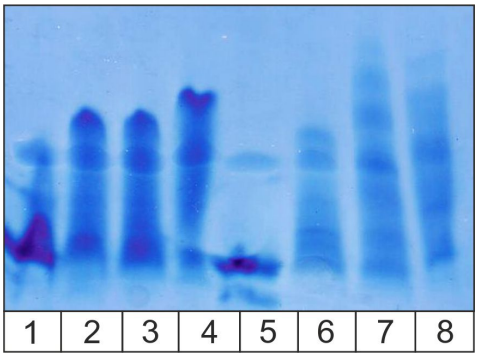

Figure 6.1: Modification of α-CT in water (lane 1 - 4) and PBS (lane 5 – 8) analyzed by SDS-PAGE. α-CT stock solutions prepared in water (lane 1) and in PBS (lane 5) served as a reference. The stock solutions were incubated with mPEG5k-furan (lane 2 and lane 6), with mPEG5k-maleimide (lane 3 and lane 7) and with a mixture of both polymers (lane 4 and lane 8) for 24 h.

For quantification, all modified species and all unmodified species were grouped and the results are presented in **Figure 6.2.** Incubation with mPEG5k-furan resulted in minor unspecific binding of less than 20 ± 0.9 % of the used amount of α-CT (pH6) (Figure 6.2 A). At pH 9, α-CT remained unaffected during incubation with mPEG5k-furan. During incubation with mPEG5k-maleimide, the amount of free α-CT decreased with increasing pH from 90 ± 2.5 % (pH 4) to 21 ± 4.3 % (pH 9). (Figure 6.2 B). This can be explained by Michael-type addition reactions of nucleophilic, surface-exposed amino acids to maleimide as already described for lysozyme.

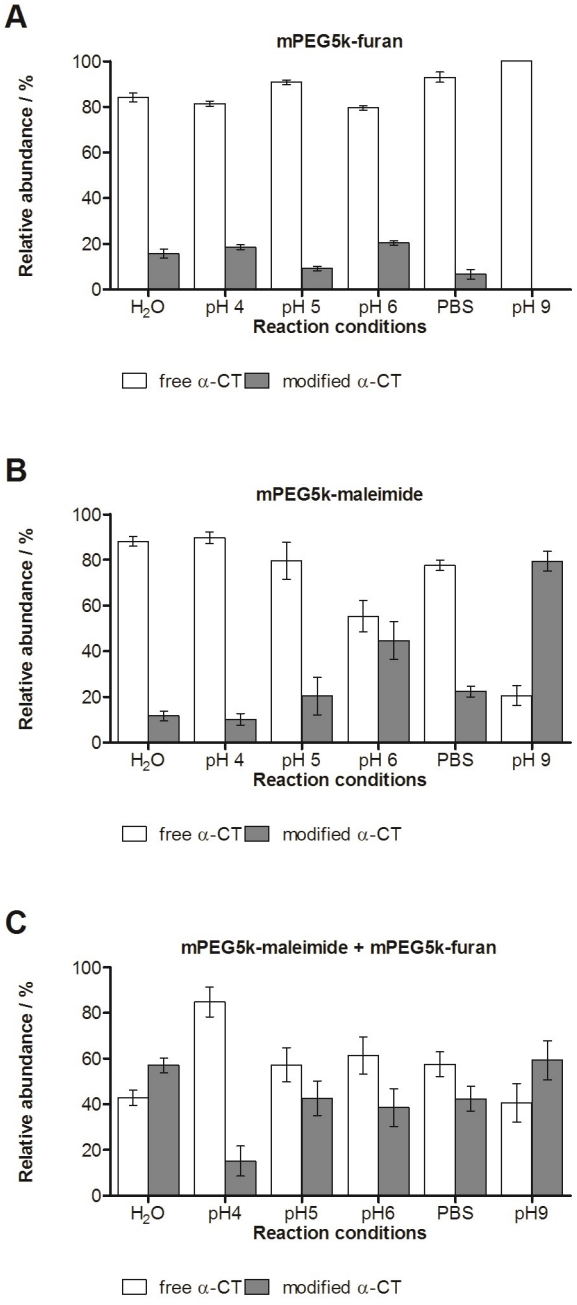

Figure 6.2: Modification of α-Chymotrypsin at different pH values. α-CT was incubated with mPEG5k-furan (A), mPEG5k-maleimide (B), and a mixture of both polymers (C) at 37 °C for 24 h. The results are shown as means ± standard deviation.

An exception was the incubation in PBS, which resulted in only 22.4 ± 2.3 % modification of α-CT, compared to 44.7 ± 8.1 % and 79.4 ± 4.3 % modification of α-CT, respectively, during incubation at pH 6 and pH 9.

Incubation with a stoichiometric mixture of both polymers also resulted in pH-dependent modifications (Figure 6.2 C). At pH 4, 85 ± 6.6 % of the total α-CT amount

remained unaffected; at pH 9, only 41 ± 8.5 % of free α-CT was detected. Incubation at pH 5, pH 6 and in PBS resulted in similar extent of modification (57 % to 61 % of free α-CT). Incubation in water resulted in a higher degree of modification (57 ± 3.4 % of modified α-CT) than expected. Due to the slightly acidic pH of ultrapure water, a degree of modification similar to that detected after incubation at pH 4 was expected. However, in contrast to a buffer the pH of ultrapure water is not exactly adjusted to a certain pH and might vary with each use. Furthermore, the pH of ultrapure water might change during the experiment due to the absence of buffer capacity. For these reasons, the detected reactivity in water might be different for each experiment. The stoichiometric mixture of mPEG5k-maleimide and mPEG5k-furan was used to mimic the conditions during hydrogel formation. Side reactions of mPEG5k-maleimide should be suppressed by the availability of a reaction partner. However, only at pH 9, a decreased extent of modification was observed after incubation with both polymers compared to mPEG5k-maleimide alone. As already observed for incubation with lysozyme (see Chap. 5), Michael-type addition reactions are preferred over Diels-Alder reactions due to the lower energy barrier of Michael additions [144].

γ-Globulin

As antibodies are of particular relevance for the clinical treatment of diseases, such as cancer, hepatitis, or rheumatoid arthritis, the compatibility of Diels-Alder hydrogels with a model antibody, γ-globulin, was investigated using SDS-PAGE. γ-Globulin is a mixture of 80 % IgG (MW: 150 kDa; R_h: 5.3nm), 10 % IgM (MW: 950 kDa; R_h: 12.7 nm), and less than 10 % IgA (MW: 162 kDa; R_h: 6.5 nm) as declared by the manufacturer [124, 165]. IgA is primarily part of the mucosal immunity and only to a small extent part of the serum [166]. IgM is the first antibody secreted in case of an upcoming infection [166]. IgM monomers are associated to pentamers, making IgM the largest antibody in human circulation [166]. IgG covers the largest part of serum antibodies [166]. Due to the high specificity, long serum-half lives and the possibility of routine production of IgG, some of the most potent drugs are based on IgG [166]. However, IgG shows a large number of surface exposed amino acids, which are prone to side reactions. For example, about half of the over 80 lysine residues of IgG are located on the protein surface [167, 168]. The more nucleophilic cysteine residues are on the other hand combined to four pairs of disulfide bonds resulting in less accessibility for modifications [167].

In **Figure 6.3,** an acrylamide gel loaded with γ-globulin after incubation with mPEG5k-maleimide, mPEG5k-furan and mixtures of both polymers in water and PBS is shown exemplarily. Protein stock solutions in water and PBS served as a reference. The individual components of γ-globulin were separated during electrophoresis. IgM migrated least and was detected near to the loading pocket due to its large size. IgG and IgA ran almost to the bottom of the gel because of their smaller size. Due to their similar size they were not clearly separated in this experimental set up.

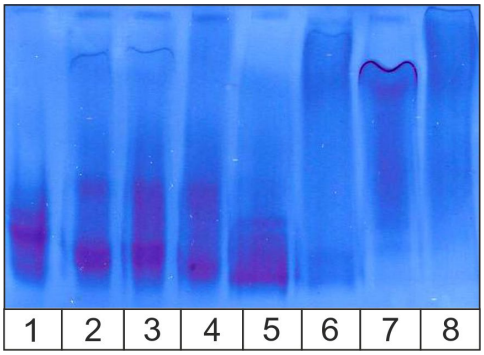

Figure 6.3: SDS-PAGE of γ-globulin after incubation in water (lane 1 - 4) and PBS (lane 5 - 8). γ-Globulin stock solutions prepared in water (lane 1) and in PBS (lane 5) served as a reference. The stock solutions were incubated with mPEG5k-furan (lane 2 and lane 6), with mPEG5k-maleimide (lane 3 and lane 7), and with a mixture of both polymers (lane 4 and lane 8) at 37 °C for 24 h.

The quantification of free and modified γ-globulin is shown in **Figure 6.4**. Free γ-globulin was defined as the sum of the detected amount of IgG, IgA, and IgM. Modified γ-globulin was the sum of all species with higher molecular weight than IgG or IgA (except IgM). Modification with mPEG5k-furan depended on the pH of the incubation medium (Figure 6.4 A). The amount of free γ-globulin decreased from 97 ± 0.6 % at pH 4 to 42 ± 2.3 % at pH 9. In pure water 87 ± 2.2 % of γ-globulin was unmodified after incubation with mPEG5k-furan. In vivo, furan is metabolized by cytochrome P450 to cis-2-butene-1,4-dial, which reacts to pyrrolin-2-one with lysine residues [169]. Under certain conditions, ring opening oxidation of furan was also observed in vitro [170, 171]. This ring opening might have occurred to a certain extent with the used mPEG5k-furan resulting in the detected side reactions with lysine residues of the protein. After incubation with mPEG5k-maleimide, pH dependent modifications were observed (Figure 6.4 B). After incubation at pH 4, γ-globulin was completely unaffected, while an increasing pH decreased the amount of free γ-globulin to 20 ± 11.8 % at pH 9. This can be explained by Michael-type addition reactions of the surface exposed nucleophilic

amino acids to the maleimide group of PEG, as already described for lysozyme and α-CT. The extent of modification after incubation in water (71 ± 5.4 % of free γ-globulin) was similar to that at pH 6 (68 ± 3.3 % of free γ-globulin). Incubation with a stoichiometric mixture of both polymers also resulted in pH-dependent modifications (Figure 6.4 C).

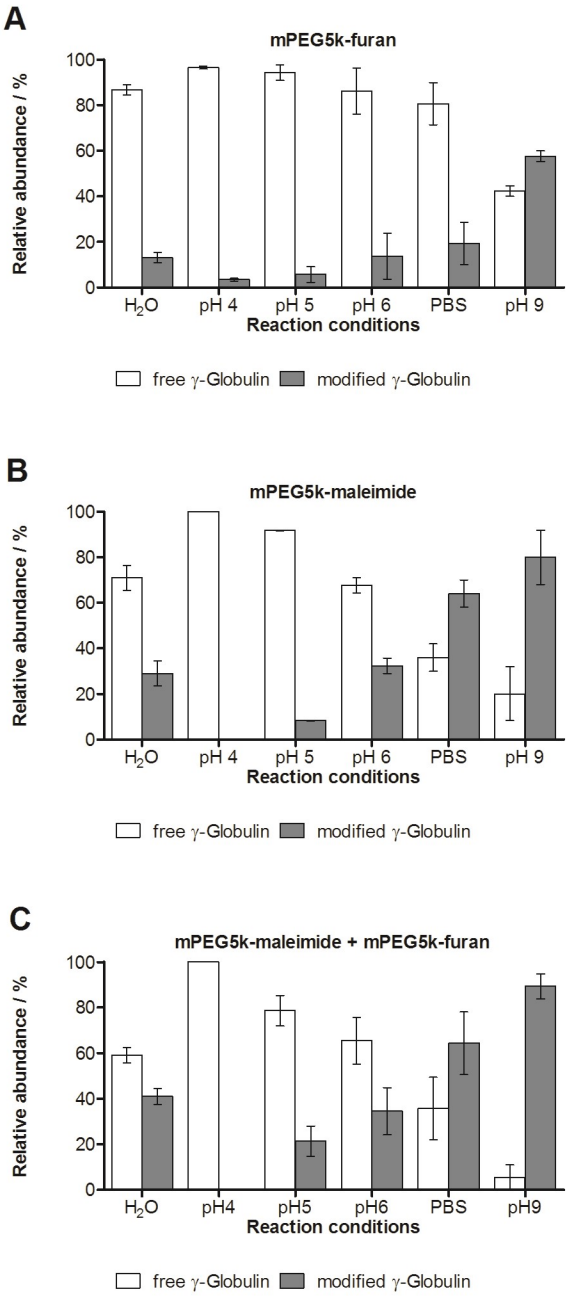

Figure 6.4: Modification of γ-globulin at different pH values analyzed by SDS-PAGE. γ-Globulin was incubated with mPEG5k-furan(A), mPEG5k-maleimide (B), and a mixture of both polymers (C). The results are shown as means ± standard deviation.

At pH 4, no modification was detected; an increasing pH resulted in an increasing degree of modification up to almost complete modification at pH 9 (6 ± 6.0 % of free γ-globulin). A suppression of side reactions by the availability of a reaction partner was not observed since Michael-type addition reactions are favored over Diels-Alder reactions as already mentioned above. A similar behavior in water and at pH 6 was observed in all three cases. Carbon dioxide dissolved in ultrapure water results in slightly acidic, but varying pH due to the absence of buffer capacity.

6.3.2. Protein Mobility in Diels-Alder Hydrogels

Protein mobility inside the Diels-Alder hydrogels was determined by FRAP in order to understand the release behavior of the used proteins [172]. FRAP is a method to investigate the diffusion of fluorescently labeled molecules in different tissues and materials [173]. For this purpose, the fluorophores are bleached in a defined area of the material by a laser. Afterwards the recovery of the fluorescence intensity in the photobleached area by diffusion of bleached molecules out of the defined area and fluorescent molecules into this area is followed by fluorescence microscopy (**Figure 6.5**) [173].

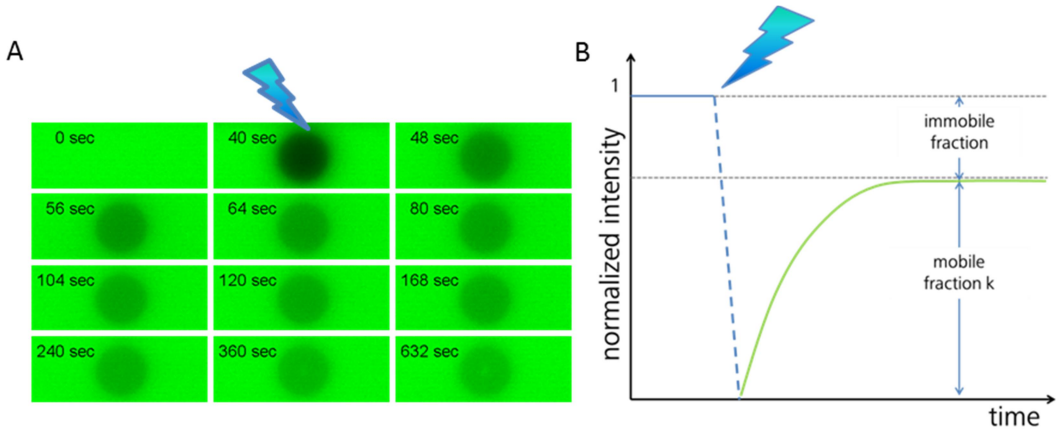

Figure 6.5: Fluorescence recovery after photobleaching. The flash symbolizes the process of photobleaching. Example of fluorescence microscope images during a typical experiment (A) and schematic diagram of the monitored intensity during an experiment (B). The initial intensity before photobleaching is represented by the blue line. The decreasing intensity during photobleaching is shown as blue dotted line. The green line represents the subsequent fluorescence recovery.

The fraction of not recovered fluorescence intensity corresponds to the immobile fraction, indicating binding of the protein to the hydrogel network [172]. The diffusion coefficient is a measure for protein mobility inside the hydrogel.

For the following experiments, proteins were labeled with Py1. Py1 is a chameleon label, which is blue and almost non-fluorescent in its free form; conjugation to primary amines of proteins (in particular ε-amino groups of lysine residues) results in red Py1-proteins with an excitation wavelength between 470 to 530 nm [174–176]. Dye, which is not bound during conjugation or cleaved of during the experiment, was non-fluorescent and cannot be detected during the measurement. This ensures that the higher mobility of the unbound dye is not included in the calculation of mobile fraction and diffusion coefficient of the protein.

The mobile fractions detected in these experiments depended on the pH during cross-linking (**Figure 6.6** A and B**)**.

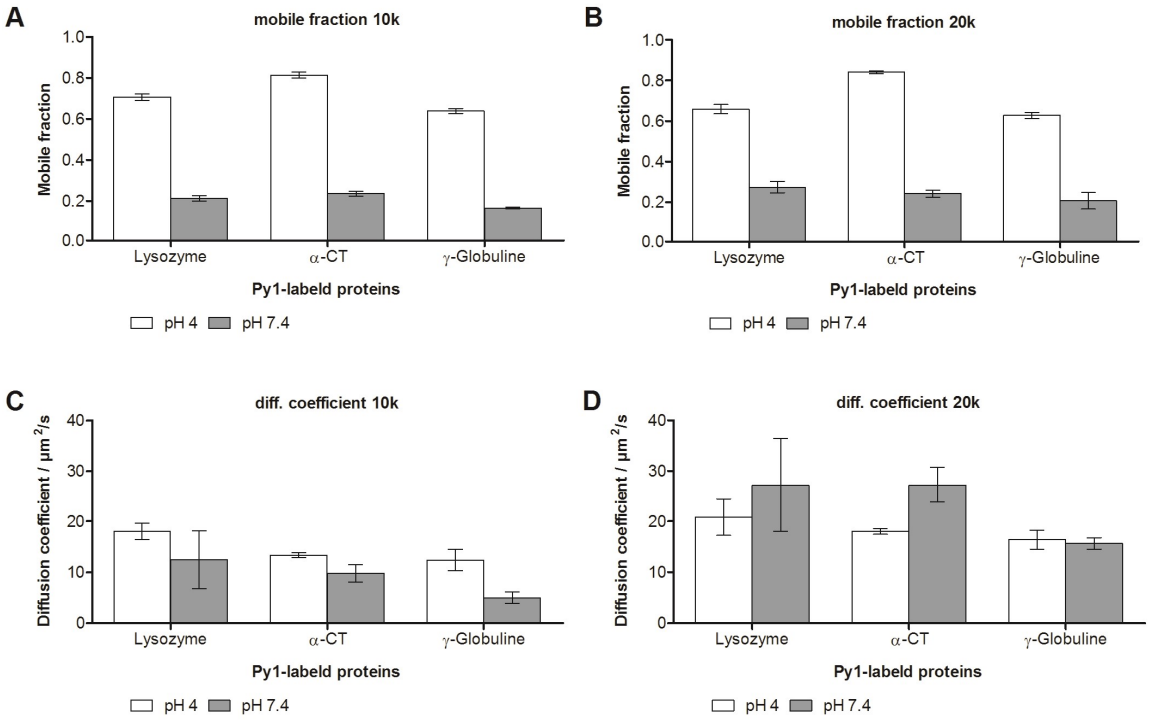

Figure 6.6: Fluorescence recovery after photobleaching. The mobility of Py1-lysozyme, Py1-α-CT and Py1-γ-globulin in Diels-Alder hydrogels (10 % polymer content) was determined after cross-linking at pH 4 and at pH 7.4. The diagrams show the mobile fraction of each protein in hydrogel preparations of 10 kDa (A) and 20 kDa (B) eight-armed PEG and the diffusion coefficients in hydrogel preparations of 10 kDa (C) and 20 kDa (D) eight-armed PEG. The results are shown as means ± standard deviation.

Cross-linking at pH 7.4 resulted in low mobile fractions of 0.16 ± 0.01 (α-CT, 8armPEG10k-hydrogel) to 0.27 ± 0.03 (lysozyme, 8armPEG20k-hydrogel). After cross-linking at pH 4, higher mobile fractions of up to 0.84 ± 0.01 (α-CT, 8armPEG20k-

hydrogel) were detected. As already discussed before, neutral or basic pH conditions promote Michael-type addition reactions between proteins and maleimide. These Michael-type addition reactions resulted in covalent protein attachment to the hydrogel backbone at pH 7.4. In this way, the fraction of mobile proteins was reduced under these conditions. Due to less pronounced Michael-type addition reactions at lower pH values, less side reactions and a higher mobile fraction were observed at pH 4. The molecular weight of PEG (10 kDa or 20 kDa) used for hydrogel preparation did not influence the mobile fraction of the incorporated proteins in the conducted experiments.

As expected, the diffusion coefficients depended on the size of the protein and the mesh size of the hydrogel (Figure 6.6 C and D) [177]. Due to the higher molecular weight of the macromonomers, the mesh size in 8armPEG20k-hydrogels (12.9 ± 0.6 nm) is larger compared to 8armPEG10k-hydrogels (5.5 ± 0.0 nm) [46]. The diffusion coefficients calculated for both types of hydrogels and literature values of diffusion coefficients in water at 20 °C are shown in **Table 6.1**.

Lysozyme is the smallest protein (R_h 2.1 nm) used in this experiment and showed the largest diffusion coefficients in all cases. Its hydrodynamic dynamic diameter is smaller than the mesh size of the used hydrogels; it was freely moving with almost equal diffusion coefficients in 8armPEG10k-hydrogels (D = 18.0 ± 1.6 $\mu m^2/s$) and 8armPEG20k-hydrogels (D = 20.8 ± 3.6 $\mu m^2/s$) after cross-linking at pH 4. After crosslinking at pH 7.4, higher diffusion coefficients were determined in 8armPEG20k-hydrogels (D = 27.2 ± 9.2 $\mu m^2/s$) compared to 8armPEG10k-hydrogels (D = 12.5 ± 5.7 $\mu m^2/s$). The diffusion coefficient of lysozyme in water at 20 °C is about 4-8 times higher (~107 $\mu m^2/s$) compared to the values measured in these experiments [178, 179]. Steric and hydrodynamic effects of the cross-linked polymer lower the diffusion coefficients of macromolecules incorporated in hydrogels compared to water [177].

The diffusion of α-CT is limited in 8armPEG10k-hydrogels because the mesh size of the hydrogel network is smaller than the hydrodynamic diameter of the protein. In 8armPEG20k-hydrogels, α-CT should be able to diffuse freely due to the larger mesh size. This is reflected by the increase of the diffusion coefficients from 13.4 ± 0.5 $\mu m^2/s$ (8armPEG10k-hydrogel) to 18.0 ± 0.6 $\mu m^2/s$ (8armPEG20k-hydrogel) at pH 4 and from 9.8 ± 1.7 $\mu m^2/s$ (8armPEG10k-hydrogel) to 27.2 ± 3.5 $\mu m^2/s$ (8armPEG20k-hydrogel) at pH 7.4. In 8armPEG20k-hydrogels the diffusion coefficient of α-CT and lysozyme were nearly the same. This is in good agreement with the values published for unhindered diffusion of α-CT and lysozyme in water (Table 6.1). The diffusion

coefficient of α-CT in water at 20 °C was about 4 - 11 times higher than in hydrogels (~108 $\mu m^2/s$) [180, 181].

γ-Globulin moved slower compared to lysozyme and α-CT in all cases due to its larger hydrodynamic diameter. This lower mobility is also reflected by the published diffusion coefficients in water. The diffusion coefficient of IgG in water at 20 °C is about 44 $\mu m^2/s$ [182–184]. The diffusion coefficient of IgM (~ 32 $\mu m^2/s$) and IgA (~ 52 $\mu m^2/s$) in water at 20 °C are slightly different [182]. In 8armPEG20k-hydrogel (16.4 ± 1.9 $\mu m^2/s$ at pH 4 and 15.6 ± 1.1 $\mu m^2/s$ at pH 7.4) higher diffusion coefficients were observed compared to 8armPEG10k-hydrogels (12.4 ± 2.1 $\mu m^2/s$ at pH 4 and 5.0 ± 1.1 $\mu m^2/s$ at pH 7.4). The main component of γ-globulin, IgG, has a hydrodynamic diameter of about 10.6 nm and is, therefore, able to diffuse freely in 8armPEG20k-hydrogels (mesh size: 12.9 nm), but not in 8armPEG10k-hydrogels (mesh size: 5.5 nm).

Table 6.1: Diffusion coefficients determined by FRAP experiments. Diffusion coefficients of lysozyme, α-CT, and γ-globulin in 8armPEG10k-hydrogels and 8armPEG20k-hydrogels in comparison to refecerence values and the corresponding hydrodynamic diameter.

Py1-protein	Hydrodynamic diameter (d_h) (nm)	D in water at 20 °C ($\mu m^2/s$)	D in 8armPEG10k-hydrogels [46] (mesh size: 5.5 ± 0.0 nm) ($\mu m^2/s$)		D in 8armPEG20k-hydrogels [46] (mesh size: 12.9 ± 0.6 nm) ($\mu m^2/s$)	
			pH 4	pH 7.4	pH 4	pH 7.4
Lysozyme	4.2[124, 155]	~ 107[178, 179]	18.0 ± 1.6	12.5 ± 5.7	20.8 ± 3.6	27.2 ± 9.2
α-CT	5.8[157]	~ 108[180, 181]	13.4 ± 0.5	9.8 ± 1.7	18.0 ± 0.6	27.2 ± 3.5
γ-Globulin	10.6 (IgG) [165] 25.4 (IgM) [165] 13.0 (IgA) [165]	~ 44[182–184] ~ 32[182] ~ 52[182]	12.4 ± 2.1	5.0 ± 1.1	16.4 ± 1.9	15.6 ± 1.1

The results of the FRAP experiments showed the dependence of protein mobility on the protein size, the mesh size of the hydrogel and the pH during cross-linking. However, the influence of swelling and degradation on the release behavior was not taken into account by FRAP experiments. It was not possible to study the changing mobility during hydrogel swelling using this set up. So, prediction of release kinetics based on FRAP experiments was not possible.

6.3.3. Protein Release from Diels-Alder Hydrogels

The suitability of Diels-Alder hydrogels for controlled protein release was investigated. To determine the influence of the pH during cross-linking, the hydrogels were prepared in PBS (pH 7.0 - 7.2) or ultrapure water, which shows a slightly acidic pH (pH 4 or pH 5) due to dissolved carbon dioxide. In order to study the influence of mesh size and cross-linking density, 8armPEG10k-hydrogels and 8armPEG20k-hydrogels were used in these experiments.

As already shown by FRAP experiments, the pH during cross-linking influences protein mobility in hydrogels. After cross-linking in water, lysozyme was completely released from 8armPEG10k-hydrogels within 24 h (94.2 ± 3.4 %) (**Figure** 6.7 A). The hydrodynamic diameter of lysozyme is smaller than the mesh size of the hydrogel; thus, lysozyme was able to diffuse freely and was released very fast. SDS-PAGE showed low degrees of modification after incubation of lysozyme with the gel precursors in water. Consequently low amounts of protein are covalently bound to the hydrogel network as verified by high mobile fractions in FRAP experiments. This allowed almost complete protein release independent of hydrogel degradation.

After cross-linking in PBS, lysozyme release proceeded in two steps. After 24 h, 35.3 ± 4.0 % of the incorporated lysozyme was released in a first burst. Afterwards, no further release was observed until a second burst after about 38 d. On day 38 and 42, the released amount abruptly increased from 37.0 ± 5.7 % to 74.3 ± 17.6 %. The release was completed at the same time as hydrogel degradation after 49 d. This is in line with the results obtained by SDS-PAGE (see Chap. 5) and FRAP. In PBS, Michael-type addition reactions of nucleophilic amino acids of lysozyme to the maleimide group occur to a greater extent than at the slightly acid reaction conditions in water. This led to protein attachment to the hydrogel backbone during cross-linking resulting in a low mobile fraction, as shown by FRAP. As a consequence, after the first burst release of unbound protein, the remaining amount of incorporated lysozyme is released during hydrogel degradation. The protein modification by the gel precursors is irreversible, so parts of the degraded gel are covalently attached to the protein even after the release is completed.

Similar results were obtained for the release of lysozyme from 8armPEG20k-hydrogels (Figure 6.7 B). Cross-linking in water limited side reactions with the gel precursors and the largest quantity of lysozyme was released within 24 h. Cross-linking in PBS resulted

in covalent attachment of lysozyme to the hydrogel network. During day 14 and 17, lysozyme release as well as hydrogel degradation were completed. It must be assumed that hydrogel fragments are irreversibly attached to lysozyme even after degradation as already mentioned above.

The release of α-CT from 8armPEG10k-hydrogels after cross-linking in water occurred somewhat slower compared to lysozyme, as expected from the diffusion coefficient and the slightly higher hydrodynamic diameter **(**Figure 6.7 C). A large amount (54.2 ± 6.2 %) of the incorporated α-CT was released over the first 24 h. The remaining amount (79.9 ± 15.7 %) was released during hydrogel swelling and degradation. The release was completed after 14 d. The high extent of modification after incubation with the gel precursors, as detected by SDS-PAGE, could not be verified. An explanation might be the undefined pH of ultrapure water. Due to the absence of buffer capacity, the pH might be different in each experiment. After cross-linking in PBS, 14.1 ± 3.1 % of the total α-CT amount was released in a first burst within 24 h. Until day 35, the release occurred very slowly. Afterwards, a second burst occurred simultaneously with hydrogel degradation. During day 35 and day 45, the amount of released α-CT increased abruptly from 23.6 ± 1.9 % to 96.0 ± 2.0 %. As detected by SDS-PAGE, incubation of α-CT with the gel precursors in PBS resulted in protein modification. These side reactions lead to covalent protein binding to the hydrogel backbone, which was also reflected in the low mobile fraction determined by FRAP experiments. Parts of the hydrogel were probably attached to the protein after degradation controlled release, as already mentioned for lysozyme.

The release profiles of α-CT from 8armPEG20k-hydrogels were similar for both cross-linking conditions (water or PBS) (Figure 6.7 D). During the first 24 h, 38.1 ± 3.3 % (cross-linking in water) and 26.2 ± 6.2 % (cross-linking in PBS) of α-CT was released in a first burst. The remaining protein amount was released during hydrogel degradation. 8armPEG20k-hydrogels degraded within 17 d (cross-linking in water) and 27 d (cross-linking in PBS), respectively. The incomplete recovery of α-CT may be caused by autolysis of the protein. The release from 8armPEG20k-hydrogels is in good agreement with the SDS-PAGE data, which showed almost the same extent of modification after incubation of α-CT with the gel precursors in water and PBS. The different results after incubation in water may be caused by the varying pH of ultrapure water due to the absence of buffer capacity as already mentioned above. In further studies, buffer should be used instead of water in all cases to standardize the conditions.

No influence of the cross-linking medium was observed for the release of γ-globulin from 8armPEG10k-hydrogels (Figure 6.7 E) and 8armPEG20k-hydrogels (Figure 6.7 F). The hydrodynamic diameter of IgG is larger than the meshes of 8armPEG10k-hydrogels and about the same size as the meshes of 8armPEG20k-hydrogels; the hydrodynamic diameter of IgA and IgM are larger than the meshes of both types of Diels-Alder hydrogels. For this reason, release is only possible during swelling and degradation, when the mesh size increases. Due to the slow degradation of 8armPEG10k-hydrogels [46], γ-globulin was released in two steps. First, the release of γ-globulin occurred very slowly; 30.1 ± 2.5 % (water) and 38.9 ± 1.3 % (PBS) of the incorporated γ-globulin was released after 28 d. During this time, the gel cylinders were visually stable. The remaining amount was rapidly released during hydrogel degradation. The release was completed after 42 d. 8armPEG20k-hydrogels degrade faster [46]; so, γ-globulin was continuously released over 14 d from 8armPEG20k-hydrogels. Due to the limited mobility of incorporated γ-globulin in all used hydrogel, covalent attachment to the hydrogel backbone would not have been detected in this experiment. However, irreversible modification of γ-globulin during cross-linking in PBS, as already mentioned for lysozyme and α-CT, is very likely. Even for the hydrogels prepared in water, the slightly acidic water inside the hydrogel is exchanged very fast by the neutral PBS surrounding the hydrogel during incubation. It should be kept in mind that Michael-type addition reactions might occur at a later time also after cross-linking in water, due to the long residence time of γ-globulin within the gel and the described increase of pH. This point should be part of further investigations. The release of proteins with attached hydrogel fragments might be problematic, because it may result in reduced bioactivity, decreased availability and increased immune responses [12, 51].

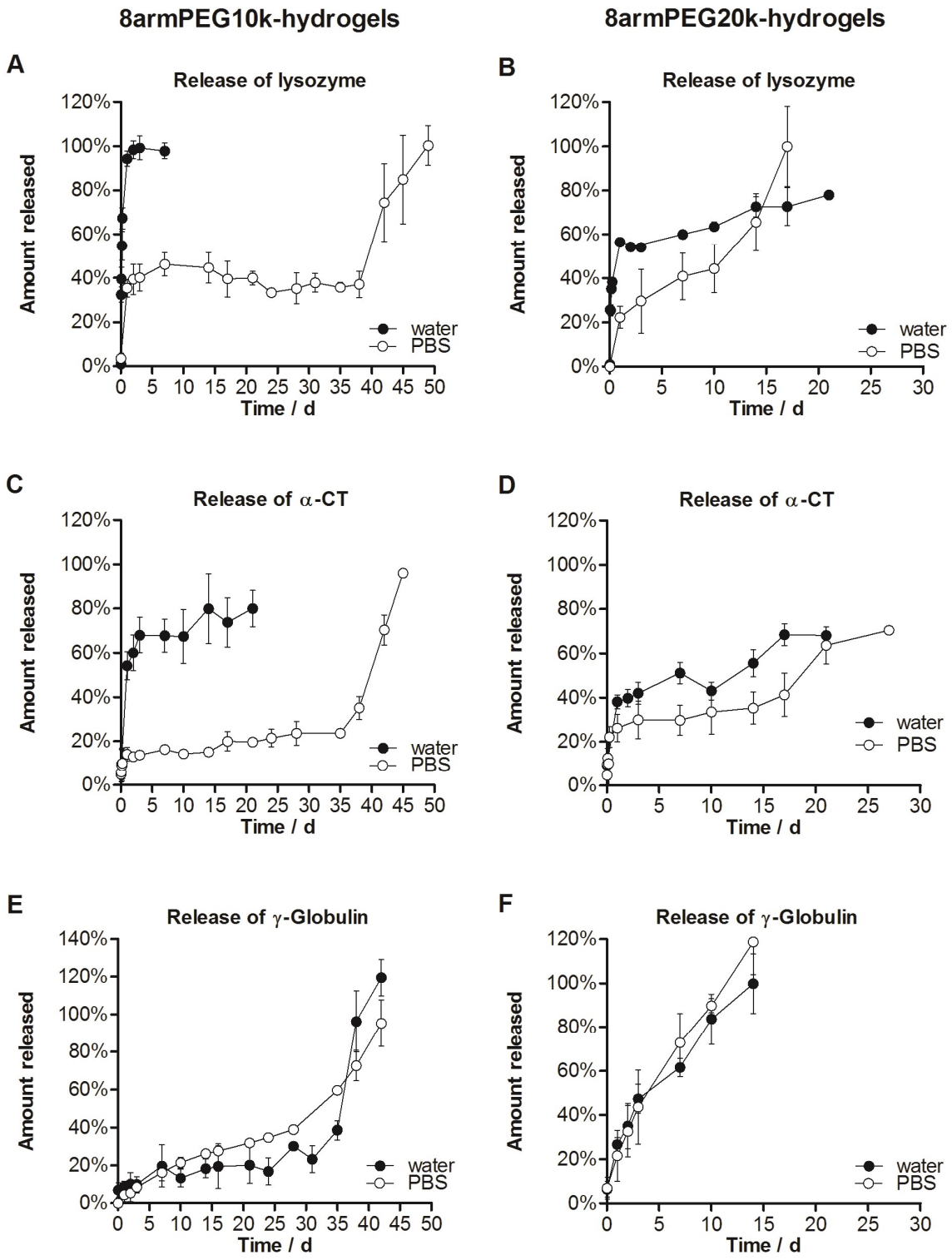

Figure 6.7: Release of lysozyme (A, B), α-Chymotrypsin (C, D) and γ-globulin (E, F) from Diels-Alder hydrogels (10k, 20k). The total polymer content of 8armPEG10k or 8armPEG20k, respectively, was 10 %. Crosslinking occurred in water (filled circle) or PBS (open circle). The results are shown as means ± standard deviation.

6.3.4. Enzymatic Activity of Lysozyme and α-CT

The protein activity after release from a carrier is an important factor in formulation development [12]. For this purpose, the activity of lysozyme and α-CT after incubation with mPEG5k-maleimide and after release from Diels-Alder hydrogels was investigated. For incubation with mPEG5k-maleimide, the same polymer amount was used as in SDS-PAGE experiments and, additionally, half and twice the quantity of polymer.

The enzymatic activity of lysozyme decreased from fully retained activity in pure water and at pH 4 to 36.0 ± 1.2 % activity after incubation with 3.66 µmol of mPEG5k-maleimide at pH 9 (**Figure 6.8**).

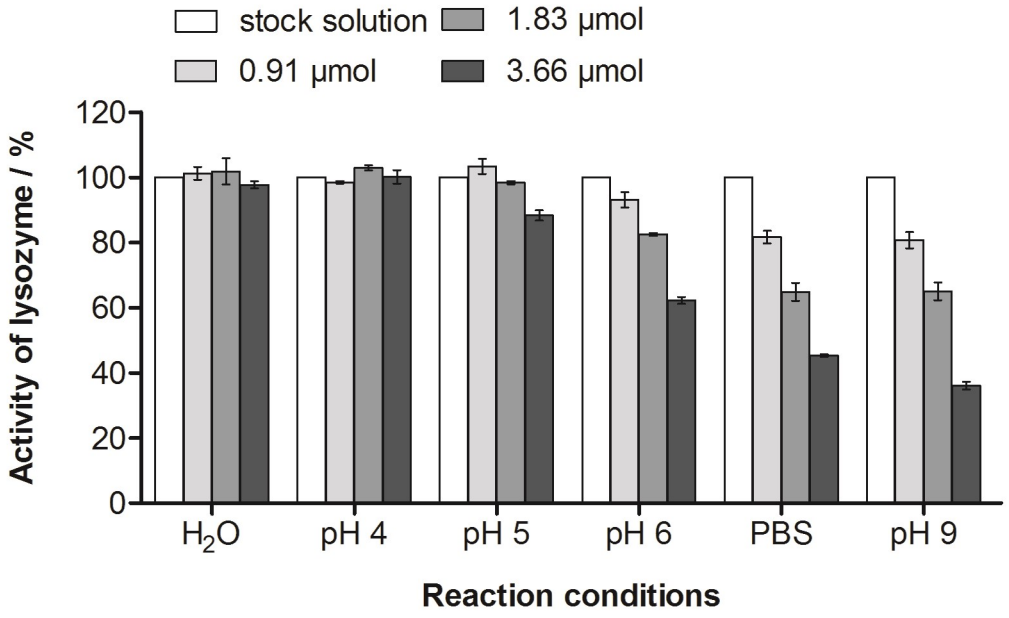

Figure 6.8: Activity of lysozyme after incubation with different amounts of mPEG5k-maleimide. The activity of the lysozyme stock solution was set to 100 %. The results are shown as means ± standard deviation.

The activity after incubation with mPEG5k-maleimide at pH 5, pH 6 and in PBS clearly depended on the used polymer amount, i.e., the amount of functional groups. At pH 6, for example, the activity decreased from 93.0 ± 2.4 % after incubation with 0.91 µmol of mPEG5k-maleimide to 82.5 ± 0.5 % after incubation with 1.83 µmol of mPEG5k-maleimide and 62.2 ± 1.1 % after incubation with 3.66 µmol of mPEG5k-maleimide, respectively. Lysozyme is known for loss of activity after covalent attachment of PEG chains [35, 84]. The observed decrease in activity after incubation with mPEG5k-

maleimide is caused by attachment of PEG chains due to Michael-type addition reactions of nucleophilic amino acids with maleimide as already described.

On the basis of all results obtained before, pH 4 was used during hydrogel preparation for the following release experiments (**Figure 6.9**). After incorporation in 8armPEG20k-hydrogels, the amount released after 24 h showed an activity of 97.1 ± 3.3 % compared to stock solution. The activity of lysozyme after incorporation in 8armPEG10k-hydrogels was somewhat lower (70.8 ± 4.6 %). This might be due to the double amount of functional groups in 8armPEG10k-hydrogels at equal polymer content and the resulting higher risk for side reactions [46]. Altogether, using pH 4 during cross-linking resulted in restricted side reactions and mostly retained activity of lysozyme after release.

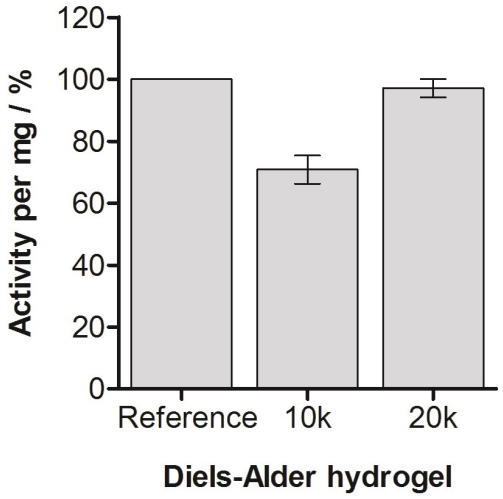

Figure 6.9: Activity of lysozyme after release from 8armPEG10k-/8armPEG20k-Diels-Alder hydrogels (10k and 20k). The results are shown as means ± standard deviation.

α-CT was more sensitive to varying pH conditions than lysozyme. Incubation of α-CT at different pH values resulted in different activities (**Figure 6.10**). Therefore, all activities were normalized to the highest activity detected (pH 4). With increasing pH, the activity of the stock solution decreased to only 3.8 ± 0.1 % at pH 9. α-CT is known for low enzymatic activity at basic pH conditions (≥ pH 8.5) [158]. The conjugation of PEG chains by Michael-type addition reactions during incubation, on the other hand, resulted in increased activity compared to the stock solution. After incubation in PBS, for example, the stock solution showed an activity of 27.9 ± 2.2 %, while the activity of the protein polymer mixture varied between 87.5 ± 2.3 % - 91.4 ± 5.1 %. Rodríguez-

Martínez et al. described the protection of α-CT by attached PEG chains against thermal inactivation during incubation at 45 °C [185]. This might explain the higher activity of α-CT after modification with mPEG5k-maleimide compared to the unmodified reference.

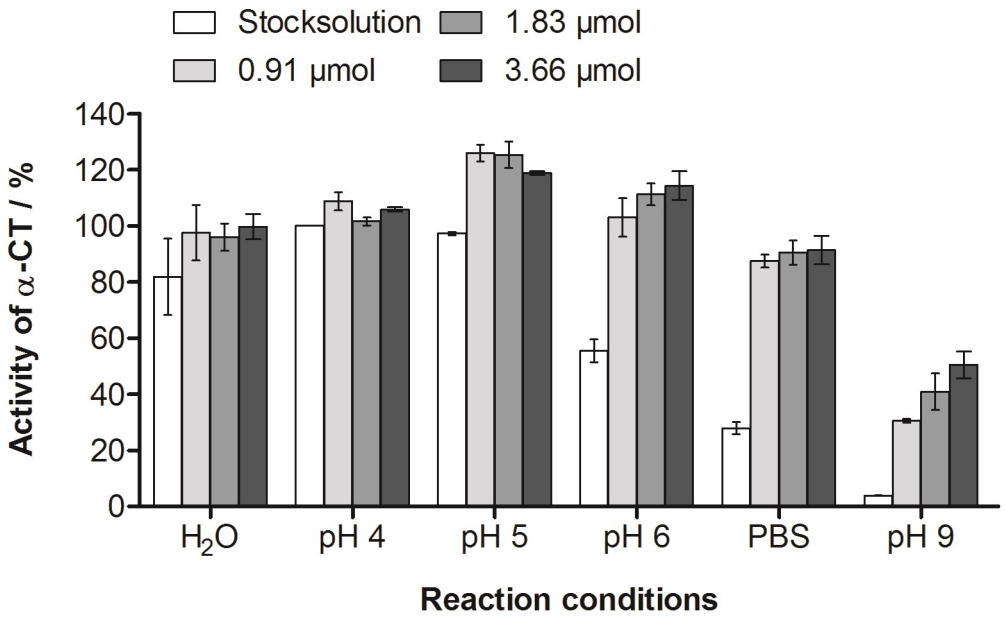

Figure 6.10: Activity of α-CT after 24h of incubation with different amounts of mPEG5k-maleimide. The activity of the stock solution with the highest activity after incubation (pH 4) was set to 100%. The results are shown as means ± standard deviation.

Similar results were obtained for α-CT released from Diels-Alder hydrogels (**Figure 6.11**). The amount released after 24 h showed an activity of 136.6 ± 4.4 % (8armPEG10k-hydrogels) and 168.9 ± 6.0 % (8armPEG20k-hydrogels), respectively. Free α-CT in solution shows autolysis resulting in decreased activity. PEGylation or immobilization in hydrogels or polymer matrices has successfully been used to improve the stability of α-CT and retain the activity [185–187]. The higher activity of α-CT released from Diels-Alder hydrogels might be explained by stabilization of proteins in hydrogels compared to proteins stored in solution [188].

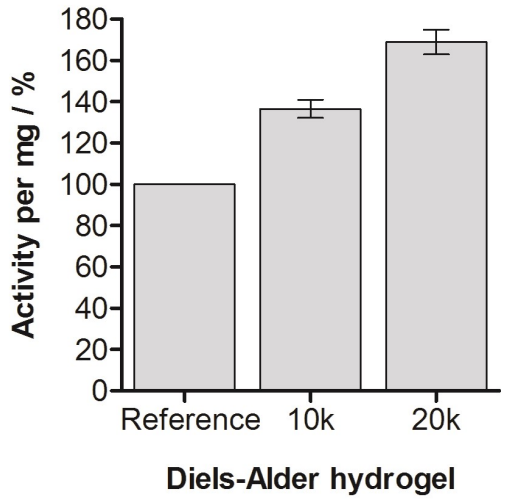

Figure 6.11: Activity of α-CT after release form Diels-Alder hydrogels related to a reference solution. The results are shown as means ± standard deviation.

6.4. Conclusion

The aim of this chapter was to investigate the suitability of Diels-Alder hydrogels as carrier for controlled delivery of protein drugs. The release kinetics could be modified by varying the network mesh size relative to the protein size. The enzymatic activity of the proteins after release could be almost completely retained or even increased by incorporating in the hydrogel compared to the reference solution. A slightly acidic pH was essential to prevent protein immobilization and inactivation during cross-linking. As already shown in Chap. 5, the pH during cross-linking of Diels-Alder hydrogels plays an important role with regard to side reactions with incorporated proteins. Especially at neutral or basic pH, Michael-type addition reactions of nucleophilic amino acids of the incorporated protein to maleimide are favored over Diels-Alder reactions. In line with the results obtained after incubation of lysozyme with mPEG5k-maleimide, α-CT and γ-globulin were modified depending on the pH conditions during incubation with mPEG5k-maleimide. The detected side reactions resulted in covalent protein attachment to the hydrogel backbone during cross-linking and influenced the protein mobility in the hydrogel, release profiles and activity of the released protein. Decreasing the pH during cross-linking prevented covalent protein binding via Michael-type addition reactions. This led to higher protein mobility inside the hydrogel and unhindered protein release, and helped to retain protein activity after release. However, protein integrity and stability should be kept in mind and investigated during

formulation development for each protein and pH value. Furthermore, there may be further strategies besides choosing the “right” pH value during cross-linking to prevent irreversible covalent protein binding. Removing the protein from the reaction site, for example by protein precipitation before cross-linking, could be one possibility. Further studies focusing on these strategies should be taken into consideration.

Chapter 7

Summary and Conclusions

7.1. Summary

The goal of this thesis was the development of suitable hydrogel formulations for the controlled delivery of protein drugs. In particular, consideration was given to protein integrity and activity during cross-linking and after release. For this purpose, two different strategies to tailor protein release were investigated; on the one hand, the reversible covalent attachment of proteins to the hydrogel backbone, on the other hand, the tailoring of the mesh size relative to the protein size.

The reversible linking of the model protein, lysozyme, was realized using hydrolytically cleavable carbamates. First, the suitability of click hydrogels as model systems for linker incorporation and release experiments was investigated. As expected, the incorporation of protein and linker caused defects in the hydrogel structure resulting in significant lower absolute values of complex shear modulus and increased swelling compared to the reference gels without linker **(Chap. 2)**. However, working with linkers would cause network defects in every hydrogel formulation. So, due to their still low swelling, high stiffness, fast gelation and non-degradability, click hydrogels were ideally suitable as model system to determine release kinetics without the influence of swelling or degradation. Nevertheless, the influence of the linker on gel properties should be kept in mind for formulation development for clinical applications.

In **Chapter 3** the suitability of carbamate linkers to control protein release was studied. SDS-PAGE experiments demonstrated that the kinetics of linker hydrolysis could successfully be controlled by the substitution pattern of the aromatic group. Depending on the used linker, linker hydrolysis took between 24 h and 28 d. This was in good agreement with the obtained release data; depending on the used linker, lysozyme release from click hydrogels lasted up to 21 d.

CD spectroscopy indicated structural integrity of the secondary structure of lysozyme after PEGylation and De-PEGylation. As verified by SDS-PAGE only the three surface lysine residues were modified due to the mild PEGylation conditions preventing structural damage. After PEG chain elimination the activity of lysozyme was restored to 73.4 % - 92.5 %, once more indicating structural integrity after cleaving off the linker group. However, PEGylation with the used carbamate linkers was not fully reversible. A maximum of 60 % of the initial dose was recovered during release. SDS-PAGE experiments provided similar results; here a recovery of maximal 63 % of free lysozyme was detected. This irreversible PEGylation may be caused by aliphatic non-degradable

site products of linker synthesis. In clinical application of degradable hydrogel systems this might cause release of protein irreversibly modified with polymer chains of the degraded hydrogel. Undefined limited activity would be the consequence. Another possible explanation might be the formation of protein aggregates due to reactions of the isocyanate formed during linker hydrolysis. In fact, lysozyme aggregates were identified by SDS-PAGE during PEG chain elimination. The presence of aggregates may result in immune response and would prevent application in humans. Further investigations should focus on the reason for incomplete PEG chain elimination and protein release and possibilities to prevent this phenomenon.
For additional analytics of PEG chain elimination a SEC method was established allowing automated sampling and standardized data evaluation and quantification (**Chap. 4**). A special manufactured heating device permitted real-time sampling. This method confirmed the elimination kinetics determined by SDS-PAGE. Elimination of Linker 2a was completed after about 26 h. As already described above, PEGylation as well as PEG chain elimination were incomplete. In contrast to SDS-PAGE experiments, no lysozyme aggregates during PEGylation and PEG chain elimination were observed using SEC. The drawback of this experimental setup was the column degradation after about 160 injections. For future experiments, sample purification would be a possibility to overcome this issue.

The second strategy, tailoring release kinetics via the hydrodynamic diameter of the drug and hydrogel mesh size was realized using Diels-Alder hydrogels. In order to vary the mesh size and hydrogel degradation, PEG derivatives with two different molecular weights (10 kDa and 20 kDa) were used. With regard to protein integrity, the Diels-Alder precursor maleimide and furan were compared to other common cross-linking mechanisms (**Chap. 5**). The study showed side reactions of all tested gel precursors. Nucleophilic amino acids, especially lysine, were modified pH-dependent in Michael-type addition reactions by maleimide, vinyl sulfone and acrylamide groups. Especially increased pH values promoted these unintended side reactions. mPEG6k-thiol resulted in pH-independent thiol-disulfide exchange reactions with cysteine residues. The incubation with mixtures of cross-linking partners only partially reduced protein modification. In some cases even higher degree of modification was observed. The degree of lysozyme modification ranged between slight PEGylation with 2 polymer chains and 88 ± 1.9 % lysozyme remaining unmodified (after incubation with a mixture

of mPEG5k-acrylamide and mPEG6k-thiol at pH4) to complete modification with up to seven PEG chains (after incubation with a mixture of mPEG5k-vinyl sulfone and mPEG6k-thiol at pH 9).

The extent of modification not only depends on the pH and the used functionalization but also on the protein. Incubation of α-CT and γ-globulin with the Diels-Alder precursors, mPEG5k-furan and mPEG5k-maleimide, resulted in modifications varying between 0 % and 89 ± 5.5 % depending on the pH and polymer functionalization (**Chap. 6**). The degree of modification would be different for each formulation and each incorporated drug and would require individual investigations. However, especially the modification of amino acids located inside the tertiary structure would result in structural breakdown associated with loss of activity, decreased availability and unintended immune response. Furthermore, modifications lead to covalent protein attachment to the hydrogel backbone limiting protein mobility and subsequent release. This was verified by FRAP and release experiments using Diels-Alder hydrogels (**Chap. 6**). For lysozyme for example, covalent attachment at pH 7.4 resulted in low mobile fractions of 0.21 ± 0.01 (8armPEG10k-hydrogel), while pH 4 prevented side reactions resulting in higher mobile fractions of 0.71 ± 0.02 (8armPEG10k-hydrogel). Release experiments showed similar results; cross-linking in slightly acidic water resulted in almost complete lysozyme release within 24 h with almost retained protein activity. Using PBS, release occurred in two steps associated with ongoing hydrogel degradation. However, one has to keep in mind that there is a very fast exchange of medium between the hydrogel and the surrounding resulting in pH shifts. For this reason, reactions between the protein and the polymer might also be possible to a later point of time. However, protein mobility and release were successfully controlled by the mesh size of the Diels-Alder hydrogel. For example, γ-globulin was released in two steps over 42 d from 8armPEG10k-hydrogels. The release from 8armPEG20k-hydrogels occurred continuously within 28 d.

7.2. Conclusion and Outlook

Overall, two different strategies, reversible covalent protein attachment via carbamate linkers and tailoring the hydrogel mesh size relative to the protein size, were investigated and successfully used to control the release of proteins; each one with individual benefits and drawbacks. For both strategies discussed here, irreversible

protein modifications represent the risk of immune reactions and restricted activity. However, on the other hand Diels-Alder hydrogels offered protection and stabilization to the protein as indicated by increasing activity of α-CT after release.

Complete prevention of side reactions between protein and polymer, complete absence of protein aggregation and the maintenance of therapeutic activity is the key challenge for the development of protein formulations. These points should be addressed in further studies in order to optimize the presented hydrogel formulation and to remove the remaining concerns.

For this purpose, careful evaluation of the formulation using reliable protein analytic is of great importance. Establishing suitable assays addressing protein quantification, activity and integrity of the protein can be tricky, but is essential for successful formulation development and should be one of the key aspects of further investigations.

References

[1] V. R. Sinha, A. Trehan, Biodegradable microspheres for protein delivery, *J. Control. Release.* 90 (2003) 261–280.

[2] T. Degim, N. Celebi, Controlled Delivery of Peptides and Proteins, *Curr. Pharm. Des.* 13 (2007) 99–117.

[3] H.-C. Mahler, G. Borchard, H. Luessen, *Protein pharmaceuticals. Formulation, analytics and delivery.* APV pharma reflexions. 3. ECV - Ed.-Cantor-Verl., Aulendorf (2010).

[4] A. L. Lehninger, D. L. Nelson, M. M. Cox, *Lehninger principles of biochemistry*. W.H. Freeman, New York (2005).

[5] S. McNicholas, E. Potterton, K. S. Wilson, M. E. M. Noble, Presenting your structures: the CCP 4 mg molecular-graphics software, *Acta Crystallogr. D. Biol. Crystallogr.* 67 (2011) 386–394.

[6] R. Diamond, Real-space refinement of the structure of hen egg-white lysozyme, *J. Mol. Biol.* 82 (1974) 371–391.

[7] S. Frokjaer, D. E. Otzen, Protein drug stability: a formulation challenge, *Nat. Rev. Drug Discov.* 4 (2005) 298–306.

[8] C. J. Fee, J. M. Van Alstine, PEG-proteins: Reaction engineering and separation issues, *Chem. Eng. Sci.* 61 (2006) 924–939.

[9] M. El Sanharawi, L. Kowalczuk, E. Touchard, S. Omri, Y. de Kozak, F. Behar-Cohen, Protein delivery for retinal diseases: From basic considerations to clinical applications, *Prog. Retin. Eye Res.* 29 (2010) 443–465.

[10] W. Wang, Protein aggregation and its inhibition in biopharmaceutics, *Int. J. Pharm.* 289 (2005) 1–30.

[11] Guidance for Industry: *Immunogenicity Assessment for Therapeutic Protein Product.* U.S. Department of Health and Human Services Food and Drug Administration, Center for Drug Evaluation and Research (CDER), Center for Biologics Evaluation and Research (CBER), Rockville, MD (2014).

[12] T. Vermonden, R. Censi, W. E. Hennink, Hydrogels for protein delivery, *Chem. Rev.* 112 (2012) 2853–2888.

[13] M. Takano, Y. Koyama, H. Nishikawa, T. Murakami, R. Yumoto, Segment-selective absorption of lysozyme in the intestine, *Eur. J. Pharmacol.* 502 (2004) 149–155.

[14] R. E. Kontermann, Strategies for extended serum half-life of protein therapeutics, *Curr. Opin. Biotechnol.* 22 (2011) 868–876.

[15] B. Leader, Q. J. Baca, D. E. Golan, Protein therapeutics: a summary and pharmacological classification, *Nat. Rev. Drug Discov.* 7 (2008) 21–39.

[16] K. Fu, A. M. Klibanov, R. Langer, *Nat. Biotechnol*. 18 (2000) 24–25.

[17] M. A. Capelle, R. Gurny, T. Arvinte, High throughput screening of protein formulation stability: Practical considerations, *Eur. J. Pharm. Biopharm.* 65 (2007) 131–148.

[18] E. Chi, S. Krishnan, T. Randolph, J. Carpenter, Physical Stability of Proteins in Aqueous Solution: Mechanism and Driving Forces in Nonnative Protein Aggregation, *Pharm. Res.* 20 (2003) 1325-1336.

[19] G. Zhu, S. R. Mallery, S. P. Schwendeman, Stabilization of proteins encapsulated in injectable poly (lactide- co-glycolide), *Nature biotechnology*. 18 (2000) 52–57.

[20] M. van de Weert, M. J. van Steenbergen, J. L. Cleland, J. Heller, W. E. Hennink, D. J. A. Crommelin, Semisolid, self-catalyzed poly(ortho ester)s as controlled-release systems: protein release and protein stability issues, *J. Pharm. Sci.* 91 (2002) 1065–1074.

[21] C. Packhaeuser, J. Schnieders, C. Oster, T. Kissel, In situ forming parenteral drug delivery systems: an overview, *Eur. J. Pharm. Biopharm.* 58 (2004) 445–455.

[22] M. van de Weert, W. E. Hennink, W. Jiskoot, Protein Instability in Poly(Lactic-co-Glycolic Acid) Microparticles, *Pharm. Res*. 17 (2000) 1159–1167.

[23] A. Lucke, J. Kiermaier, A. Göpferich, Peptide Acylation by Poly(α-Hydroxy Esters), *Pharm. Res*. 19 (2002) 175-181.

[24] B. Qiu, S. Stefanos, J. Ma, A. Lalloo, B. A. Perry, M. J. Leibowitz, P. J. Sinko, S. Stein, A hydrogel prepared by in situ cross-linking of a thiol-containing poly(ethylene glycol)-based copolymer: a new biomaterial for protein drug delivery, *Biomaterials.* 24 (2003) 11–18.

[25] C. Hiemstra, L. J. van der Aa, Z. Zhong, P. J. Dijkstra, J. Feijen, Novel in Situ Forming, Degradable Dextran Hydrogels by Michael Addition Chemistry: Synthesis, Rheology, and Degradation, *Macromolecules.* 40 (2007) 1165–1173.

[26] B. Maiser, F. Dismer, J. Hubbuch, Optimization of random PEGylation reactions by means of high throughput screening, *Biotechnol. Bioeng.* 111 (2014) 104–114.

[27] M. Malkoch, R. Vestberg, N. Gupta, L. Mespouille, P. Dubois, A. F. Mason, J. L. Hedrick, Q. Liao, C. W. Frank, K. Kingsbury, C. J. Hawker, Synthesis of well-defined hydrogel networks using Click chemistry, *Chem. Commun.* (2006) 2774–2776.

[28] V. D. Bock, H. Hiemstra, J. H. van Maarseveen, Cu^{I}-Catalyzed Alkyne–Azide "Click" Cycloadditions from a Mechanistic and Synthetic Perspective, *Eur. J. Org. Chem.* 2006 (2006) 51–68.

[29] J. L. Vanderhooft, M. Alcoutlabi, J. J. Magda, G. D. Prestwich, Rheological Properties of Cross-Linked Hyaluronan-Gelatin Hydrogels for Tissue Engineering, *Macromol. Biosci.* 9 (2009) 20–28.

[30] P. Gupta, K. Vermani, S. Garg, Hydrogels: from controlled release to pH-responsive drug delivery, *Drug Discov. Today.* 7 (2002) 569–579.

[31] T. Canal, N. A. Peppas, Correlation between mesh size and equilibrium degree of swelling of polymeric networks, *J. Biomed. Mater. Res.* 23 (1989) 1183–1193.

[32] J. L. Drury, D. J. Mooney, Hydrogels for tissue engineering: scaffold design variables and applications, *Biomaterials.* 24 (2003) 4337–4351.

[33] S. Udenfriend, S. Stein, P. Bohlen, W. Dairman, W. Leimgruber, M. Weigele, Fluorescamine: A Reagent for Assay of Amino Acids, Peptides, Proteins, and Primary Amines in the Picomole Range, *Science.* 178 (1972) 871–872.

[34] F. Brandl, M. Henke, S. Rothschenk, R. Gschwind, M. Breunig, T. Blunk, J. Tessmar, A. Göpferich, Poly(Ethylene Glycol) Based Hydrogels for Intraocular Applications, *Adv. Eng. Mater.* 9 (2007) 1141–1149.

[35] N. Hammer, F. P. Brandl, S. Kirchhof, A. M. Goepferich, Cleavable carbamate linkers for controlled protein delivery from hydrogels, *J. Control. Release.* 183 (2014) 67–76.

[36] E. D. Goddard-Borger, R. V. Stick, An Efficient, Inexpensive, and Shelf-Stable Diazotransfer Reagent: Imidazole-1-sulfonyl Azide Hydrochloride, *Org. Lett.* 9 (2007) 3797–3800.

[37] C. Yan, D. J. Pochan, Rheological properties of peptide-based hydrogels for biomedical and other applications, *Chem. Soc. Rev.* 39 (2010) 3528.

[38] E. Engleder, C. Honeder, J. Klobasa, M. Wirth, C. Arnoldner, F. Gabor, Preclinical evaluation of thermoreversible triamcinolone acetonide hydrogels for drug delivery to the inner ear, *Int. J. Pharm.* 471 (2014) 297–302.

[39] E. Lallana, F. Fernandez-Trillo, A. Sousa-Herves, R. Riguera, E. Fernandez-Megia, Click Chemistry with Polymers, Dendrimers, and Hydrogels for Drug Delivery, *Pharm. Res.* 29 (2012) 902–921.

[40] A. Uliniuc, M. Popa, T. Hamaide, M. Dobromir, New approaches in hydrogel synthesis - Click chemistry: A review, *Cell. Chem. Technol.* (2012) 1–11.

[41] V. V. Rostovtsev, L. G. Green, V. V. Fokin, K. B. Sharpless, A Stepwise Huisgen Cycloaddition Process: Copper(I)-Catalyzed Regioselective "Ligation" of Azides and Terminal Alkynes*, Angew. Chem. Int. Ed.* 41 (2002) 2596–2599.

[42] M. Shibayama, Structure-mechanical property relationship of tough hydrogels, *Soft Matter.* 8 (2012) 8030–8038.

[43] K. S. Anseth, C. N. Bowman, L. Brannon-Peppas, Mechanical properties of hydrogels and their experimental determination, *Biomaterials.* 17 (1996) 1647–1657.

[44] E. A. Phelps, N. O. Enemchukwu, V. F. Fiore, J. C. Sy, N. Murthy, T. A. Sulchek, T. H. Barker, A. J. García, Maleimide Cross-Linked Bioactive PEG Hydrogel Exhibits Improved Reaction Kinetics and Cross-Linking for Cell Encapsulation and In Situ Delivery, *Adv. Mater.* 24 (2012) 64–70.

[45] S. K. Patel, S. Malone, C. Cohen, J. R. Gillmor, R. H. Colby, Elastic modulus and equilibrium swelling of poly(dimethylsiloxane) networks, *Macromolecules.* 25 (1992) 5241–5251.

[46] S. Kirchhof, F. P. Brandl, N. Hammer, A. M. Goepferich, Investigation of the Diels–Alder reaction as a cross-linking mechanism for degradable poly(ethylene glycol) based hydrogels, *J. Mater. Chem. B.* 1 (2013) 4855–4864.

[47] S. Thirumaleshwar, P. K. Kulkarni, D. V. Gowda, Liposomal Hydrogels: A Novel Drug Delivery System for Wound Dressing, *Curr. Drug ther.* 7 (2012) 212–218.

[48] S. H. M. Söntjens, D. L. Nettles, M. A. Carnahan, L. A. Setton, M. W. Grinstaff, Biodendrimer-Based Hydrogel Scaffolds for Cartilage Tissue Repair, *Biomacromolecules.* 7 (2006) 310–316.

[49] D. V. Goeddel, D. G. Kleid, F. Bolivar, H. L. Heyneker, D. G. Yansura, R. Crea, T. Hirose, A. Kraszewski, K. Itakura, A. D. Riggs, Expression in Escherichia coli of chemically synthesized genes for human insulin, *Proc. Natl. Acad. Sci.* 76 (1979) 106–110.

[50] V. F. M. Segers, R. T. Lee, Local delivery of proteins and the use of self-assembling peptides, *Drug Discov. Today*. 12 (2007) 561–568.

[51] C.-C. Lin, K. Anseth, PEG Hydrogels for the Controlled Release of Biomolecules in Regenerative Medicine, *Pharm. Res.* 26 (2009) 631–643.

[52] R. G. Schoenmakers, P. van de Wetering, D. L. Elbert, J. A. Hubbell, The effect of the linker on the hydrolysis rate of drug-linked ester bonds, *J. Control. Release.* 95 (2004) 291–300.

[53] K. H. Bouhadir, G. M. Kruger, K. Y. Lee, D. J. Mooney, Sustained and controlled release of daunomycin from cross-linked poly(aldehyde guluronate) hydrogels, *J. Pharm. Sci.* 89 (2000) 910–919.

[54] J. R. Tauro, R. A. Gemeinhart, Matrix Metalloprotease Triggered Delivery of Cancer Chemotherapeutics from Hydrogel Matrixes, *Bioconjug. Chem.* 16 (2005) 1133–1139.

[55] X. Zhao, J. Milton Harris, Novel degradable poly(ethylene glycol) hydrogels for controlled release of protein, *J. Pharm. Sci.* 87 (1998) 1450–1458.

[56] A. H. Zisch, M. P. Lutolf, M. Ehrbar, G. P. Raeber, S. C. Rizzi, N. Davies, H. Schmökel, D. Bezuidenhout, V. Djonov, P. Zilla, J. A. Hubbell, Cell-demanded release of VEGF from synthetic, biointeractive cell ingrowth matrices for vascularized tissue growth, *FASEB J.* 17 (2003) 2260–2262.

[57] D. Seliktar, A. H. Zisch, M. P. Lutolf, J. L. Wrana, J. A. Hubbell, MMP-2 sensitive, VEGF-bearing bioactive hydrogels for promotion of vascular healing, *J. Biomed. Mater. Res.* 68 (2004) 704–716.

[58] M. E. Davis, Local myocardial insulin-like growth factor 1 (IGF-1) delivery with biotinylated peptide nanofibers improves cell therapy for myocardial infarction, *Proc. Natl. Acad. Sci.* 103 (2006) 8155–8160.

[59] E. Verheyen, S. van der Wal, H. Deschout, K. Braeckmans, S. de Smedt, A. Barendregt, W. E. Hennink, C. F. van Nostrum, Protein macromonomers containing reduction-sensitive linkers for covalent immobilization and glutathione triggered release from dextran hydrogels, *J. Control. Release*. 156 (2011) 329–336.

[60] K. C. Koehler, K. S. Anseth, C. N. Bowman, Diels–Alder Mediated Controlled Release from a Poly(ethylene glycol) Based Hydrogel, *Biomacromolecules*. 14 (2013) 538–547.

[61] M. Roberts, M. Bentley, J. Harris, Chemistry for peptide and protein PEGylation, *Adv. Drug Deliv. Rev*. 54 (2002) 459–476.

[62] A. Lucke, E. Fustella, J. Teßmar, A. Gazzaniga, A. Göpferich, The effect of poly(ethylene glycol)–poly(d,l-lactic acid) diblock copolymers on peptide acylation, *J. Control. Release.* 80 (2002) 157–168.

[63] S. Lee, R. B. Greenwald, J. McGuire, K. Yang, C. Shi, Drug Delivery Systems Employing 1,6-Elimination: Releasable Poly(ethylene glycol) Conjugates of Proteins, *Bioconjug. Chem.* 12 (2001) 163–169.

[64] F. Brandl, N. Hammer, T. Blunk, J. Tessmar, A. Goepferich, Biodegradable Hydrogels for Time-Controlled Release of Tethered Peptides or Proteins, *Biomacromolecules.* 11 (2010) 496–504.

[65] A. Natarajan, C.-Y. Xiong, A. Huguette, G. L. DeNardo, S. J. DeNardo, Characterization of Site-Specific ScFv PEGylation for Tumor-Targeting Pharmaceuticals, *Bioconjug. Chem.* 16 (2005) 113–121.

[66] C. A. Schneider, W. S. Rasband, K. W. Eliceiri, NIH Image to ImageJ: 25 years of image analysis, *Nat Meth.* 9 (2012) 671–675.

[67] G. Böhm, R. Muhr, R. Jaenicke, Quantitative analysis of protein far UV circular dichroism spectra by neural networks, *Protein Engineering.* 5 (1992) 191–195.

[68] D. Shugar, The Measurment of lysozyme activity and the ultra-violet inactivation of lysozyme, *Biochim. Biophys. Acta*. 8 (1952) 302-309.

[69] M. M. Bradford, A rapid and sensitive method for the quantitation of microgram quantities of protein utilizing the principle of protein-dye binding, *Anal. Biochem.* 72 (1976) 248–254.

[70] R. B. Greenwald, A. Pendri, C. D. Conover, H. Zhao, Y. H. Choe, A. Martinez, K. Shum, S. Guan, Drug Delivery Systems Employing 1,4- or 1,6-Elimination: Poly(ethylene glycol) Prodrugs of Amine-Containing Compounds, *J. Med. Chem.* 42 (1999) 3657–3667.

[71] R. B. Greenwald, K. Yang, H. Zhao, C. D. Conover, S. Lee, D. Filpula, Controlled release of proteins from their poly(ethylene glycol) conjugates: drug delivery systems employing 1,6-elimination, *Bioconjug. Chem.* 14 (2003) 395–403.

[72] R. B. Greenwald, Y. H. Choe, C. D. Conover, K. Shum, D. Wu, M. Royzen, Drug Delivery Systems Based on Trimethyl Lock Lactonization: Poly(ethylene glycol) Prodrugs of Amino-Containing Compounds, *J. Med. Chem.* 43 (2000) 475–487.

[73] H. Zhao, K. Yang, A. Martinez, A. Basu, R. Chintala, H.-C. Liu, A. Janjua, M. Wang, D. Filpula, Linear and branched bicin linkers for releasable PEGylation of macromolecules: controlled release in vivo and in vitro from mono- and multi-PEGylated proteins, *Bioconjug. Chem.* 17 (2006) 341–351.

[74] R. B. Greenwald, Y. H. Choe, J. McGuire, C. D. Conover, Effective drug delivery by PEGylated drug conjugates, *Adv. Drug Deliv. Rev.* 55 (2003) 217–250.

[75] D. Filpula, H. Zhao, Releasable PEGylation of proteins with customized linkers, *Adv. Drug Deliv. Rev.* 60 (2008) 29–49.

[76] L. W. Dittert, T. Higuchi, Rates of hydrolysis of carbamate and carbonate esters in alkaline solution, *J. Pharm. Sci.* 52 (1963) 852–857.

[77] A. Williams, Alkaline hydrolysis of substituted phenyl N-phenylcarbamates. Structure-reactivity relationships consistent with an E1cB mechanism, *J. Chem. Soc., Perkin Trans.* 2 (1972) 808–812.

[78] A. F. Hegarty, L. N. Frost, Elimination-addition mechanism for the hydrolysis of carbamates. Trapping of an isocyanate intermediate by an o-amino-group, *J. Chem. Soc., Perkin Trans.* 2 (1973) 1719–1728.

[79] A. F. Hegarty, L. N. Frost, J. H. Coy, Question of amide group participation in carbamate hydrolysis, *J. Org. Chem.* 39 (1974) 1089–1093.

[80] J. Hansen, N. Mørk, H. Bundgaard, Phenyl carbamates of amino acids as prodrug forms for protecting phenols against first-pass metabolism, *Int. J. Pharm.* 81 (1992) 253–261.

[81] J. L. Bolton, S. B. Turnipseed, J. A. Thompson, Influence of quinone methide reactivity on the alkylation of thiol and amino groups in proteins: studies utilizing amino acid and peptide models, *Chem. Biol. Interact.* 107 (1997) 185–200.

[82] G. V. Kleopina, N. A. Kravchenko, E. D. Kaverzneva, Role of the 6-amino groups of lysine in lysozyme, *Russ. Chem. Bull.* 14 (1965) 806–812.

[83] E. Verheyen, L. Delain-Bioton, S. van der Wal, N. el Morabit, A. Barendregt, W. E. Hennink, C. F. van Nostrum, Conjugation of Methacrylamide Groups to a Model Protein via a Reducible Linker for Immobilization and Subsequent Triggered Release from Hydrogels, *Macromol. Biosci.* 10 (2010) 1517–1526.

[84] M. J. Roberts, J. Milton Harris, Attachment of degradable poly(ethylene glycol) to proteins has the potential to increase therapeutic efficacy, *J. Pharm. Sci.* 87 (1998) 1440–1445.

[85] M. Morpurgo, E. A. Bayer, M. Wilchek, N-hydroxysuccinimide carbonates and carbamates are useful reactive reagents for coupling ligands to lysines on proteins, *J. Biochem. Biophys. Methods.* 38 (1999) 17–28.

[86] A. F. Hegarty, L. N. Frost, Isocyanate intermediates in Elcb mechanism of carbamate hydrolysis, *J. Chem. Soc., Chem. Commun.* (1972) 500.

[87] D. J. Woodcock, A carbamate anion-isocyanate equilibrium, *Chem. Commun.* (1968) 267–268.

[88] W. E. Brown, A. H. Green, T. E. Cedel, J. Cairns, Biochemistry of protein-isocyanate interactions: a comparison of the effects of aryl vs. alkyl isocyanates, *Environ. Health Perspect.* 72 (1987) 5–11.

[89] O. G. Hampe, Conformation of lysozyme in aqueous solution. Effect of ionic strength and protein concentration, *Eur. J. Biochem.* 31 (1972) 32–37.

[90] J. A. Rodríguez-Martínez, I. Rivera-Rivera, K. Griebenow, Prevention of benzyl alcohol-induced aggregation of chymotrypsinogen by PEGylation, *J. Pharm. Pharmacol.* 63 (2011) 800–805.

[91] L. M. Gaetke, C. K. Chow, Copper toxicity, oxidative stress, and antioxidant nutrients, *Toxicology.* 189 (2003) 147–163.

[92] C. M. Nimmo, M. S. Shoichet, Regenerative Biomaterials that "Click": Simple, Aqueous-Based Protocols for Hydrogel Synthesis, Surface Immobilization, and 3D Patterning, *Bioconjug. Chem.* 22 (2011) 2199–2209.

[93] S. Zalipsky, N. Mullah, C. Engbers, M. U. Hutchins, R. Kiwan, Thiolytically Cleavable Dithiobenzyl Urethane-Linked Polymer-Protein Conjugates as Macromolecular Prodrugs: Reversible PEGylation of Proteins, *Bioconjug. Chem.* 18 (2007) 1869–1878.

[94] I. L. Koumenis, Z. Shahrokh, S. Leong, V. Hsei, L. Deforge, G. Zapata, Modulating pharmacokinetics of an anti-interleukin-8 F(ab′)2 by amine-

specific PEGylation with preserved bioactivity, *Int. J. Pharm.* 198 (2000) 83–95.

[95] T. Kim, H. Lee, T. G. Park, Pegylated recombinant human epidermal growth factor (rhEGF) for sustained release from biodegradable PLGA microspheres, *Biomaterials.* 23 (2002) 2311–2317.

[96] M. Diwan, T. G. Park, Pegylation enhances protein stability during encapsulation in PLGA microspheres, *J. Control. Release.* 73 (2001) 233–244.

[97] M.-I. Aguilar, *HPLC of peptides and proteins. Methods and protocols*. Methods in molecular biology. 251. Humana Press, Totowa, N.J (2004).

[98] B. J. Compton, L. Kreilgaard, Chromatographic Analysis of Therapeutic Proteins, *Anal. Chem.* 66 (1994) 1175A-1180A.

[99] W. Conze, J. Christel, A. Sprauer, V. Noedinger, E. Mueller, Characterization of PEGylated lysozyme by size exclusion and ion exchange chromatography, *LC-GC Eur.* (2008) 48–49.

[100] Y.-S. Wang, S. Youngster, M. Grace, J. Bausch, R. Bordens, D. F. Wyss, Structural and biological characterization of pegylated recombinant interferon alpha-2b and its therapeutic implications, *Adv. Drug Deliv. Rev.* 54 (2002) 547–570.

[101] A. Moosmann, J. Christel, H. Boettinger, E. Mueller, Analytical and preparative separation of PEGylated lysozyme for the characterization of chromatography media, *J. Chromatogr. A*. 1217 (2010) 209–215.

[102] O. Kinstler, G. Molineux, M. Treuheit, D. Ladd, C. Gegg, Mono-N-terminal poly(ethylene glycol)–protein conjugates, *Adv. Drug Deliv. Rev.* 54 (2002) 477–485.

[103] K. Štulík, V. Pacáková, M. Tichá, Some potentialities and drawbacks of contemporary size-exclusion chromatography, *J. Biochem. Biophys. Methods.* 56 (2003) 1–13.

[104] E. Müller, D. Josic, T. Schröder, A. Moosmann, Solubility and binding properties of PEGylated lysozyme derivatives with increasing molecular weight on hydrophobic-interaction chromatographic resins, *J. Chromatogr. A.* 1217 (2010) 4696–4703.

[105] K. Mayolo-Deloisa, M. E. Lienqueo, B. Andrews, M. Rito-Palomares, J. A. Asenjo, Hydrophobic interaction chromatography for purification of monoPEGylated RNase A, *J. Chromatogr. A.* 1242 (2012) 11–16.

[106] D. Berek, Size exclusion chromatography - A blessing and a curse of science and technology of synthetic polymers, *J. Sep. Sci.* 33 (2010) 315–335.

[107] T. Arakawa, D. Ejima, T. Li, J. S. Philo, The critical role of mobile phase composition in size exclusion chromatography of protein pharmaceuticals, *J. Pharm. Sci.* 99 (2010) 1674–1692.

[108] C. J. Fee, J. M. Van Alstine, Prediction of the Viscosity Radius and the Size Exclusion Chromatography Behavior of PEGylated Proteins, *Bioconjug. Chem.* 15 (2004) 1304–1313.

[109] W. Kopaciewicz, F. E. Regnier, Nonideal size-exclusion chromatography of proteins: Effects of pH at low ionic strength, *Anal. Biochem.* 126 (1982) 8–16.

[110] P. L. Dubin, J. M. Principi, Optimization of size-exclusion separation of proteins on a Superose column, *J. Chromatogr. A.* 479 (1989) 159–164.

[111] F. E. Regnier, K. M. Gooding, High-performance liquid chromatography of proteins, *Anal. Biochem.* 103 (1980) 1–25.

[112] J. J. Ratto, S. R. O'Conner, A. R. Distler, G.-M. Wu, D. Hummel, M. J. Treuheit, A. C. Herman, J. M. Davis, Ethanol-sodium chloride-phosphate mobile phase for size-exclusion chromatography of poly(ethylene glycol) modified proteins, *J. Chromatogr. A.* 763 (1997) 337–344.

[113] J. Christel, W. Conze, A. Sprauer, V. Noedinger, E. Mueller, Characterization studies of PEGylated lysozyme using TSK-GEL HPLC columns, *LCGC North Am.* (2010) 23–25.

[114] N. A. Peppas, P. Bures, W. Leobandung, H. Ichikawa, Hydrogels in pharmaceutical formulations, *Eur. J. Pharm. Biopharm.* 50 (2000) 27–46.

[115] T. R. Hoare, D. S. Kohane, Hydrogels in drug delivery: Progress and challenges, *Polymer.* 49 (2008) 1993–2007.

[116] A. S. Sawhney, C. P. Pathak, J. A. Hubbell, Bioerodible hydrogels based on photopolymerized poly(ethylene glycol)-co-poly(α-hydroxy acid) diacrylate macromers, *Macromolecules.* 26 (1993) 581–587.

[117] J. L. West, J. A. Hubbell, Photopolymerized hydrogel materials for drug delivery applications, *Reactive Polymers*. 25 (1995) 139–147.

[118] R. Censi, T. Vermonden, M. J. van Steenbergen, H. Deschout, K. Braeckmans, S. C. de Smedt, C. F. van Nostrum, P. di Martino, W. E. Hennink, Photopolymerized thermosensitive hydrogels for tailorable diffusion-controlled protein delivery, *J. Control. Release.* 140 (2009) 230–236.

[119] M. B. Mellott, K. Searcy, M. V. Pishko, Release of protein from highly cross-linked hydrogels of poly(ethylene glycol) diacrylate fabricated by UV polymerization, *Biomaterials.* 22 (2001) 929–941.

[120] M. B. Browning, E. Cosgriff-Hernandez, Development of a Biostable Replacement for PEGDA Hydrogels, *Biomacromolecules.* 13 (2012) 779–786.

[121] D. L. Elbert, A. B. Pratt, M. P. Lutolf, S. Halstenberg, J. A. Hubbell, Protein delivery from materials formed by self-selective conjugate addition reactions, *J. Control. Release.* 76 (2001) 11–25.

[122] P. van de Wetering, A. T. Metters, R. G. Schoenmakers, J. A. Hubbell, Poly(ethylene glycol) hydrogels formed by conjugate addition with controllable swelling, degradation, and release of pharmaceutically active proteins, *J. Control. Release.* 102 (2005) 619–627.

[123] M. P. Lutolf, J. A. Hubbell, Synthesis and Physicochemical Characterization of End-Linked Poly(ethylene glycol)-co-peptide Hydrogels Formed by Michael-Type Addition, *Biomacromolecules.* 4 (2003) 713–722.

[124] C. Hiemstra, Z. Zhong, M. J. van Steenbergen, W. E. Hennink, J. Feijen, Release of model proteins and basic fibroblast growth factor from in situ forming degradable dextran hydrogels, *J. Control. Release.* 122 (2007) 71–78.

[125] T. Nie, A. Baldwin, N. Yamaguchi, K. L. Kiick, Production of heparin-functionalized hydrogels for the development of responsive and controlled growth factor delivery systems, *J. Control. Release.* 122 (2007) 287–296.

[126] E. A. Phelps, D. M. Headen, W. R. Taylor, P. M. Thulé, A. J. García, Vasculogenic bio-synthetic hydrogel for enhancement of pancreatic islet engraftment and function in type 1 diabetes, *Biomaterials.* 34 (2013) 4602–4611.

[127] J. Yu, X. Xu, F. Yao, Z. Luo, L. Jin, B. Xie, S. Shi, H. Ma, X. Li, H. Chen, In situ covalently cross-linked PEG hydrogel for ocular drug delivery applications, *Int. J. Pharm.* 470 (2014) 151–157.

[128] C. M. Nimmo, S. C. Owen, M. S. Shoichet, Diels−Alder Click Cross-Linked Hyaluronic Acid Hydrogels for Tissue Engineering, *Biomacromolecules.* 12 (2011) 824–830.

[129] H. Tan, J. P. Rubin, K. G. Marra, Direct Synthesis of Biodegradable Polysaccharide Derivative Hydrogels Through Aqueous Diels-Alder Chemistry, *Macromol. Rapid Commun.* 32 (2011) 905–911.

[130] C. T. Huynh, M. K. Nguyen, D. S. Lee, Injectable Block Copolymer Hydrogels: Achievements and Future Challenges for Biomedical Applications, *Macromolecules.* 44 (2011) 6629–6636.

[131] G. T. Hermanson, *Bioconjugate techniques*. Academic Press, Amsterdam, Netherlands (2013).

[132] M. A. Gauthier, H.-A. Klok, Peptide/protein–polymer conjugates: synthetic strategies and design concepts, *Chem. Commun.* (2008) 2591–2611.

[133] C. C. F. Blake, D. F. Koenig, G. A. Mair, A. C. T. North, D. C. Phillips, V. R. Sarma, Structure of Hen Egg-White Lysozyme: A Three-dimensional Fourier Synthesis at 2 Å Resolution, *Nature.* 206 (1965) 757–761.

[134] D. Suckau, M. Mak, M. Przybylski, Protein surface topology-probing by selective chemical modification and mass spectrometric peptide mapping, *Proc. Natl. Acad. Sci.* 89 (1992) 5630–5634.

[135] T. Masuda, N. Ide, N. Kitabatake, Structure-Sweetness Relationship in Egg White Lysozyme: Role of Lysine and Arginine Residues on the Elicitation of Lysozyme Sweetness, *Chem. Senses.* 30 (2005) 667–681.

[136] C. M. Smales, C. H. Moore, L. F. Blackwell, Characterization of Lysozyme-Estrone Glucuronide Conjugates. The Effect of the Coupling Reagent on the Substitution Level and Sites of Acylation, *Bioconjug. Chem.* 10 (1999) 693–700.

[137] M. A. Gauthier, H.-A. Klok, Arginine-Specific Modification of Proteins with Polyethylene Glycol, *Biomacromolecules.* 12 (2011) 482–493.

[138] C. Li, D. S. Moore, R. C. Rosenberg, Circular dichroism studies of diethyl pyrocarbonate-modified histidine in hen egg white lysozyme, *J. Biol. Chem.* 268 (1993) 11090–11096.

[139] C. E. Hoyle, A. B. Lowe, C. N. Bowman, Thiol-click chemistry: a multifaceted toolbox for small molecule and polymer synthesis, *Chem. Soc. Rev.* 39 (2010) 1355.

[140] P. Guire, Differences in tryptophan exposure between chicken egg-white lysozyme and bovine α-lactalbumin, *Biochim. Biophys. Acta - Protein Structure.* 221 (1970) 383–386.

[141] M. Morpurgo, F. M. Veronese, D. Kachensky, J. M. Harris, Preparation and Characterization of Poly(ethylene glycol) Vinyl Sulfone, *Bioconjug. Chem.* 7 (1996) 363–368.

[142] M. Friedman, J. F. Cavins, J. S. Wall, Relative Nucleophilic Reactivities of Amino Groups and Mercaptide Ions in Addition Reactions with α,β-Unsaturated Compounds, *J. Am. Chem. Soc.* 87 (1965) 3672–3682.

[143] B. D. Mather, K. Viswanathan, K. M. Miller, T. E. Long, Michael addition reactions in macromolecular design for emerging technologies, *Prog. Polym. Sci.* 31 (2006) 487–531.

[144] S.-Y. Tang, J. Shi, Q.-X. Guo, Accurate prediction of rate constants of Diels–Alder reactions and application to design of Diels–Alder ligation, *Org. Biomol. Chem.* 10 (2012) 2673.

[145] J. A. Cadée, de Groot, C. J, W. Jiskoot, W. den Otter, W. E. Hennink, Release of recombinant human interleukin-2 from dextran-based hydrogels, *J. Control. Release.* 78 (2002) 1–13.

[146] C.-C. Lin, A. Metters, Enhanced Protein Delivery from Photopolymerized Hydrogels Using a Pseudospecific Metal Chelating Ligand, *Pharm. Res.* 23 (2006) 614-622.

[147] W. Wang, S. Singh, D. L. Zeng, K. King, S. Nema, Antibody structure, instability, and formulation, *J. Pharm. Sci.* 96 (2007) 1–26.

[148] O. Jeon, S. J. Song, H. S. Yang, S.-H. Bhang, S.-W. Kang, M. A. Sung, J. H. Lee, B.-S. Kim, Long-term delivery enhances in vivo osteogenic efficacy of bone morphogenetic protein-2 compared to short-term delivery, *Biochem. Bioph. Res. Co.* 369 (2008) 774–780.

[149] G. A. Peyman, E. M. Lad, D. M. Moshfeghi, Intravitreal injection of therapeutic agents, *Retina (Philadelphia, Pa.)*. 29 (2009) 875–912.

[150] S. R. van Tomme, G. Storm, W. E. Hennink, In situ gelling hydrogels for pharmaceutical and biomedical applications, *Int. J. Pharm.* 355 (2008) 1–18.

[151] F. Wu, T. Jin, Polymer-Based Sustained-Release Dosage Forms for Protein Drugs, Challenges, and Recent Advances, *AAPS PharmSciTech*. 9 (2008) 1218–1229.

[152] N. Hammer, F. P. Brandl, S. Kirchhof, V. Messmann, A. M. Goepferich, Protein Compatibility of Selected Cross-linking Reactions for Hydrogels, *Macromol. Biosci.* 15 (2015) 405–413.

[153] F. Brandl, F. Kastner, R. M. Gschwind, T. Blunk, J. Teßmar, A. Göpferich, Hydrogel-based drug delivery systems: Comparison of drug diffusivity and release kinetics, *J. Control. Release.* 142 (2010) 221–228.

[154] R. J. Solá, K. Griebenow, Chemical glycosylation: New insights on the interrelation between protein structural mobility, thermodynamic stability, and catalysis, *FEBS Letters.* 580 (2006) 1685–1690.

[155] E. W. Merrill, K. A. Dennison, C. Sung, Partitioning and diffusion of solutes in hydrogels of poly(ethylene oxide), *Biomaterials.* 14 (1993) 1117–1126.

[156] L. Callewaert, C. W. Michiels, Lysozymes in the animal kingdom, *J. Biosci.* 35 (2010) 127–160.

[157] T. Schönknecht, D. Pörschke, Electrooptical analysis of α-chymotrypsin at physiological salt concentration, *Biophysical Chemistry.* 58 (1996) 21–28.

[158] A. Kumar, P. Venkatesu, Overview of the Stability of α-Chymotrypsin in Different Solvent Media, *Chem. Rev.* 112 (2012) 4283–4307.

[159] P. P. Berna, N. T. Mrabet, J. van Beeumen, B. Devreese, J. Porath, M. A. Vijayalakshmi, Residue accessibility, hydrogen bonding, and molecular recognition: metal-chelate probing of active site histidines in chymotrypsins, *Biochemistry.* 36 (1997) 6896–6905.

[160] F. Bordusa, Proteases in Organic Synthesis, *Chem. Rev.* 102 (2002) 4817–4868.

[161] Z. He, Z. Zhang, Solvation energy and thermal stability of hydrophilization-modified alpha-chymotrypsin, *J. Protein Chem.* 18 (1999) 557–564.

[162] K. Takahashi, Further studies on the reactions of phenylglyoxal and related reagents with proteins, *J. Biochem.* 81 (1977) 403–414.

[163] M. W. Pandit, M. S. Rao, Studies on self-association of proteins. The self-association of alpha-chymotrypsin at pH 8.3 and ionic strength 0.05, *Biochemistry.* 13 (1974) 1048–1055.

[164] M. L. Simon, K. Lászió, M. Kotormán, B. Szajáni, A comparative study of conformational stabilities of trypsin and α-chymotrypsin, *Acta Biologica Szegediensis*. 45 (2001) 43–49.

[165] J. K. Armstrong, R. B. Wenby, H. J. Meiselman, T. C. Fisher, The Hydrodynamic Radii of Macromolecules and Their Effect on Red Blood Cell Aggregation, *Biophys. J.* 87 (2004) 4259–4270.

[166] K.-T. Shade, R. Anthony, Antibody Glycosylation and Inflammation, *Antibodies.* 2 (2013) 392–414.

[167] Y. Feng, Z. Zhu, W. Chen, P. Prabakaran, K. Lin, D. Dimitrov, Conjugates of Small Molecule Drugs with Antibodies and Other Proteins, *Biomedicines.* 2 (2014) 1–13.

[168] R. S. Larson, V. Menard, H. Jacobs, S. W. Kim, Physicochemical Characterization of Poly(ethylene glycol)-Modified Anti-GAD Antibodies, *Bioconjug. Chem.* 12 (2001) 861–869.

[169] M. B. Phillips, M. M. Sullivan, P. W. Villalta, L. A. Peterson, Covalent Modification of Cytochrome c by Reactive Metabolites of Furan, *Chem. Res. Toxicol.* 27 (2013) 129–135.

[170] T. Montagnon, D. Kalaitzakis, M. Triantafyllakis, M. Stratakis, G. Vassilikogiannakis, Furans and singlet oxygen – why there is more to come from this powerful partnership, *Chem. Commun.* 50 (2014) 15480–15498.

[171] L. A. Badovskaya, L. V. Povarova, Oxidation of furans (Review), *Chem. Heterocycl. Comp.* 45 (2009) 1023-1034.

[172] T. Meyvis, S. de Smedt, P. van Oostveldt, J. Demeester, Fluorescence Recovery After Photobleaching: A Versatile Tool for Mobility and Interaction Measurements in Pharmaceutical Research, *Pharm. Res.* 16 (1999) 1153–1162.

[173] H. Deschout, K. Raemdonck, J. Demeester, S. C. De Smedt, K. Braeckmans, FRAP in Pharmaceutical Research: Practical Guidelines and Applications in Drug Delivery, *Pharm. Res.* 31 (2014) 255–270.

[174] B. K. Wetzl, S. M. Yarmoluk, D. B. Craig, O. S. Wolfbeis, Chameleon Labels for Staining and Quantifying Proteins, *Angew. Chem. Int. Ed.* 43 (2004) 5400–5402.

[175] B. K. Hoefelschweiger, A. Duerkop, O. S. Wolfbeis, Novel type of general protein assay using a chromogenic and fluorogenic amine-reactive probe, *Anal. Biochem.* 344 (2005) 122–129.

[176] R. J. Meier, M.-S. Steiner, A. Duerkop, O. S. Wolfbeis, SDS-PAGE of Proteins Using a Chameleon-Type of Fluorescent Prestain, *Anal. Chem.* 80 (2008) 6274–6279.

[177] K. B. Kosto, W. M. Deen, Diffusivities of macromolecules in composite hydrogels, *AIChE J.* 50 (2004) 2648–2658.

[178] S. B. Dubin, G. Feher, G. B. Benedek, Study of the chemical denaturation of lysozyme by optical mixing spectroscopy, *Biochemistry.* 12 (1973) 714–720.

[179] J. R. Colvin, The Size And Shape Of Lysozyme, *Can. J. Chem*. 30 (1952) 831–834.

[180] R. R. Walters, J. F. Graham, R. M. Moore, D. J. Anderson, Protein diffusion coefficient measurements by laminar flow analysis: Method and applications, *Anal. Biochem*. 140 (1984) 190–195.

[181] E. N. Vasina, P. Déjardin, Adsorption of α-Chymotrypsin onto Mica in Laminar Flow Conditions. Adsorption Kinetic Constant as a Function of Tris Buffer Concentration at pH 8.6, *Langmuir.* 20 (2004) 8699–8706.

[182] W. M. Saltzman, M. L. Radomsky, K. J. Whaley, R. A. Cone, Antibody diffusion in human cervical mucus, *Biophys. J.* 66 (1994) 508–515.

[183] K. Burczak, T. Fujisato, M. Hatada, Y. Ikada, Protein permeation through poly(vinyl alcohol) hydrogel membranes, *Biomaterials.* 15 (1994) 231–238.

[184] B. A. Askonas, C. P. Farthing, J. H. Humphrey, The significance of multiple antibody components in serum of immunized rabbits, *Immunology.* 3 (1960) 336–351.

[185] J. A. Rodríguez-Martínez, I. Rivera-Rivera, R. J. Solá, K. Griebenow, Enzymatic activity and thermal stability of PEG-α-chymotrypsin conjugates, *Biotechnol. Lett.* 31 (2009) 883–887.

[186] S. J. Novick, J. S. Dordick, Preparation of Active and Stable Biocatalytic Hydrogels for Use in Selective Transformations, *Chem. Mater.* 10 (1998) 955–958.

[187] J. Kim, T. J. Kosto, J. C. Manimala, E. B. Nauman, J. S. Dordick, Preparation of enzyme-in-polymer composites with high activity and stability, *AIChE J*. 47 (2001) 240–244.

[188] L. Gai, D. Wu, A Novel Reversible pH-Triggered Release Immobilized Enzyme System, *Appl. Biochem. Biotechnol.* 158 (2009) 747–760.

List of Figures

List of Tables

Appendix

Acronyms

^{1}H-NMR ..... proton nuclear magnetic resonance
8armPEG10k ..... eight-armed poly(ethylene glycol) with a molecular weight of 10 kDa
8armPEG20k ..... eight-armed poly(ethylene glycol) with a molecular weight of 20 kDa
BSA ..... bovine serum albumin
CD spectroscopy ..... circular dichroism spectroscopy
$CDCl_3$ ..... deuterated chloroform
CuAAC ..... copper(I)-catalyzed azide-alkyne cycloaddition
DCC ..... N,N'-dicyclohexylcarbodiimide
DCM ..... methylene chloride
DCU ..... N,N'-dicyclohexylurea
DIAD ..... diisopropyl azodicarboxylate
DSC ..... N,N'-discuccinimidyl carbonate
EPO ..... erythropoietin
FRAP ..... fluorescence recovery after photobleaching
HOSu ..... N-hydroxysuccinimide
HPLC ..... high-performance liquid chromatography
IgG ..... Immunoglobulin G
LHRH ..... luteinizing hormone–releasing hormone
MALDI TOF MS ..... matrix-assisted laser desorption ionization mass spectrometry
mPEG ..... methoxy poly(ethylene glycol)
NHS ..... N-hydroxysuccinimide
PBS ..... phosphate-buffered saline
PEG ..... poly(ethylene glycol)
PEGylation ..... modification with PEG
pI ..... isoelectric point, isoelectric point
PLA ..... polylactic- acid
PLGA ..... poly(lactic-co-glycolic acid)
PPh_3 ..... triphenylphosphine
R_h ..... hydrodynamic radius
SC ..... linker groups activated with discuccinimidyl carbonate
SDS-PAGE ..... sodium dodecyl sulfate polyacrylamide gel electrophoresis
SEC ..... size exclusion chromatography
TEMED ..... tetramethylethylenediamine
TRIS 2-amino-2-hydroxymethyl-propane-1,3-diol
α-CT ..... α-Chymotrypsin

Symbols

c……..concentration
D…….....diffusion coefficient
d_h…….hydrodynamic diameter
δ……..chemical shift
$F(t)$……..fluorescence intensity of the region of interest normalized to full scale
$f(t)$……normalized intensity of the bleached region of interest.
$f(0)$……...normalized intensity of the region of interest directly after bleaching.
$f(pre)$……...normalized intensity of the region of interest before bleaching
$f(t)$……....normalized fluorescence intensity of the bleached region of interest
$|G^*|$…….....absolute value of the complex shear modulus
G'……storage modulus
G''……...loss modulus
$I_{ref}(pre)$……fluorescence intensity of the reference region before bleaching
$I_{ref}(t)$……fluorescence intensity of the reference region at each time point t
$I_{roi}(pre)$……fluorescence intensity of the region of interest before bleaching.
$I_{roi}(t)$……fluorescence intensity of the region of interest at each time point t
I_0……..modified Bessel function of the first kind zero order
I_1……..modified Bessel function of the first kind first order
k……...mobile fraction
λ_{em}……...emission wavelength
λ_{ex}……excitation wavelength
M_0……weight before incubation
M_t…….weight at certain time t
R_h…….hydrodynamic radius
T_D……diffusion time
w……..radius of the bleached region of interest

List of Publications

Publications in Scientific Journals

[1] S. Kirchhof, M. Abrami, V. Messmann, **Nadine Hammer**, A.M. Goepferich, M. Grassi, et al. Diels–Alder hydrogels for controlled antibody release: Correlation between mesh size and release rate. *Mol. Pharmaceutics*, 12 (2015): 3358–3368. doi:10.1021/acs.molpharmaceut.5b00375.

[2] S. Kirchhof, M. Gregoritza, V. Messmann, **Nadine Hammer**, A.M. Goepferich, F.P. Brandl. Diels-Alder hydrogels with enhanced stability: First step toward controlled release of bevacizumab. *Eur. J. Pharm. Biopharm*, 96 (2015): 217–225. doi:10.1016/j.ejpb.2015.07.024.

[3] **Nadine Hammer**, F.P. Brandl, S. Kirchhof, V. Messmann, A.M. Goepferich. Protein compatibility of selected cross-linking reactions for hydrogels. *Macromol. Biosci*. 15 (2015): 405–413. doi:10.1002/mabi.201400379. **(Chapter 5)**

[4] S. Kirchhof, A. Strasser, H.-J. Wittmann, V. Messmann, **Nadine Hammer**, A.M. Goepferich, et al. New insights into the cross-linking and degradation mechanism of Diels-Alder hydrogels. *J. Mater. Chem. B.,* 3 (2015): 449–457. doi:10.1039/C4TB01680G.

[5] **Nadine Hammer**, F.P. Brandl, S. Kirchhof, A.M. Goepferich. Cleavable carbamate linkers for controlled protein delivery from hydrogels. *J. Control. Release,* 183 (2014): 67–76. doi:10.1016/j.jconrel.2014.03.031. **(Chapter 3)**

[6] S. Kirchhof, F.P. Brandl, **Nadine Hammer**, A.M. Goepferich. Investigation of the Diels–Alder reaction as a cross-linking mechanism for degradable poly(ethylene glycol) based hydrogels. *J. Mater. Chem. B,* 1 (2013): 4855–4864. doi:10.1039/c3tb20831a.

[7] F.P. Brandl, **Nadine Hammer**, T. Blunk, J.K. Tessmar, A.M. Goepferich. Biodegradable hydrogels for time-controlled release of tethered peptides or proteins. *Biomacromolecules,* 11 (2010): 496–504. doi:10.1021/bm901235g.

Conference Abstracts

[1] **Nadine Hammer**, F.P. Brandl, S. Kirchhof, A.M. Goepferich. Carbamate linkers for controlled protein release from hydrogels. PBP World Meeting, Lisbon, Portugal (2014).

[2] S. Kirchhof, F.P. Brandl, **Nadine Hammer**, A.M. Goepferich. Degradable poly(ethylene glycol) based hydrogels cross-linked by Diels-Alder click reaction. PBP World Meeting, Lisbon, Portugal (2014).

[3] **Nadine Hammer**, F.P. Brandl, S. Kirchhof, A.M. Goepferich. Degradation controlled protein release from Diels-Alder hydrogels. ACS National Meeting & Exposition, Indianapolis, IN, USA (2013).

[4] **Nadine Hammer**, F.P. Brandl, S. Kirchhof, A.M. Goepferich. Protein mobility in Diels-Alder hydrogels. CRS German Local Chapter Meeting, Ludwigshafen, Germany (2013).

[5] S. Kirchhof, F.P. Brandl, **Nadine Hammer**, A.M. Goepferich. Degradation of Diels-Alder hydrogels: Exploring the mechanism. ACS National Meeting & Exposition, Indianapolis, IN, USA (2013).

[6] S. Kirchhof, F.P. Brandl, **Nadine Hammer**, A.M. Goepferich. Diels-Alder hydrogels with defined mesh size for controlled drug delivery. CRS German Local Chapter Meeting, Ludwigshafen, Germany (2013).

[7] S. Kirchhof, F.P. Brandl, **Nadine Hammer**, V. Messmann, A.M. Goepferich. Poly(ethylene glycol) based Diels-Alder hydrogels for biomedical applications. Annual Meeting & Exposition of the Society for Biomaterials, Boston, MA, USA (2013).

[8] F.P. Brandl, S. Kirchhof, **Nadine Hammer**, V. Messmann, A.M. Goepferich. Development and pharmaceutical technological applications of Diels-Alder hydrogels. DPhG Jahrestagung, Greifswald, Germany (2012).

[9] **Nadine Hammer**, F.P. Brandl, S. Kirchhof, V. Messmann, J.K. Tessmar, A.M. Goepferich. Hydrogels for drug delivery: Hydrolytically cleavable carbamate linkers for time controlled protein release. DPhG Jahrestagung, Greifswald,

Germany (2012).

[10] **Nadine Hammer**, F.P. Brandl, S. Kirchhof, J.K. Tessmar, A.M. Goepferich. Hydrogels for drug delivery: Hydrolytically cleavable linkers for time controlled protein release. CRS German Local Chapter Meeting, Würzburg, Germany (2012).

[11] **Nadine Hammer**, F.P. Brandl, S. Kirchhof, J.K. Tessmar, A.M. Goepferich. Time controlled protein delivery by hydrolytically cleavable poly(ethylene glycol) linkers. World Biomaterials Congress, Chengdu, China (2012).

[12] S. Kirchhof, F.P. Brandl, **Nadine Hammer**, J.K. Tessmar, A.M. Goepferich. Application of the Diels-Alder reaction as a new cross-linking mechanism for poly(ethylene glycol) based hydrogels. ACS National Meeting & Exposition, Philadelphia, PA, USA (2012).

[13] S. Kirchhof, F.P. Brandl, **Nadine Hammer**, V. Messmann, J.K. Tessmar, A.M. Goepferich. Hydrogels for drug delivery: Influence of macromer branching on characteristics of poly(ethylene glycol) based hydrogels. DPhG Jahrestagung, Greifswald, Germany (2012).

[14] S. Kirchhof, F.P. Brandl, **Nadine Hammer**, J.K. Tessmar, A.M. Goepferich. Investigation of novel poly(ethylene glycol) based hydrogels as delivery systems for peptides and proteins. CRS German Local Chapter Meeting, Würzburg, Germany (2012).

[15] **Nadine Hammer**, F.P. Brandl, J.K. Tessmar, A.M. Goepferich. Hydrogels for drug delivery: Time controlled protein release by hydrolytically cleavable carbamates. DGBM Jahrestagung, Gießen, Germany (2011).

Acknowledgments

An dieser Stelle möchte ich mich ganz herzlich bei all jenen bedanken, die mich bei der Umsetzung dieser Arbeit maßgeblich unterstützt haben.

Meinen besonderen Dank möchte ich Herrn Prof. Dr. Achim Göpferich aussprechen für die Möglichkeit an diesem Thema zu arbeiten, für die kontinuierliche Unterstützung und die Möglichkeit zur Umsetzung eigener Ideen und Ansätze. Die wissenschaftlichen Diskussionen und Anregungen waren sehr hilf- und lehrreich für mich. Ganz besonders bedanken möchte ich mich für die Möglichkeit meine Ergebnisse auf nationalen und internationalen Konferenzen zu präsentieren. Dies waren sehr wertvolle Erfahrungen für mich.

Herrn Dr. Ferdinand Brandl danke ich besonders für die freundschaftliche und engagierte Betreuung des Projekts. Die vielen Ratschläge und Tipps, selbst aus der Ferne, waren sehr hilfreich zur Umsetzung der Experimente und zur Interpretation der Ergebnisse. Insbesondere möchte ich mich für seine Hilfe und Unterstützung und die zahlreichen konstruktiven Diskussionen bei der Erstellung zahlreicher Manuskripte bedanken.

Herrn Dr. habil. Jörg Teßmar danke ich für seine Hilfsbereitschaft, die vielen Anregungen und Ideen, besonders in schwierigen Zeiten, und die freundschaftliche Zusammenarbeit bei der Praktikumsbetreuung.

Frau PD Dr. Miriam Breunig danke ich für die hilfreichen und anregenden wissenschaftlichen Diskussionen.

Dr. Helmut Durchschlag und Klaus-Jürgen Tiefenbach danke ich ganz herzlich für die Hilfestellung, Unterstützung und Beratung bei der Aufnahme und Auswertung der CD-Spektren.
Dr. Robert Meier danke ich sehr für die Markierung verschiedener Proteine mit verschiedenen Fluoreszenzfarbstoffen. Danke für die Idee zur Verwendung eine Chamäleonlabels.

Prof. Dr. Jens Schlossmann und seinem Team danke ich für die Erlaubnis zur Nutzung des ChemiDoc™ MP gel imaging Systems, das mir die Dokumentation und Auswertung der SDS-PAGE Versuche sehr erleichtert hat.

Frau Viktoria Meßmann danke herzlich ich für die zuverlässige und stets gut gelaunte Unterstützung bei der Durchführung der Experimente.

Für die finanzielle Förderung des Projekts „Bioabbaubare Hydrogele für die lokale Verabreichung von Protein- und Nukleinsäurewirkstoffen am Auge“ (GO 565/16-1) bedanke ich mich bei der Deutschen Forschungsgemeinschaft.

Nicht zuletzt möchte ich mich bei allen derzeitigen und ehemaligen Kolleginnen und Kollegen am Lehrstuhl für Pharmazeutische Technologie für die gute und freundschaftliche Zusammenarbeit und die schöne gemeinsame Zeit bedanken.
Mein besonderer Dank gilt dabei:

Meinen Labormitbewohnerinnen Dr. Sonja Bauhuber und Julia Köhler für die gemeinsame Zeit, die vielen fachlichen und nicht-fachlichen Gespräche, ihre konstruktive Unterstützung im Laboralltag und ihre Freundschaft.

Luise Tomasetti, Johanna Lempp und Dr. Eva Esser für die engagierte und lustige Zusammenarbeit im Praktikum und die gemeinsame Zeit.

Dr. Eva Esser und Dr. Robert Hennig für die tolle Begleitung auf jeweils unvergesslichen Reisen.

Dr. Martina Kessler für die Aufmunterungen in schlechten Zeiten.

Dr. Susanne Kirchhof für die Zusammenarbeit im „Hydrogel-Projekt“.

Magdalena Seitz, Veronica Scheidler und Theresa Ferstl für die Unterstützung im Labor.

Angelika Berié, Andrea Blaimer, Stefan Kolb, Renate Liebl, Edith Schindler und Eva Wrobel für ihre vielfältige technische und organisatorische Hilfe.

Mein ganz besonderer Dank gilt meiner Familie und allen Freunden, die mich auf diesem Weg begleitet und unterstützt und auch in schwierigen Phasen ertragen haben.

Erklärung

Hiermit erkläre ich, dass ich die vorliegende Arbeit selbst verfasst und keine anderen als die angegebenen Hilfsmittel verwendet habe.

Regensburg, den 13.03.2017

Nadine Hammer